Distributed Cooperative Positioning for Next Generation Mobile Radio Systems

Siwei Zhang

A Thesis submitted for the Degree of
Master of Science

Institute for Communications and Navigation

Prof. Dr. Christoph Günther

Supervised by Dr.-Ing. R. Raulefs
Dipl.-Ing. K. Giger

Munich, September 2011

Institute for Communications and Navigation

Technische Universität München
Theresienstrasse 90
80333 Munich

Abstract

In GNSS-denied areas (e.g. deep urban canyon, indoor, etc.) navigation is still possible by using terrestrial radio signals. However, for the conventional terrestrial positioning the accuracy is limited by the number of available base stations (BS) with the line-of-sight (LOS) condition and the corresponding ranging accuracies. The problem can be solved by using the additional ranging measurements between neighboring mobile terminals (MT) in a peer-to-peer fashion. This approach is called cooperative positioning. So far, the research in this area was mainly focused on the simple models and neglected the system constraints. In this thesis, we look into the cooperative positioning within the framework of the next generation mobile radio system based on OFDM (orthogonal frequency-division multiplexing). We propose a nature-inspired mobility model to increase the robustness of the particle filter, and a link evaluation scheme to reduce the effect of error propagation. Then we take the features of OFDM signals into consideration to derive several theoretical bounds for the ranging and positioning performance. Finally, we consider the resources limitation of a real system and propose some resource allocation schemes.

Contents

List of Abbreviations

3G:	Third generation
AI:	Artificial intelligence
AWGN:	Additive white Gaussian noise
BS:	Base station
CDF:	Cumulative distribution function
CRLB:	Cramér-Rao lower bound
CSI:	Channel state information
DLR:	Deutsches Zentrum für Luft- und Raumfahrt (German Aerospace Center)
DOP:	Dilution of precision
EKF:	Extended Kalman filter
FDMA:	Frequency division multiple access
FIM:	Fisher information matrix
GLOS:	Geometric line-of-sight
GN:	Gauss-Newton method
GNSS:	Global navigation satellite system
H-SPAWN:	Hybrid sum-product algorithm over a wireless network
iff:	If and only if
KF :	Kalman filter
LF :	Lévy-flight
LOS:	Line-of-sight
LT:	Lévy track
MLF:	Modified Lévy-flight
MLF_LT:	Modified Lévy-flight and Lévy track
MT:	Mobile terminal
NE:	Nash equilibrium
NLOS:	Non-line-of-sight
OFDM:	Orthogonal frequency division multiplexing
OFDMA:	Orthogonal frequency division multiplexing access
PDF:	Probability density function
PF:	Particle filter
RMS:	Root mean square
RSS:	Received signal strength
RWP:	Random way point

RTD:	Round trip delay
SINR:	Signal to noise ratio
SNR:	Signal to interference and noise ratio
SPAWN:	Sum-product algorithm over a wireless network
TDMA:	Time division multiple access
TDOA:	Time difference of arrival
TOA:	Time of arrival
UWB:	Ultra-wideband
WDOP:	Weighted dilution of precision
WNA:	White noise acceleration

List of Notation

Positioning Aspects

K	Number of BSs
M	Number of MTs
L	Total number of the links
MT_i	The i^{th} MT node
BS^k	The k^{th} BS node
$\vec{r}_i$	Position vector ofMT_i
$\vec{r}^k$	Position vector of BS^k
$d_{i,j}$	Distance from MT_j to MT_i
d_i^k	Distance from BS^k to MT_i
ρ_i^k	Terrestrial range of BS^k to MT_i link
$\rho_{i,j}$	Cooperative range of MT_i to MT_i link
η_i^k	Terrestrial range noise of BS^k to MT_i link
$\eta_{i,j}$	Cooperative range noise of MT_i to MT_i link
K_i	Number of the neighboring BSs of MT_i
M_i	Number of the neighboring MTs of MT_i
$\mathbb{B}_i$	Index set of MT_i's neighboring BSs
$\mathbb{M}_i$	Index set of MT_i's neighboring MTs
$(\sigma_i^k)^2$	Ranging variance of the terrestrial link $BS^k \rightarrow MT_i$
$(\sigma_{i,j})^2$	Ranging variance of the cooperative link $MT_j \rightarrow MT_i$
c	Speed of the light
τ	Propagation Delay
ε	Noise on top of the delay estimation
$R_{i,j}$	Communication Range from MT_j to MT_i
R_i^k	Communication Range from BS^k to MT_i
ρ	Ranging measurement
$x^{k(i)}$	Quantity x referring to the k^{th} neighboring BS of MT_i
$x_{j(i)}$	Quantity x referring to the j^{th} neighboring MT of MT_i
ρ_i^{BS}	Vector of all the terrestrial ranging measurements of MT_i
$\rho_{i,\text{ MT}}$	Vector of all the cooperative ranging measurements of MT_i
$\rho_{\text{MT}}^{\text{BS}}$	Vector of all the terrestrial ranges of all the MTs
$\rho_{\text{MT, MT}}$	Vector of all the cooperative ranges of all the MTs

ρ_{MT}	Vector of all the ranges(terrestrial and cooperative) of all the MTs
ϱ_i	Targeting accuracy of MT_i
$r_{\mathrm{pj,i}}^{\mathrm{BS}}$	Non-cooperative projection vector
$H_{\mathrm{nc},i}$	Non-cooperative geometric matrix of MT_i
$C_{\mathrm{nc},i}$	Non-cooperative covariance matrix of MT_i
$r_{\mathrm{pj,i,\ MT}}$	Cooperative projection vector
$\vec{e}_i^{\,k}$	Unitary vector from BS^k to MT_i
$H_{\mathrm{c},i}$	Cooperative component of the overall geometric matrix of MT_i
$C_{\mathrm{c},i}$	Cooperative component of the overall covariance matrix of MT_i
$\vec{e}_{i,j}$	Unitary vector from MT_j to MT_i
H_i	Overall geometric matrix of MT_i
C_i	Overall covariance matrix of MT_i
$r_{\mathrm{pj,i}}$	Overall projection vector
ρ_i	Vector of all the ranging measurements of MT_i
$x_{[t]}$	Quantity x at time step t
$x_{[t_0:t_1]}$	Vector of quantity x from time step t_0 to time step t_1
$x^{\{p\}}$	Quantity x referring to the p^{th} particle in the particle filter
N_p	Number of particles
$w_{i,[t]}^{\{p\}}$	Weight for p^{th} particle of i^{th} MT at time step t
$q(\cdot)$	Proposal importance density
L_f	Flight length of the Lévy Flight mobility model, where $L_f \sim \mathcal{L}(\mu_f, \ell_f)$
t_p	Pause time of the Lévy Flight mobility model, where $t_p \sim \mathcal{L}(\mu_p, \ell_p)$
a_v	Exponential factor of the Lévy Flight mobility model
b_v	Scale factor of the Lévy Flight mobility model
φ_f	Flight direction of the Lévy Flight mobility model, where $\varphi_f \sim \mathcal{U}[0, 2\pi]$
β	Confidence factor
$\tilde{\sigma}_{i,j}$	Equivalent (or weighted) variance of $MT_j \rightarrow MT_i$ link
ϵ_{jx}	Estimation error of MT_j on the x dimension
ϵ_{jy}	Estimation error of MT_j on the y dimension
α	General notation for the parameter to be estimated
g	General notation for the observation
$\mathrm{CRLB}[x]$	CRLB (scaler or matrix) of quantity x
$J[x]$	FIM of quantity x
$J_{\mathrm{nc}}[\vec{r}_i]$	Non-cooperative positioning FIM for MT_i
$\mathrm{CRLB}_{\mathrm{nc}}[\vec{r}_i]$	Non-cooperative positioning CRLB for MT_i
$J_{\mathrm{nc}}[\vec{r}_{\mathrm{MT}}]$	Non-cooperative positioning FIM for all the MTs
$\mathrm{CRLB}_{\mathrm{nc}}[\vec{r}_{\mathrm{MT}}]$	Non-cooperative positioning CRLB for all the MTs
$J_{\mathrm{c}}[\vec{r}_{\mathrm{MT}}]$	Cooperative component of the positioning FIM for all the MTs
$J_{[}\vec{r}_{\mathrm{MT}}]$	Overall positioning FIM for all the MTs
$\mathrm{CRLB}_{[}\vec{r}_{\mathrm{MT}}]$	Overall positioning CRLB for all the MTs

$c^{-1}_{\mathrm{bi,i,j}}$	Weight for a bi-directional link between MT_i and MT_j
$C^{-1}_{c,\mathrm{bi},i^{-1}}$	Cooperative weight matrix for all the bi-directional links of MT_i
H_{c,i^-}	Cooperative geometric matrix
$\delta_{i,j}$	Link selection factor
$\tilde{C}^{-1}_{\mathrm{c,bi},i}$	Cooperative weight matrix for all the bi-directional links of MT_i with mutual neighbors
$\tilde{H}_{\mathrm{c},i}$	Cooperative geometric matrix with mutual neighbors

System Aspects

$s(t)$	OFDM signal in time domain
N	Number of subcarriers
S_n	The information carried by the n^{th} subcarriers
PL	Pathloss
σ_0^2	Variance of thermal noise
ϑ	Attenuation factor
f_{sc}	Subcarrier spacing
f_{c}	Carrier frequency
T	Sampling period
SNR_n	SNR for the n^{th} subcarriers
N_{th}	Thermal noise
$P_{\mathrm{tx},n}$	Transmit power of the n^{th} subcarriers
σ^2_{ofdm}	Ranging variance with the OFDM signal
$r(iT-\tau)$	A sampled time domain received signal
$\mathbb{N}_i^k$	Index set of subcarriers used by the $BS_k \rightarrow MT_i$ link
$\mathbb{N}_{i,j}$	Index set of subcarriers used by the $MT_j \rightarrow MT_i$ link
T_{pro}	Processing time
E	Efficiency function
F	Fairness function
f_{cost}	Cost function for the centralized resource allocation scheme
ν_{c}	Tradeoff factor for the centralized resource allocation scheme
$\mathrm{SC}_{\mathrm{MT,opt}}$	Global optimal resource allocation solution
N_{res}	Number of the resources
Price_i	Price offered by MT_i in the bidding game
$\mathrm{CRLB}[\vec{r}_i]_{\mathrm{loc}}$	Local approximation of the positioning CRLB for MT_i
sc_n	Resource allocation strategy that using the subcarrier n
$n_{\mathrm{sc},i}$	Number of the subcarriers used by MT_i
Δ_i	Relative need of improvement for MT_i
p_{intf}	Probability of having interference if a subcarrier is used by two links
$p_{i,j,\mathrm{one}}$	Probability that a specific subcarrier from MT_i is interfered by MT_j
ζ	Percentage factor
$p_{i,\mathrm{get}}$	probability of getting new subcarriers for MT_i

$p_{i,\text{release}}$	probability of releasing occupied subcarriers for MT_i
ν_{dc}	Tradeoff factor for the decentralized resource allocation scheme

Mathematics

$\hat{x}$	Estimation of quantity x
$\mathcal{E}[x]$	Expectation of variable x
var[x]	Variance of variable x
$\lvert x\rvert$	Absolute value of number x
$\lvert S\rvert$	Cardinality of set S (number of the members)
$\lVert x\rVert$	Euclidean norm of the vector x
det[A]	Determinant of the matrix A
Trace[A]	Trace of the matrix A
$x \sim \mathcal{N}(\mu, \sigma^2)$	Random variable x follows the normal distribution with the mean μ and the variance σ^2
$x \sim \mathcal{L}(\mu, \ell)$	Random variable x follows the Lévy distribution with the location factor μ and the scale factor ℓ
$x \sim \mathcal{U}[a, b]$	Random variable x follows the Uniform distribution in the interval $[a, b]$
$p(x\lvert y)$	Conditional probability density function of r.v. x given r.v. y
$p(x, y)$	Joint probability density function of r.v. x and y
$x_{i^{\text{th}}}$	i^{th} order Maclaurin expansion of variable x
a_i	The i^{th} agent in game theory
$\lambda_{m(i)}$	The m^{th} strategy for a_i
$\lambda_{\bar{m}(i)}$	The optimal strategy for a_i
Λ_i	Strategy set for a_i
$u_{m(i)}$	Utility function for a_i by applying $\lambda_{m(i)}$

Chapter 1

Introduction

1.1 Background

In wireless communications the location awareness becomes one of the crucial needs which makes terrestrial positioning a hot topic. The idea is to estimate a mobile terminal (MT)'s position by the features of the mobile radio signal. It is considered as an assisting or an alternative technology of global navigation satellite system (GNSS) [1]. The main reason is that there are normally not enough navigation satellites visible or the satellite signal is too weak in the public indoor (e.g. shopping mall) and urban canyon (e.g. street of metropolis) scenarios. However, in these scenarios the mobile terminal (MT)'s location information is much of interest [2]. In [3], the authors gave a theoretical overview of the fundamentals of positioning with ultra-wideband (UWB) radios. In [4] Yuan et al. focused on the Cramér-Rao Lower Bound (CRLB) of terrestrial positioning. In [5] the authors looked into a real third generation (3G) mobile radio system and made comparisons between the performances of the 3G terrestrial and satellite based positioning. They concluded that 3G terrestrial positioning is a low cost but inaccurate alternative to GNSS.

Positioning metrics

For positioning with wireless networks the metrics can be divided into two main categories: a) geometric based and b) fingerprint based. For the first category some geometric values (e.g. distance, angle, etc.) are measured, and the position is estimated according to the geometric relationship. Distance can be measured by time of arrival (TOA), time difference of arrival (TDOA), round trip delay (RTD) and received signal strength (RSS)[3], [4]. The first three are referred as time based metrics, whereas the last one is power based. For a multiple antenna device, we can also measure the angle of arrival (AOA) to estimate the position. For any geometric based positioning, a sufficient number of reference points are required. Moreover, a line-of-sight (LOS) condition will be beneficial. For the fingerprint based positioning, the MT searches in the database to find a pre-measured pattern

which matches the characteristic of the currently received signal. The environment constraint for fingerprinting is less critical because the performance does not rely on the LOS condition. However, a large database is required [6]. Hybrid metrics for positioning were also investigated, which fuses multiple metrics together. For example, in [7] Qi et al. proposed a hybrid TOA-RSS distance estimation scheme. A critical distance is defined. The algorithm chooses between TOA and RSS by comparing the pre-estimated distance to the critical distance.

Positioning algorithms

Numerous positioning algorithms have been developed. Based on where the information is collected and the position is estimated, the positioning algorithms can be divided into two types: a) centralized algorithms and b) decentralized algorithms. For a centralized algorithm, there is a central unit which collects all the available information from the nodes, and globally calculates the estimates for all the MTs. An algorithm is decentralized if each MT calculates its own estimate only based on the locally accessible information (e.g. messages from neighbors). For centralized approaches, all the information needs to be forwarded to the center unit. When the network is dense, the communication capacity of the center unit becomes a bottleneck which increases the processing delay. On the contrary, for an MT using decentralized algorithms, the processing delay does not depend on the number of MTs [8].

The current position of an MT is normally correlated to the previous positions [9]. The positioning algorithms can also be distinguished by whether the time-correlations of the MT's track are considered. A static positioning algorithm only uses the snapshot information and ignores the old information, e.g. non-linear least-square estimator with Gauss-Newton method (GN) [10]. Whereas dynamic algorithm also takes the historical information as well as the movement model into account, e.g. Kalman filter (KF), extended Kalman filter (EKF), particle filter (PF), etc. [9].

Cooperative positioning

For the conventional terrestrial positioning, only the base stations (BSs) are considered as the reference points. This technique is also called non-cooperative positioning. The mobile networks are originally designed for communications. For each MT, normally only one BS is required to establish a communication link. Therefore, the number of BSs with LOS condition may also be insufficient for positioning (up to 3 BSs per 1000 m^2) [11]. On the contrary, in the public indoor and urban scenarios, the MTs network is quite dense (10-100 MTs per 1000 m^2) [11]. It is easier to find some MTs around with LoS condition [10]. Moreover, with the introduction of relays, the peer-to-peer communication is frequently discussed within the framework of the next generation mobile radio system [12]. The positioning accuracy could

be enhanced by the aid of peer-to-peer links. This technique is called cooperative positioning. The main idea is that MTs additionally use the measurement from peer-to-peer links together with the neighboring MTs' position information to localize themselves cooperatively. In [8], [13], the usage of cooperative positioning in wireless communication system is introduced. The cooperative positioning variance is theoretically lower bounded by the CRLB which can be found in [14], [15], etc.

A severe problem of cooperative positioning is called error propagation [16]: Because of the interaction between MTs, the estimation errors are propagated. If an MT trusts the unreliable information from neighboring MTs, its estimation accuracy may be reduced. In [17] Wymeersch et al. looked into the network topology and belief propagation, and presented an algorithm named SPAWN (sum-product algorithm over a wireless network) to use the neighbors' information appropriately. Caceres et al. adapted the work from Wymeersch to a GNSS-terrestrial hybrid system and came up with a Hybrid-SPAWN algorithm (H-SPAWN) in [18]. Another solution to reduce the error propagation effect is to discard the unreliable information. A discarding scheme was proposed in [19] where the information of a neighboring MT will be discarded if its CRLB is bigger than a certain threshold. In [16], Savarese et al. used a two stages algorithm to eliminate the initial estimation error propagation. At the first stage, only the non-cooperative positioning is applied to get a rough estimation. Then the estimation is refined by cooperative positioning. For the refinement stage, a trust factor is presented to reduce the error propagation effect.

1.2 Contributions and Outline of the Thesis

The main contributions of this thesis are:

Novel schemes to improve the positioning performance: A nature-inspired mobility model named Lévy-flight (LF) is used by the PF. The pattern of the LF can be described as long distance walk interrupted by short strolling. It is considered as an efficient movement model to find a randomly located target in a map [20]. PF becomes more efficient and robust by applying the LF. A low complexity link evaluation scheme is proposed which transfers neighbor's estimation uncertainty into the measurement error variance. With this scheme an MT is able to use neighbors' information locally with a rational trust strategy to reduce the error propagation effect.

Derivation of theoretical bounds for positioning problems with the features of an OFDM signal: The CRLBs of non-cooperative and cooperative positioning are derived which takes the feature of an orthogonal frequency-division multiplexing (OFDM) system (i.e. subcarrier index, pathloss-measurement variance dependency, etc.) into account. It gives a clearer idea of the achievable estimation accuracy of a specific OFDM cooperative positioning system compared to previous

work [14], [8], [15]. A local approximation of the cooperative positioning CRLB is proposed by using the link evaluation scheme.

Investigation of resource allocation schemes with the real system constraint: In a real system, resources are limited. With this constraint, we propose several resource allocation schemes based on the previously derived CRLBs. We also explore the usage of game theory in the resource allocation schemes especially for the decentralized case.

The rest of this thesis is organized as follow:

In Chapter 2 the system model with the corresponding notations are defined. In Chapter 3 we introduce two distributed cooperative positioning algorithms namely: distributed Gauss-Newton (GN) and distributed particle filter (PF). For PF, we additionally introduce the LF mobility model. We also raise a low complexity link evaluation scheme. It combines neighbors' estimation variance with the distance measurement variance to obtain an equivalent measurement variance.

In Chapter 4 we investigate the positioning CRLBs in general and the CRLB of ranging variance with an OFDM signal. Then we look into a specific OFDM cooperative positioning system and derive the modified positioning CRLBs with the features of an OFDM signal.

In Chapter 5, we consider the impact of limited resources on the positioning accuracy and propose several resource allocation schemes. We use the CRLBs derived in Chapter 4 as a core factor to allocate the limited resource. A greedy centralized approach, a partial decentralized bidding game and two pure decentralized allocation games are presented.

In Chapter 6 the simulation results and the analysis are shown which include the performances of the proposed link evaluation scheme, resource allocation schemes, etc.

In Chapter 7 we conclude the thesis and list potential topics for future research.

Chapter 2

System Model

In this chapter, we define the system model as well as the corresponding notations. More particularly, we introduce the scenario including the definitions of node and neighbor. The measurement model together with a ranging protocol is defined. The problem and system descriptions are raised at the end of this chapter.

2.1 Scenario Setup

We setup our scenario by defining nodes and neighbors.

Nodes

We consider a network with K BSs $(BS^1, \ldots, BS^K)$ and M MTs $(MT_1, \ldots, MT_M)$[1]. We use 2-dimensional coordinate vectors to indicate the location of *nodes* (BSs and MTs):

$$\text{BS:} \quad \vec{r}^{\,k} = [x^k, y^k]^T, \quad \forall k \in (1, \ldots, K) \tag{2.1}$$

$$\text{MT:} \quad \vec{r}_i \; = [x_i \, , y_i \,]^T, \quad \forall i \in (1, \ldots, M). \tag{2.2}$$

The position estimations of the MTs are denoted as:

$$\hat{\vec{r}}_i \; = [\hat{x}_i \, , \hat{y}_i \,]^T, \quad \forall i \in (1, \ldots, M). \tag{2.3}$$

Neighbors

For MT_i, any BS within a certain predefined communication range is considered as a neighboring BS:

$$k \in \mathbb{B}_i, \quad |\mathbb{B}_i| = K_i,^2 \quad \text{iff}^3 \quad d_i^k \leq R_i^k, \tag{2.4}$$

[1] In general, for better distinction we use superscript to indicate variables related to BS and subscript to MT.

[2] $|S|$ denotes the cardinality of the set S (number of the members).

[3] read as 'if and only if'.

where $d_i^k = \|\vec{r}_i - \vec{r}^k\|$ is the distance between BS^k and MT_i ($\|\cdot\|$ denotes the Euclidean norm), $\mathbb{B}_i$ is the index set of MT_i's neighboring BSs which contains K_i entities and R_i^k is the threshold of communication range. Similarly, we can define the neighboring MTs of MT_i as:

$$j \in \mathbb{M}_i, \quad |\mathbb{M}_i| = M_i, \quad \text{iff } d_{i,j} \leq R_{i,j}, \tag{2.5}$$

with the true distance $d_{i,j} = \|\vec{r}_i - \vec{r}_j\|$, the index set of neighboring MTs $\mathbb{M}_i$ with M_i entities, and the communication range threshold $R_{i,j}$.

Note: For better expression, in the remaining of the thesis we also use $x^{k(i)}$ to denote the quantity x referring to the k^{th} neighboring BS of MT_i and use $x_{j(i)}$ to denote the one referring to the j^{th} neighboring MT of MT_i.

2.2 Ranging

We mainly use TOA measurements for ranging. For simplicity we assume all the nodes are fully synchronized (i.e. there is no clock offset between nodes)[4]. The signals propagate with the speed of light ($c = 299792458$ m/s). In general, the ranging measurement: ρ [m] is the estimated propagation delay $\hat{\tau}$ [s] multiplied by c:

$$\begin{aligned} \rho &= \hat{\tau} \cdot c = (\tau + \varepsilon) \cdot c \\ &= \tau \cdot c + \varepsilon \cdot c = d + \eta, \end{aligned} \tag{2.6}$$

where d is the true distance (known as the geometric line-of-sight (GLOS) distance), $\tau \triangleq d/c$ is the expected delay, ε is the noise of the delay estimation and η is the corresponding ranging error. From Equation (2.6) we can see for TOA the ranging error is proportional to the delay estimation error.

Terrestrial ranging

For non-cooperative positioning, MT only do conventional BS-to-MT ranging with its neighboring BSs, which we call *terrestrial ranging*. We assume the range of $BS^{k(i)}$ to MT_i: $\rho_i^{k(i)}$ is the true distance $d_i^{k(i)}$ with some noise $\eta_i^{k(i)}$:

$$\rho_i^{k(i)} = d_i^{k(i)} + \eta_i^{k(i)} \tag{2.7}$$

Note: In some publications, 'terrestrial' may be used to describe all the ground-based positioning technique [15]. However in the remaining part of this thesis, unless stated otherwise it exclusively refers to the conventional BS-to-MT positioning schemes in order to distinct from cooperative ones.

[4]If the system is asynchronous, we can use RTD or TDOA for instead.

Cooperative ranging

For cooperative positioning, besides the terrestrial ranging, MTs also measure the distance from neighboring MTs via peer-to-peer links, called *cooperative ranging*:

$$\rho_{i,j(i)} = d_{i,j(i)} + \eta_{i,j(i)}, \tag{2.8}$$

where $\rho_{i,j(i)}$ and $\eta_{i,j(i)}$ indicate the ranging and the measurement noise for the $MT_{j(i)} \rightarrow MT_i$ link (measured by MT_i) respectively. In the simplest setup, all measurement noise can be assumed as independent additive white Gaussian noise (AWGN) with an identical variance σ^2 for each dimension:

$$\eta_i^{k(i)}, \eta_{i,j(i)} \sim \mathcal{N}(0, \sigma^2). \tag{2.9}$$

In a more realistic analysis like investigating the optimal resource allocation scheme for a real OFDM system, the noise variance normally depends on the link parameters, e.g. link length (i.e. d_i^k and $d_{i,j}$), occupied subcarriers, transmit power, shadowing, thermal noise, interference, etc.

Ranging protocol assumption

For a real system, due to the resource limitation and the security reason, maybe not all the MTs are willing to cooperate with others. The willingness to cooperate and the motivation of MTs could also be an interesting topic in this area. However, for simplicity, we assume all the nodes following a non-selfish ranging protocol: When a node receive a ranging request with specified resource if only the resource is available, it will agree to use this resource for the requested ranging link. If the resource is not available, it will reject the request and send back a notification. The ranging request can either come from a centralized coordinator, or from a neighboring MT directly.

2.3 System Setup

Problem description

BSs are synchronized, always know their location information perfectly and offer this information to MTs. On the contrary, an MT is not aware of its exact position. The goal of the system is to estimate MTs' positions as accurately as possible or with certain targeting accuracy: ϱ_i [m]. An MT collects other nodes' position information and measures distance to make an estimate based on some positioning algorithms. In the mean time, MTs also offer their own position estimates to each other. In general, BSs are stationary whereas MTs move with certain mobility model. Sometimes a BS can also move and lose its position reliability (e.g. WiFi access point, femtocell base station, etc.). In this case it will be considered as a special MT and adjusts

its own position information. Vice versa, when an MT has a very accurate location estimate, it also has the possibility to become a BS, helping others without affected by the error propagation.

System description

The system is modeled in a discrete time step sense to guarantee the fairness (i.e. all nodes are processing at the same time). The system runs in several stages, which are: initialization, communications, resource allocation, movement, measurement and position estimate. In the initialization stage, each node is initialized based on a certain assumption, which could be deterministically located with a predefined position or statistically distributed following certain distributions. Based on the application, the initial estimate can be the true position, the noisy position information or random values. In the communications stage, each of the nodes broadcasts a message which contains its location information as well as some control signal. The control signal could be the reliability of its own location information, the resource it occupied, the environment of its neighborhood, etc. The resource allocation stage begins after nodes receive the messages from neighbors. Resources will be allocated by the centralized coordinator or by the node itself individually based on certain allocation scheme. In the moving stage, each node moves to a new position with certain mobility model unless its mobility is defined as stationary. In the measurement stage, each node makes range measurements with certain metric(s). Then in a location estimate stage, a new position estimate can be obtained by combining the measurements and neighbors' position information which is read from the received messages. At the end, it goes back to the communications stage, where a node creates a new message with the new estimate and then broadcasts it again. The system moves to the next time step. A system flowchart can be seen in Figure 2.1.

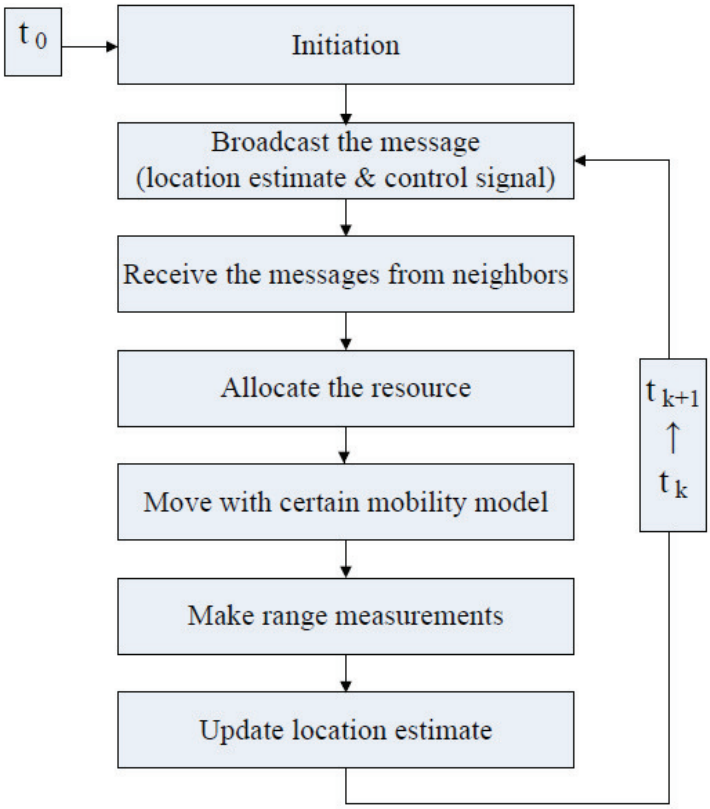

Figure 2.1: The flowchart of the system setup

Chapter 3

Distributed Cooperative Positioning Algorithms

In this chapter, two distributed cooperative positioning algorithms are introduced, namely distributed Gauss-Newton (GN) and distributed particle filter (PF). For the PF, a nature-inspired mobility model called Lévy-flight (LF) is introduced to improve the performance. In the second part of this chapter, a link evaluation scheme is raised to reduce the error propagation effect caused by cooperation.

3.1 Distributed Gauss-Newton (GN) Algorithm

The position can be estimated by a static approach, e.g. weighted non-linear least squares estimator and the non-linearity can be solved by numerical algorithms like Gauss-Newton[21], [22], [23].

For non-cooperative positioning, MT_i has K_i neighboring BSs $\left(BS^{1(i)}, \ldots, BS^{K_i(i)}\right)$, the position estimate $\hat{\vec{r}}_i$ is:

$$\hat{\vec{r}}_i = \arg\min_{\vec{r}_i'} \left((\rho_i^{\mathrm{BS}} + r_{\mathrm{pj},i}^{\mathrm{BS}} - H_{\mathrm{nc},i}\, \vec{r}_i^{\,\prime})^T C_{\mathrm{nc},\,i}^{-1} (\rho_i^{\mathrm{BS}} + r_{\mathrm{pj},i}^{\mathrm{BS}} - H_{\mathrm{nc},i}\, \vec{r}_i^{\,\prime}) \right) \tag{3.1}$$

where $H_{\mathrm{nc},i}$ is the non-cooperative geometric matrix:

$$H_{\mathrm{nc},i} \triangleq \begin{pmatrix} \frac{(\vec{r}_i - \vec{r}^{\,1(i)})^T}{d_i^{1(i)}} \\ \vdots \\ \frac{(\vec{r}_i - \vec{r}^{\,K_i(i)})^T}{d_i^{K_i(i)}} \end{pmatrix} = \begin{pmatrix} (\vec{e}_i^{\,1(i)})^T \\ \vdots \\ (\vec{e}_i^{\,K_i(i)})^T \end{pmatrix}, \tag{3.2}$$

$C_{\mathrm{nc},\,i}$ is the non-cooperative ranging noise covariance matrix, which is diagonal when

ranging errors from different links are uncorrelated:

$$C_{\mathrm{nc},\,i} = \begin{pmatrix} (\sigma_i^{1(i)})^2 & \cdots & 0 \\ 0 & \ddots & 0 \\ 0 & \cdots & (\sigma_i^{K_i(i)})^2 \end{pmatrix}, \tag{3.3}$$

The vector of terrestrial ranging measurements ρ_i^{BS} and a vector of position-to-link projections $r_{\mathrm{pj},i}^{\mathrm{BS}}$ are defined as:

$$\rho_i^{\mathrm{BS}} \triangleq \begin{pmatrix} \rho_i^{1(i)} \\ \vdots \\ \rho_i^{K_i(i)} \end{pmatrix}, \quad r_{\mathrm{pj},i}^{\mathrm{BS}} \triangleq \begin{pmatrix} (\vec{e}_i^{1(i)})^T \vec{r}^{1(i)} \\ \vdots \\ (\vec{e}_i^{K_i(i)})^T \vec{r}^{K_i(i)} \end{pmatrix}. \tag{3.4}$$

The solution of Equation 3.1 is:

$$\hat{\vec{r}}_i = (H_{\mathrm{nc},i}^T C_{\mathrm{nc},\,i}^{-1} H_{\mathrm{nc},i})^{-1} H_{\mathrm{nc},i}^T C_{\mathrm{nc},\,i}^{-1} (\rho_i^{\mathrm{BS}} + r_{\mathrm{pj},i}^{\mathrm{BS}}). \tag{3.5}$$

It is not linear because $H_{\mathrm{nc},i}$ contains $\vec{r}_i$ (Equation (3.2)). We set an initial guess for $\vec{r}_i$ and iteratively update $H_{\mathrm{nc},i}$ and then $\vec{r}_i$ to get the estimate. The term $(H_{\mathrm{nc},i}^T C_{\mathrm{nc},\,i}^{-1} H_{\mathrm{nc},i})^{-1}$ - denoted as weighted dilution of precision (WDOP) shows the variance of the positioning estimation.

For cooperative positioning, MT_i additionally uses M_i neighboring MTs and their position estimates $\hat{\vec{r}}_{j(i)}, j \in [1, \ldots, M_i]$ to locate itself. If we assume the estimates of neighboring MTs are the true positions without the estimation error, the solution of cooperative GN can be obtained by extending Equation (3.5):

$$\hat{\vec{r}}_i = (H_i^T C_i^{-1} H_i)^{-1} H_i^T C_i^{-1} (\rho_i + r_{\mathrm{pj},i}), \tag{3.6}$$

where the overall geometric matrix (H_i), covariance matrix (C_i), measurements vector (ρ_i) and projections vector ($r_{\mathrm{pj},i}$) can be obtained by extending the non-cooperative ones with the cooperative components:

$$H_i = \begin{pmatrix} H_{\mathrm{nc},i} \\ H_{\mathrm{c},i} \end{pmatrix}, \quad C_i = \begin{pmatrix} C_{\mathrm{nc},\,i} & 0 \\ 0 & C_{\mathrm{c},\,i} \end{pmatrix}, \tag{3.7}$$

$$\rho_i = \begin{pmatrix} \rho_i^{\mathrm{BS}} \\ \rho_{i,\mathrm{MT}} \end{pmatrix}, \quad r_{\mathrm{pj},i} = \begin{pmatrix} r_{\mathrm{pj},i}^{\mathrm{BS}} \\ r_{\mathrm{pj},i,\mathrm{MT}} \end{pmatrix}, \tag{3.8}$$

The cooperative components are defined as follow:

$$\text{Cooperative geometic matrix: } H_{\mathrm{c},i} \triangleq \begin{pmatrix} \frac{\left(\vec{r}_i - \hat{\vec{r}}_{1(i)}\right)^T}{d_{i,1(i)}} \\ \vdots \\ \frac{\left(\vec{r}_i - \hat{\vec{r}}_{M_i(i)}\right)^T}{d_{i,M_i(i)}} \end{pmatrix} = \begin{pmatrix} \left(\vec{e}_{i,1(i)}\right)^T \\ \vdots \\ \left(\vec{e}_{i,M_i(i)}\right)^T \end{pmatrix}, \quad (3.9)$$

$$\text{Cooperative covariance matrix: } C_{\mathrm{c},i} \triangleq \begin{pmatrix} \left(\sigma_{i,1(i)}\right)^2 & \cdots & 0 \\ 0 & \ddots & 0 \\ 0 & \cdots & \left(\sigma_{i,M_i(i)}\right)^2 \end{pmatrix}, \quad (3.10)$$

$$\text{Cooperative measurements vector: } \rho_{i,\mathrm{MT}} \triangleq \begin{pmatrix} \rho_{i,1(i)} \\ \vdots \\ \rho_{i,M_i(i)} \end{pmatrix}, \quad (3.11)$$

$$\text{Cooperative projections vector: } r_{\mathrm{pj},i,\mathrm{MT}} \triangleq \begin{pmatrix} \left(\vec{e}_{i,1(i)}\right)^T \hat{\vec{r}}_{1(i)} \\ \vdots \\ \left(\vec{e}_{i,M_i(i)}\right)^T \hat{\vec{r}}_{M_i(i)} \end{pmatrix}. \quad (3.12)$$

3.2 Distributed Particle Filter (PF) Algorithm

The positions of a MT are normally correlated in time. This time correlation is also known as the mobility model. By using the mobility model, the estimation's accuracy can be improved especially when the number of measurements is not sufficient. This kind of positioning is also referred to as *tracking*, which can be solved by the Particle Filter [24],[25]. The PF is a Monte Carlo (MC) method and directly works with the posterior probability density function (PDF). The main idea of the PF is creating many samples (particles) to approximate the posterior PDF in a discrete fashion. In general, the procedure of the PF can be divided into four stages:

1. Prediction: First moving all the particles according to their old states and the a priori state transformation function (also known as mobility model).

2. Weight update: Evaluating each particle based on the observation(s) and calculating the new weight to construct a quantized version of the posterior PDF approximation.

3. Estimation: The estimation can be obtained from the combination of all the particles (e.g. using the weighted mean).

4. Resampling: Discarding the particles with small weight and duplicating the ones with high weight. It is used to reduce effect of degeneracy, i.e. after several iterations, most of the particles have very small weights and hardly contribute to the estimate.

At the prediction stage, an appropriate mobility model could significantly reduce the complexity (by decreasing the sufficient number of particles). Meanwhile, it can also increase the robustness of the system. We use a novel nature-inspired mobility model for the PF which will be introduced in Subsection 3.2.1. The particles' weights can be calculated recursively from the overall posterior PDF function.

Note: We use $x_{[t]}$ to denote the quantity x referring to the time step t, $x_{[t_1:t_2]}$ to denote the collection of x from time step t_1 to time step t_2(inclusive) and $x^{\{p\}}$ to denote x referring to the p^{th} particle.

With the same cooperative setup as in Section 3.1, for MT_i the overall posterior PDF till time step t can be reformulated by Bayesian rule and Markov property as following:

$$\begin{aligned} p\left(\vec{r}_{i,[0:t]}|\rho_{i,[1:t]}\right) =& \frac{p\left(\rho_{i,[1:t-1]},\rho_{i,[t]},\vec{r}_{i,[0:t]}\right)}{p\left(\rho_{i,[1:t]}\right)} \\ =& \frac{p\left(\rho_{i,[t]}|\vec{r}_{i,[0:t]},\rho_{i,[1:t-1]}\right)\cdot p\left(\vec{r}_{i,[0:t]}|\rho_{i,[1:t-1]}\right)}{p\left(\rho_{i,[t]}|\rho_{i,[1:t-1]}\right)} \\ =& \frac{p\left(\rho_{i,[t]}|\vec{r}_{i,[0:t]},\rho_{i,[1:t-1]}\right)\cdot p\left(\vec{r}_{i,[t]}|\vec{r}_{i,[0:t-1]},\rho_{i,[1:t-1]}\right)}{p\left(\rho_{i,[t]}|\rho_{i,[1:t-1]}\right)} \\ & \cdot p\left(\vec{r}_{i,[0:t-1]}|\rho_{i,[1:t-1]}\right) \\ \propto & \underbrace{p\left(\rho_{i,[t]}|\vec{r}_{i,[t]}\right)}_{\text{likelihood function}}\cdot\underbrace{p\left(\vec{r}_{i,[t]}|\vec{r}_{i,[t-1]}\right)}_{\text{a priori function}}\cdot\underbrace{p\left(\vec{r}_{i,[0:t-1]}|\rho_{i,[1:t-1]}\right)}_{\text{posterior from last time step}}. \end{aligned} \tag{3.13}$$

We use N_p particles to recreate a discrete posterior approximation:

$$p\left(\vec{r}_{i,[0:t]}|\rho_{i,[1:t]}\right) \approx \sum_{p=1}^{N_p} w_{i,[t]}^{\{p\}}\cdot\delta\left(\vec{r}_{i,[0:t]}-\vec{r}_{i,[0:t]}^{\{p\}}\right), \tag{3.14}$$

where $\delta(\cdot)$ is the Dirac function, and $w_{i,[t]}^{\{p\}}$ is the weight of particle p at time step t:

$$w_{i,[t]}^{\{p\}} \propto \frac{p\left(\vec{r}_{i,[0:t]}^{\{p\}}|\rho_{i,[1:t]}\right)}{q\left(\vec{r}_{i,[0:t]}^{\{p\}}|\rho_{i,[1:t]}\right)}. \tag{3.15}$$

$q\left(\vec{r}_{i,[0:t]}^{\{p\}}|\rho_{i,[1:t]}\right)$ is a proposal importance density. Combining Equations (3.13), (3.14) and (3.15), the weight can be obtained recursively:

$$w_{i,[t]}^{\{p\}} \propto w_{i,[t-1]}^{\{p\}}\cdot\frac{p\left(\rho_{i,[t]}|\vec{r}_{i,[t]}^{\{p\}}\right)\cdot p\left(\vec{r}_{i,[t]}^{\{p\}}|\vec{r}_{i,[t-1]}^{\{p\}}\right)}{q\left(\vec{r}_{i,[t]}^{\{p\}}|\vec{r}_{i,[0:t-1]}^{\{p\}},\rho_{i,[t]}\right)}. \tag{3.16}$$

If we further set the proposal importance density equals to the a priori, i.e.:

$$q\left(\vec{r}_{i,[t]}^{\{p\}}|\vec{r}_{i,[0:t-1]}^{\{p\}},\rho_{i,[t]}\right) = p\left(\vec{r}_{i,[t]}^{\{p\}}|\vec{r}_{i,[t-1]}^{\{p\}}\right), \tag{3.17}$$

Equation (3.16) can be simplified as:

$$w_{i,[t]}^{\{p\}} \propto w_{i,[t-1]}^{\{p\}} \cdot p\left(\rho_{i,[t]}|\vec{r}_{i,[t]}^{\{p\}}\right). \tag{3.18}$$

The posterior at time step t can be approximated by:

$$p\left(\vec{r}_{i,[0:t]}|\rho_{i,[1:t]}\right) \approx \sum_{p=1}^{N_p} w_{i,[t]}^{\{p\}} \delta\left(\vec{r}_{i,[t]} - \vec{r}_{i,[t]}^{\{p\}}\right). \tag{3.19}$$

The position of MT_i can be estimated as the weighted mean of all the particles:

$$\hat{\vec{r}}_{i,[t]} = \sum_{p=1}^{N_p} w_{i,[t]}^{\{p\}} \cdot \vec{r}_{i,[t]}^{\{p\}}. \tag{3.20}$$

The likelihood function $p\left(\rho_{i,[t]}|\vec{r}_{i,[t]}^{\{p\}}\right)$ denotes how likely is the p^{th} particle observing all the measurements performed by MT_i. Assuming the measurements are independent from each other, $p\left(\rho_{i,[t]}|\vec{r}_{i,[t]}^{\{p\}}\right)$ can be written as a product of the individual likelihood functions:

$$p\left(\rho_{i,[t]}|\vec{r}_{i,[t]}^{\{p\}}\right) = \prod_{k=1(i)}^{K_i(i)} p\left(\rho_{i,[t]}^{k}|\vec{r}_{i,[t]}^{\{p\}}\right) \cdot \prod_{j=1(i)}^{M_i(i)} p\left(\rho_{i,j,[t]}|\vec{r}_{i,[t]}^{\{p\}}\right). \tag{3.21}$$

If the ranging noise is normally distributed, Equation (3.21) becomes:

$$\begin{aligned} p\left(\rho_{i,[t]}|\vec{r}_{i,[t]}^{\{p\}}\right) =& \frac{1}{(2\pi)^{(K_i(i)+M_i(i))/2}} \prod_{k=1(i)}^{K_i(i)} \frac{1}{\sigma_{i,[t]}^{k}} \exp\left(\frac{\left(\rho_{i,[t]}^{k} - \|\vec{r}_{i,[t]}^{\{p\}} - \vec{r}_{[t]}^{k}\|\right)^2}{2\left(\sigma_{i,[t]}^{k}\right)^2}\right) \\ & \cdot \prod_{j=1(i)}^{M_i(i)} \frac{1}{\sigma_{i,j,[t]}} \exp\left(\frac{\left(\rho_{i,j,[t]} - \|\vec{r}_{i,[t]}^{\{p\}} - \hat{\vec{r}}_{j,[t]}\|\right)^2}{2\left(\sigma_{i,j,[t]}\right)^2}\right). \end{aligned} \tag{3.22}$$

From Equation (3.13) we can see the PF takes all the former observations into account and directly works with the posterior PDF unlike GN.

3.2.1 A Nature-Inspired Mobility Model for Particle Filter

In this subsection, we introduce a nature-inspired mobility model called *Lévy-flight (LF)* and a modified version for the PF.

Lévy-Flight Mobility Model

LF is a nature-inspired mobility model. The pattern of this model can be widely observed in animal forging tracks like seabirds, jackals, spider monkey, shark, etc. [20].

Furthermore, it can describe the human movement behavior in numerous scenarios in a statistical sense [26]. Also known as Levy walk, it is based on the Levy distribution which models continuous non-negative random variables with the fat-tail-PDF property. Due to the fat-tail-PDF effect, the object's movement appears to be the combination of some short strolling with low speed and some long distance walk with relatively high velocity. For multi-objects, some of the objects will stay still or cruise locally while others may walk towards destinations far away. It is believed that this long walk interrupted by some short strolling model chosen by nature is very efficient for finding a target randomly located in the map.

The LF can be obtained as follow [26]:
Firstly the flight length L_f and the pause time t_p are generated with Levy distribution i.e. $L_f \sim \mathcal{L}(\mu_f, \ell_f)$ and $t_p \sim \mathcal{L}(\mu_p, \ell_p)$, where $x \sim \mathcal{L}(\mu, \ell)$ denotes the random variable x following the Levy distribution with the location factor μ and the scale factor ℓ. Secondly, the flying speed v_f corresponding to the flight length is calculated by $v_f = (L_f)^{a_v}/b_v$,where a_v is the exponential factor and b_v is the scale factor. With these two factor, the speed-distance relationship can be easily controlled. At last, we generate an uniform distributed flight direction φ_f i.e. $\varphi_f \sim \mathcal{U}[0, 2\pi]$, where $x \sim \mathcal{U}[a, b]$ denotes the random variable x is uniformly distributed in the interval $[a, b]$. An object moves in the direction φ_f with speed v_f until the moving length achieves L_f. It stays at that point for time t_p and then a new flight is generated. The pseudo code of generating a LF model can be found in Algorithm 1.

There are some other random mobility models which are commonly used like the random way point (RWP) and the white noise acceleration (WNA). For the RWP, the object moves to a randomly picked destination with a constant velocity. Then a new walk is triggered. For the WNA, at each time step, a zero-mean Gaussian distributed acceleration is generated to change the velocity [9]. The comparison of RWP, WNA and LF can be seen in Figure 3.1.

Algorithm 1 Generating a LF

$GenerateNewFlight = true$
for time step t **do**
  if $GenerateNewFlight == true$ **then**
    Generate a new flight:
    $L_f \sim \mathcal{L}(\mu_f, \ell_f)$
    $t_p \sim \mathcal{L}(\mu_p, \ell_p)$
    $\varphi_f \sim \mathcal{U}[0, 360]$
    $v_f = \frac{1}{b_v}(L_f)^{a_v}$
    $flight\_steps = \left\lceil \frac{L_f}{v_f} \right\rceil$
    $GenerateNewFlight = false$
  end if
  if $flight\_step \neq 0 \,\&\, t_p > 0$ **then**
    Flight:
    $\vec{r}_{[t]} = \vec{r}_{[t-1]} + T_{\text{step}} \begin{bmatrix} \cos\varphi_f \\ \sin\varphi_f \end{bmatrix} v_f$
    $flight\_steps - -$
  else if $flight\_step == 0 \,\&\, t_p > 0$ **then**
    Pause:
    $\vec{r}_{[t]} = \vec{r}_{[t-1]}$
    $t_p = t_p - T_{\text{step}}$
  else
    Trigger a new flight:
    $GenerateNewFlight = true$
  end if
end for

The initial coordinate $\vec{r}_0$ and the time step period T_{step} is known.

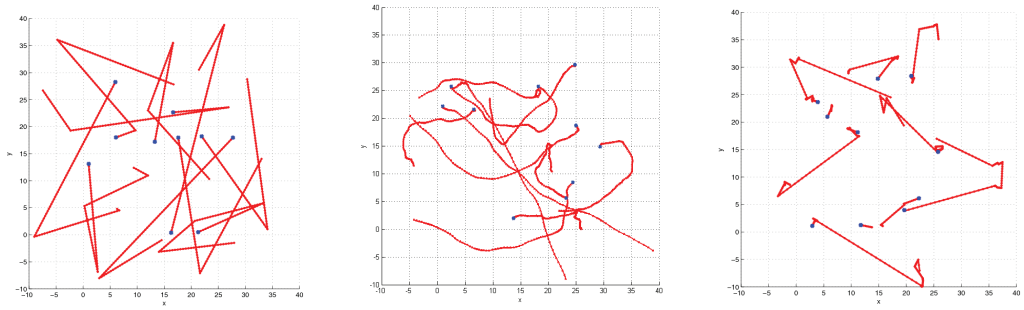

(a) RWP (b) WNA (c) LF

Figure 3.1: Tracks comparison of RWP, WNA and LF. 10 objects move for 100 time steps.

Levy-Flight Based Mobility Model for Particle Filter

In Artificial Intelligence (AI), researchers have already tried to apply LF for searching the global optimum. For example, in [20], LF is applied for a new proposed swarm intelligent searching algorithm called Cuckoo Search. There are some similarities between particle filter and swarm intelligence. For example both of them are based on evaluating many samples. Therefore, for the prediction stage of PF, we create several LF based mobility model for the PF namely *Modified Levy Flight (MLF)*, *Levy Track (LT)* and *Modified Levy Flight and Levy Track (MLF_LT)*. For the MLF, instead of moving forward to achieve the Levy distributed flight length, a new flight direction and velocity are generated similar as Algorithm 1 for each particle at each time step. For LT, we additionally take the previous estimated node velocity (difference between two previous position estimates) into account. The whole particle cloud firstly moves together with the old estimated velocity, then spreads similarly as in MLF. It allows particles to online-update the velocity knowledge which brings a significant gain when the node moving straightforward with stable speed. However when the node suddenly changes the direction, it will take longer time for particle cloud to catch up, or even worse, it may lose the track. At the end, we split the particle could into two parts, the first part moves with MLF and the latter one moves with LT. It combines the advantages of both and we call it MLF_LT. The pseudo codes of the MLF and MLF_LT can be found in Algorithm 2. The particle clouds with the WNA, MLF and MLF_LT are shown in Figure 3.2. We can see that with the MLF and MLF_LT the main particle clouds concentrate on the believed crucial area while a few particles explore in a wider region. Comparing the MLF_LT with the MLF, the first one has two clouds which will be more robust for both the cases of moving straightforward and changing the direction.

Algorithm 2 LF based mobility model for the PF

for time step t **do**
  for particle p **do**
    $L_f^{\{p\}} \sim \mathcal{L}(\mu_f, \ell_f)$
    $\varphi_f^{\{p\}} \sim \mathcal{U}[0, 360]$
    $v_f^{\{p\}} = \frac{1}{b_v}(L_f^{\{p\}})^{a_v}$
    if $model == MLF$ **then**

$$\vec{r}_{[t]}^{\{p\}} = \vec{r}_{[t-1]}^{\{p\}} + T_{\text{step}} \begin{bmatrix} \cos\varphi_f^{\{p\}} \\ \sin\varphi_f^{\{p\}} \end{bmatrix} v_f^{\{p\}}$$

    else if $model == LT$ **then**

$$\vec{r}_{[t]}^{\{p\}} = \vec{r}_{[t-1]}^{\{p\}} + T_{\text{step}} \begin{bmatrix} \cos\varphi_f^{\{p\}} \\ \sin\varphi_f^{\{p\}} \end{bmatrix} v_f^{\{p\}} + T_{\text{step}} \hat{\vec{v}}_{[t-1]}$$

    else if $model == MLF\_LT$ **then**
      if $j \in$ first half of the particles **then**

$$\vec{r}_{[t]}^{\{p\}} = \vec{r}_{[t-1]}^{\{p\}} + T_{\text{step}} \begin{bmatrix} \cos\varphi_f^{\{p\}} \\ \sin\varphi_f^{\{p\}} \end{bmatrix} v_f^{\{p\}}$$

      else

$$\vec{r}_{[t]}^{\{p\}} = \vec{r}_{[t-1]}^{\{p\}} + T_{\text{step}} \begin{bmatrix} \cos\theta_f^{\{p\}} \\ \sin\theta_f^{\{p\}} \end{bmatrix} v_f^{\{p\}} + T_{\text{step}} \hat{\vec{v}}_{[t-1]}$$

      end if
    end if
  end for
  $\hat{\vec{v}}_t = \frac{1}{T_{\text{step}}}(\hat{\vec{r}}_{[t]} - \hat{\vec{r}}_{[t-1]})$
end for

$\hat{\vec{r}}_{[t]}$ is the coordinate estimate of the **node** at the step t feeded from the estimation stage of the PF (Equation (3.20)). $\hat{\vec{v}}_{[t]}$ is the **node**'s velocity estimate.

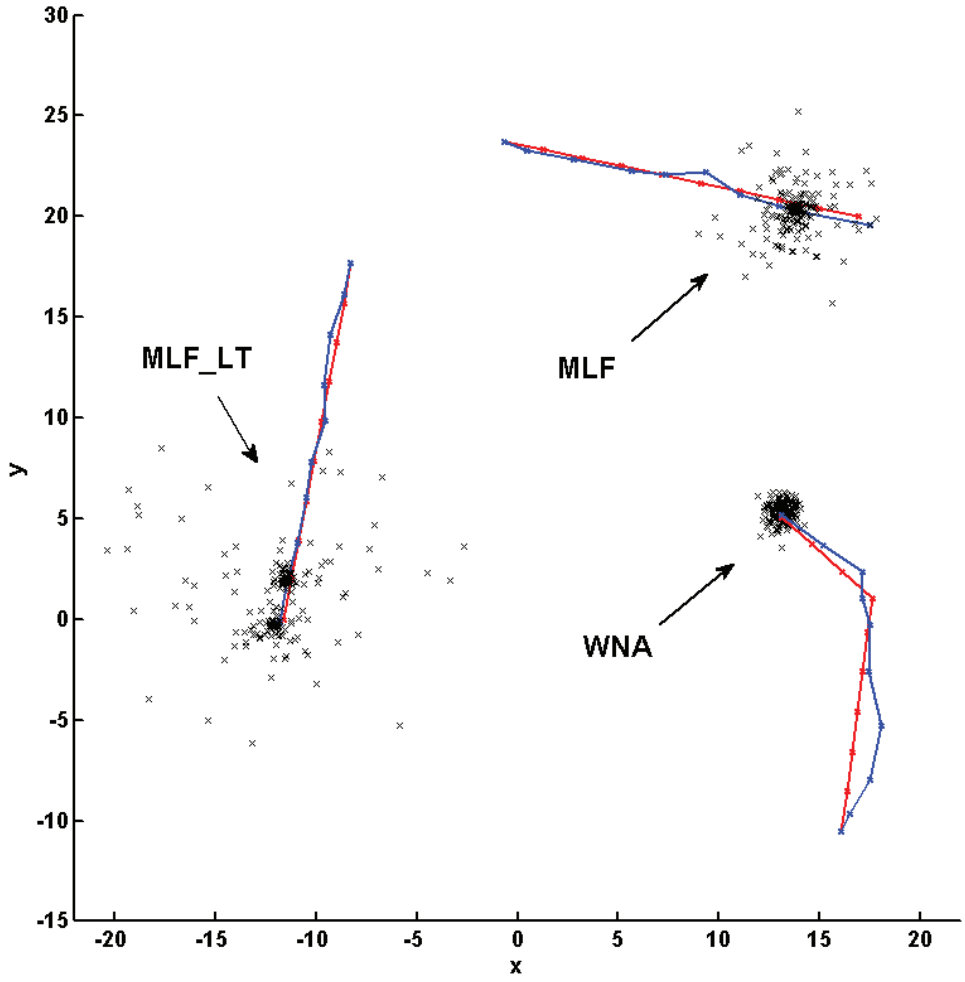

Figure 3.2: The particle clouds of WNA, MLF and MLF_LT: the red curves are the tracks connecting the true positions, whereas the blue ones are the tracks connecting the estimates.

3.3 Link Evaluation

For cooperative positioning the MTs' position estimates are exchanged, which leads to the effect of error propagation. There are ways to reduce this effect, e.g. belief propagation [17], [18], information discarding [19], etc. Another approach is to weight the ranging links differently. In [16] a link is weighted by its type (BS-to-MT link or peer-to-peer link). In this section, we first introduce a weighting scheme similar as in [16], which differs the links by their types. Then a rational link evaluation scheme with low complexity is proposed.

3.3.1 Weighting by Type

The error is only propagated through the peer-to-peer links. Therefore, it is reasonable to trust the cooperative ranging less than the terrestrial ranging. We define a confidence factor $\beta \in (0, 1]$. For the cooperative link $MT_j \to MT_i$, instead of using the true ranging variance $(\sigma_{i,j})^2$ for estimation, we use a weighted variance $(\tilde{\sigma}_{i,j})^2$:

$$(\tilde{\sigma}_{i,j})^2 = \frac{1}{\beta} \cdot (\sigma_{i,j})^2. \tag{3.23}$$

$\beta = 1$ denotes trusting both the cooperative and terrestrial link equally, whereas $\beta \to 0$ means totally distrusting the cooperative links (equivalent to non-cooperative positioning). A simulation result can be found in Figure 3.3. We can see that the performance is sensitive to the confidence factor. Weighting the cooperative links with an appropriate confidence factor can bring some improvement, however assigning an inappropriate one may even decrease the accuracy. A reasonable confidence factor could be obtained from experience or some online learning algorithm.

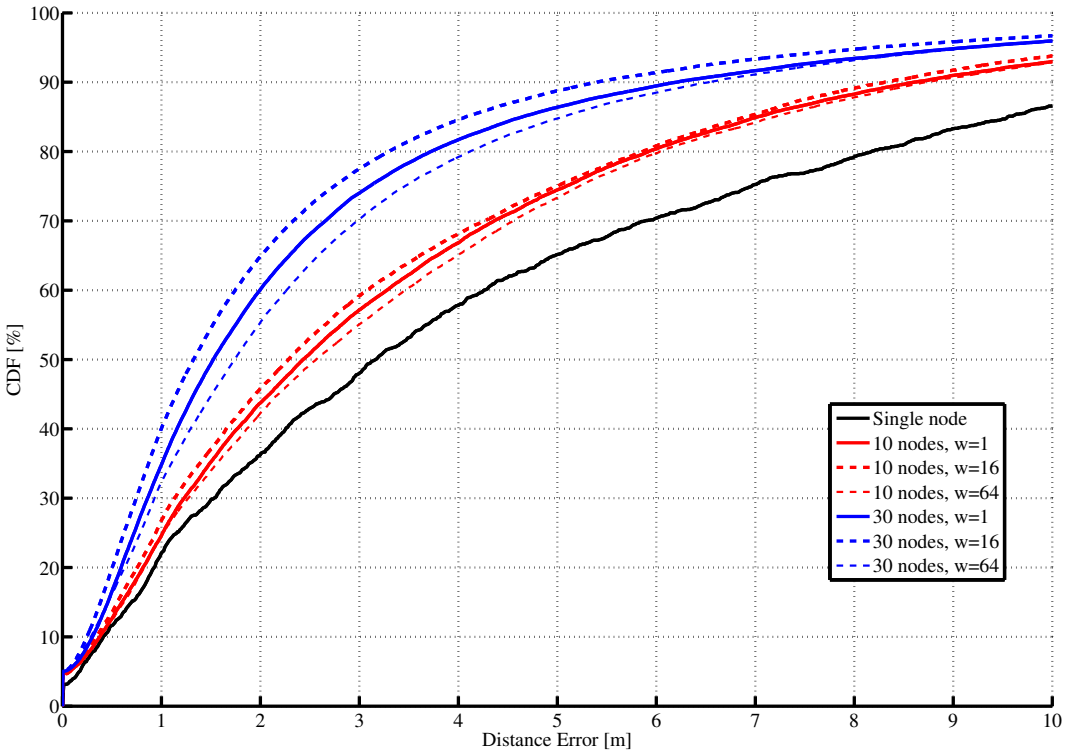

Figure 3.3: Simulation result of using the link type to weight. 9 MTs are uniformly located in a 30×30 map, the ranging variances of all the links are set to 0.09 m^2. The communication range is 7 m

3.3.2 Rational Weighting

If we additionally know the accuracy of the neighbors' estimations, a more rational weighting scheme can be found. For peer-to-peer link $MT_j \rightarrow MT_i$, we assume the ranging measurement error and the MT_j's estimation error in each dimension are normally distributed with known variances, i.e.:

$$\begin{aligned} \hat{x}_j &= x_j + \epsilon_{j_x}, \quad \epsilon_{j_x} \sim \mathcal{N}(0, \sigma_{j_x}^2), \\ \hat{y}_j &= y_j + \epsilon_{j_y}, \quad \epsilon_{j_y} \sim \mathcal{N}(0, \sigma_{j_y}^2), \\ \rho_{i,j} &= d_{i,j} + \eta_{i,j}, \quad \eta_{i,j} \sim \mathcal{N}(0, \sigma_{i,j}^2). \end{aligned} \tag{3.24}$$

We combine M_j's estimation variance with the ranging variance to get an equivalent ranging variance, i.e.:

$$\tilde{\sigma}_{i,j}^2 = f(\sigma_{j_x}^2, \sigma_{j_y}^2, \sigma_{i,j}^2). \tag{3.25}$$

The equivalent ranging variances can be used to replace the true ones in the positioning algorithms. By doing so, we can consider the M_j's estimation as the position without noise, but the ranging measurements are less reliable. It transfers the cooperative positioning problem into an equivalent non-cooperative positioning one without losing the information of the estimations' inaccuracy of neighboring MTs. The equivalent ranging variance $(\tilde{\sigma}_{i,j})^2$ can be derived as follow:

$$\begin{aligned} \rho_{i,j} =& \sqrt{(x_i - x_j)^2 + (y_i - y_j)^2} + \eta_{i,j} \\ =& \sqrt{(x_i - \hat{x}_j + \epsilon_{j_x})^2 + (y_i - \hat{y}_j + \epsilon_{j_y})^2} + \eta_{i,j}, \end{aligned} \tag{3.26}$$

and

$$\triangle \hat{x}_{i,j} \triangleq x_i - \hat{x}_j, \quad \triangle \hat{y}_{i,j} \triangleq y_i - \hat{y}_j, \quad \hat{d}_{i,j} \triangleq \sqrt{(x_i - \hat{x}_j)^2 + (y_i - \hat{y}_j)^2}. \tag{3.27}$$

The equivalent ranging variance states:

$$
\begin{aligned}
(\tilde{\sigma}_{i,j})^2 &= \mathcal{E}\left[(\rho_{i,j} - \hat{d}_{i,j})^2\right] \\
&= \mathcal{E}\left[\left(\sqrt{(\triangle\ \hat{x}_{i,j} + \epsilon_{j_x})^2 + (\triangle\ \hat{y}_{i,j} + \epsilon_{j_y})^2} + \eta_{i,j} - \sqrt{\triangle\ \hat{x}_{i,j}^2 + \triangle\ \hat{y}_{i,j}^2}\right)^2\right] \\
&= \mathcal{E}\left[(\triangle\ \hat{x}_{i,j} + \epsilon_{j_x})^2 + (\triangle\ \hat{y}_{i,j} + \epsilon_{j_y})^2 + \hat{d}_{i,j}^2 + \eta_{i,j}^2\right] \\
&\quad + \underbrace{\mathcal{E}\left[2\eta_{i,j}\sqrt{(\triangle\ \hat{x}_{i,j} + \epsilon_{j_x})^2 + (\triangle\ \hat{y}_{i,j} + \epsilon_{j_y})^2}\right]}_{=0} - \underbrace{\mathcal{E}\left[2\hat{d}_{i,j}\eta_{i,j}\right]}_{=0} \\
&\quad - \mathcal{E}\left[\underbrace{2\hat{d}_{i,j}\sqrt{(\triangle\ \hat{x}_{i,j} + \epsilon_{j_x})^2 + (\triangle\ \hat{y}_{i,j} + \epsilon_{j_y})^2}}_{\triangleq g(\epsilon_{j_x}, \epsilon_{j_y})}\right] \\
&= \mathcal{E}\left[\epsilon_{j_x}^2\right] + \mathcal{E}\left[\epsilon_{j_y}^2\right] + \mathcal{E}\left[\eta_{i,j}^2\right] + 2\mathcal{E}\left[\hat{d}_{i,j}^2\right] + 2\mathcal{E}\left[\triangle\ \hat{x}_{i,j}\epsilon_{j_x}\right] + 2\mathcal{E}\left[\triangle\ \hat{y}_{i,j}\epsilon_{j_y}\right] \\
&\quad - \mathcal{E}\left[g(\epsilon_{j_x}, \epsilon_{j_y})\right] \\
&= \sigma_{j_x}^2 + \sigma_{j_y}^2 + (\sigma_{i,j})^2 + 2\mathcal{E}\left[\hat{d}_{i,j}^2\right] + 2\mathcal{E}\left[\triangle\ \hat{x}_{i,j}\epsilon_{j_x}\right] + 2\mathcal{E}\left[\triangle\ \hat{y}_{i,j}\epsilon_{j_y}\right] \\
&\quad - \mathcal{E}\left[g(\epsilon_{j_x}, \epsilon_{j_y})\right].
\end{aligned} \tag{3.28}
$$

$g(\epsilon_{j_x}, \epsilon_{j_y})$ can be polynomialized by taking the two variables Maclaurin expansion:

$$
\begin{aligned}
g(\epsilon_{j_x}, \epsilon_{j_y}) &= g(0,0) + \epsilon_{j_x}\frac{\partial g(0,0)}{\partial \epsilon_{j_x}} + \epsilon_{j_y}\frac{\partial g(0,0)}{\partial \epsilon_{j_y}} \\
&\quad + \frac{1}{2!}\left(\epsilon_{j_x}^2\frac{\partial^2 g(0,0)}{\partial \epsilon_{j_x}^2} + 2\epsilon_{j_x}\epsilon_{j_y}\frac{\partial^2 g(0,0)}{\partial \epsilon_{j_x}\partial \epsilon_{j_y}} + \epsilon_{j_y}^2\frac{\partial^2 g(0,0)}{\partial \epsilon_{j_y}^2}\right) + \cdots
\end{aligned} \tag{3.29}
$$

$g(\epsilon_{j_x}, \epsilon_{j_y})$ can be approximated by the fist order expansion:

$$
\begin{aligned}
g(\epsilon_{j_x}, \epsilon_{j_y}) &\approx g(0,0) + \epsilon_{j_x}\frac{\partial g(0,0)}{\partial \epsilon_{j_x}} + \epsilon_{j_y}\frac{\partial g(0,0)}{\partial \epsilon_{j_y}} \\
&= 2\hat{d}_{i,j}^2 + 2\ \triangle\ \hat{x}_{i,j}\epsilon_{j_x} + 2\ \triangle\ \hat{y}_{i,j}\epsilon_{j_y}.
\end{aligned} \tag{3.30}
$$

Inserting Equation (3.30) into Equation (3.28):

$$
\begin{aligned}
(\tilde{\sigma}_{i,j})^2 &\approx (\tilde{\sigma}_{i,j})_{1^{\text{st}}}^2 \\
&= (\sigma_{i,j})^2 + \sigma_{j_x}^2 + \sigma_{j_y}^2.
\end{aligned} \tag{3.31}
$$

If we approximate $g(\epsilon_{j_x}, \epsilon_{j_y})$ with the second order expansion, the equivalent ranging variance becomes:

$$\begin{aligned}(\tilde{\sigma}_{i,j})^2 &\approx (\tilde{\sigma}_{i,j})^2_{2^{\text{nd}}} \\ &= (\sigma_{i,j})^2 + \sigma^2_{j_x} + \sigma^2_{j_y} - \mathcal{E}\left[\frac{1}{2!}(\epsilon^2_{j_x}\frac{\partial^2 g(0,0)}{\partial \epsilon^2_{j_x}} + 2\epsilon_{j_x}\epsilon_{j_y}\frac{\partial^2 g(0,0)}{\partial \epsilon_{j_x}\partial \epsilon_{j_y}} + \epsilon^2_{j_y}\frac{\partial^2 g(0,0)}{\partial \epsilon^2_{j_y}})\right] \\ &= \sigma^2_{i,j} + \sigma^2_{j_x} + \sigma^2_{j_y} - \mathcal{E}\left[\epsilon^2_{j_x}\frac{\triangle\, \hat{y}^2_{i,j}}{\hat{d}^2_{i,j}} + \epsilon^2_{j_y}\frac{\triangle\, \hat{x}^2_{i,j}}{\hat{d}^2_{i,j}} - 2\epsilon_{j_x}\epsilon_{j_y}\frac{\triangle\, \hat{x}_{i,j}\, \triangle\, \hat{y}_{i,j}}{\hat{d}^2_{i,j}}\right]. \quad (3.32)\end{aligned}$$

With $\hat{\theta}_{i,j} \triangleq \text{angle}\left(\vec{r}_i - \hat{\vec{r}}_j\right)$, [1] the last term of Equation (3.32) can be reformulated as:

$$\begin{aligned}&\mathcal{E}\left[\epsilon^2_{j_x}\frac{\triangle\, \hat{y}^2_{i,j}}{\hat{d}^2_{i,j}} + \epsilon^2_{j_y}\frac{\triangle\, \hat{x}^2_{i,j}}{\hat{d}^2_{i,j}} - 2\epsilon_{j_x}\epsilon_{j_y}\frac{\triangle\, \hat{x}_{i,j}\, \triangle\, \hat{y}_{i,j}}{\hat{d}^2_{i,j}}\right] \\ &= \mathcal{E}\left[\epsilon^2_{j_x}\sin^2\hat{\theta}_{i,j} + \epsilon^2_{j_y}\cos^2\hat{\theta}_{i,j} - 2\epsilon_{j_x}\epsilon_{j_y}\sin\hat{\theta}_{i,j}\cos\hat{\theta}_{i,j}\right]\end{aligned} \quad (3.33)$$

If we consider $\hat{\theta}_{i,j}$ as the observation, Equation (3.33) can be written as:

$$\begin{aligned}&\mathcal{E}\left[\epsilon^2_{j_x}\frac{\triangle\, \hat{y}^2_{i,j}}{\hat{d}^2_{i,j}} + \epsilon^2_{j_y}\frac{\triangle\, \hat{x}^2_{i,j}}{\hat{d}^2_{i,j}} - 2\epsilon_{j_x}\epsilon_{j_y}\frac{\triangle\, \hat{x}_{i,j}\, \triangle\, \hat{y}_{i,j}}{\hat{d}^2_{i,j}}\right] \\ &= \sin^2\hat{\theta}_{i,j}\mathcal{E}\left[\epsilon^2_{j_x}\right] + \cos^2\hat{\theta}_{i,j}\mathcal{E}\left[\epsilon^2_{j_y}\right] - 2\sin\hat{\theta}_{i,j}\cos\hat{\theta}_{i,j}\mathcal{E}\left[\epsilon_{j_x}\epsilon_{j_y}\right] \\ &= \sin^2\hat{\theta}_{i,j}\sigma^2_{j_x} + \cos^2\hat{\theta}_{i,j}\sigma^2_{j_y} - 2\sin\hat{\theta}_{i,j}\cos\hat{\theta}_{i,j}\mathcal{E}\left[\epsilon_{j_x}\right]\mathcal{E}\left[\epsilon_{j_y}\right] \\ &= \sin^2\hat{\theta}_{i,j}\sigma^2_{j_x} + \cos^2\hat{\theta}_{i,j}\sigma^2_{j_y}. \quad (3.34)\end{aligned}$$

The equivalent ranging variance can be approximated as:

$$(\tilde{\sigma}_{i,j})^2 \approx (\sigma_{i,j})^2 + \cos^2\hat{\theta}_{i,j}\sigma^2_{j_x} + \sin^2\hat{\theta}_{i,j}\sigma^2_{j_y}. \quad (3.35)$$

In a cooperative positioning system, $\hat{\theta}_{i,j}$ can be estimated by the old location estimate. Another way to estimate $\hat{\theta}_{i,j}$ is getting a rough location estimate at first.

If there is no a priori knowledge of $\hat{\theta}_{i,j}$, we further define $\cos\phi \triangleq \frac{\epsilon_{j_x}}{\sqrt{\epsilon^2_{j_x}+\epsilon^2_{j_y}}}$,

[1] angle$(\cdot)$ denotes the angle of a vector, w.r.t the x axis.

Equation (3.33) can then be reformulated as:

$$\begin{aligned}
&\mathcal{E}\left[\epsilon_{j_x}^2 \frac{\triangle \hat{y}_{i,j}^2}{\hat{d}_{i,j}^2} + \epsilon_{j_y}^2 \frac{\triangle \hat{x}_{i,j}^2}{\hat{d}_{i,j}^2} - 2\epsilon_{j_x}\epsilon_{j_y} \frac{\triangle \hat{x}_{i,j} \triangle \hat{y}_{i,j}}{\hat{d}_{i,j}^2}\right] \\
&= \mathcal{E}\left[(\epsilon_{j_x} \sin\hat{\theta}_{i,j} - \epsilon_{j_y} \cos\hat{\theta}_{i,j})^2\right] \\
&= \mathcal{E}\left[(\epsilon_{j_x}^2 + \epsilon_{j_y}^2)(\cos\phi \sin\hat{\theta}_{i,j} - \sin\phi \cos\hat{\theta}_{i,j})^2\right] \\
&= \mathcal{E}\left[(\epsilon_{j_x}^2 + \epsilon_{j_y}^2) \sin^2(\hat{\theta}_{i,j} - \phi)\right] \\
&\leq \mathcal{E}\left[(\epsilon_{j_x}^2 + \epsilon_{j_y}^2)\right] \\
&= \sigma_{j_x}^2 + \sigma_{j_y}^2.
\end{aligned} \tag{3.36}$$

Because $\mathcal{E}\left[(\epsilon_{j_x} \sin\hat{\theta}_{i,j} - \epsilon_{j_y} \cos\hat{\theta}_{i,j})^2\right] \geq 0$ we can obtain:

$$\mathcal{E}\left[\epsilon_{j_x}^2 \frac{\triangle \hat{y}_{i,j}^2}{\hat{d}_{i,j}^2} + \epsilon_{j_y}^2 \frac{\triangle \hat{x}_{i,j}^2}{\hat{d}_{i,j}^2} - 2\epsilon_{j_x}\epsilon_{j_y} \frac{\triangle \hat{x}_{i,j} \triangle \hat{y}_{i,j}}{\hat{d}_{i,j}^2}\right] \geq 0. \tag{3.37}$$

Combining Equation (3.32), (3.36) and (3.37), the second order expanded equivalent ranging variance can be constrained by:

$$(\tilde{\sigma}_{i,j,\text{low}})^2 \leq (\tilde{\sigma}_{i,j})_{2^{\text{nd}}}^2 \leq (\tilde{\sigma}_{i,j,\text{up}})^2, \tag{3.38}$$

where

$$(\tilde{\sigma}_{i,j,\text{low}})^2 = \sigma_{i,j}^2 \tag{3.39}$$

and

$$(\tilde{\sigma}_{i,j,\text{up}})^2 = \sigma_{i,j}^2 + \sigma_{j_x}^2 + \sigma_{j_y}^2. \tag{3.40}$$

Then $(\tilde{\sigma}_{i,j})_{2^{\text{nd}}}^2$ can be described as:

$$(\tilde{\sigma}_{i,j})_{2^{\text{nd}}}^2 = \sigma_{i,j}^2 + \kappa_x \sigma_{j_x}^2 + \kappa_y \sigma_{j_y}^2, \tag{3.41}$$

where $\kappa_x, \kappa_y \in [0, 1]$. From Equation (3.35) we can see κ_x and κ_y are the estimated angle information and have the relationship as $\kappa_x + \kappa_y = 1$. If the estimated angle information is not available we use the average: $\kappa_x = \kappa_y = 1/2$. Then $(\tilde{\sigma}_{i,j})^2$ becomes:

$$(\tilde{\sigma}_{i,j})^2 \approx (\sigma_{i,j})^2 + \frac{1}{2}(\sigma_{j_x}^2 + \sigma_{j_y}^2). \tag{3.42}$$

A comparison of the true variance, the first order expansion, the second order expansions with and without the angle information can be found in Figure 3.4 - 3.6. It shows that, for the small location variances, the performances are similar. When the location variances are large, the second order expansions are much closer to the real variance. When the location variances of different dimensions are changing, the second order expansion with the angle information out performs the other two.

With the equivalent ranging variance, MT is able to work with only local information. The error propagation effect is reduced which improves the performance of distributed cooperative positioning algorithms. It can also be used to fuse the mobility information, i.e. if the variance of neighbor's mobility is also known, it is straightforward to get an equivalent ranging variance combining the uncertainty of ranging, neighbors' estimate and neighbors' movement. The link evaluation scheme raised in this section can be also used in other place. In Chapter 4 the link evaluation scheme helps MT approximating a lower bound of the estimation variance locally with only a limited amount of communications. In Chapter 5, the link evaluation scheme is one of the essential factors to control the resource allocation schemes. The derivation of the equivalent variance is based on the assumption of knowing the neighbors' position estimation variance and the ranging variance which are statistic features and cannot be extracted without massive samples. Meanwhile, online learning the variances by massive observations may not fulfill the real time requirement. In next chapter, we will introduce a theoretical bound for these variances which can be used to substitute the real variances.

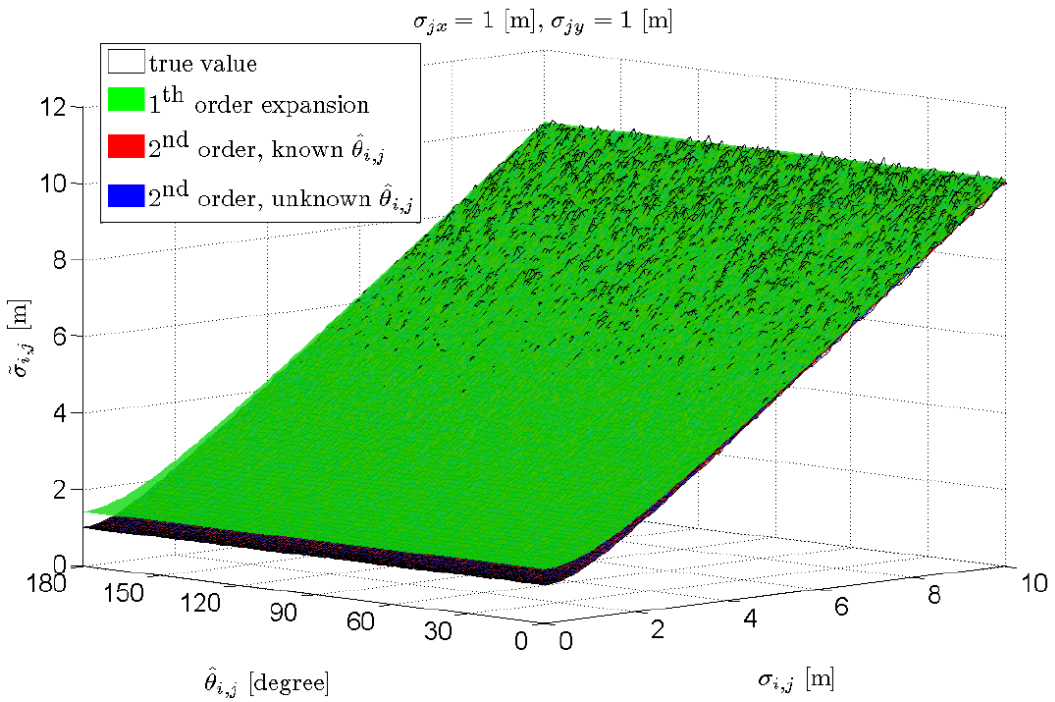

Figure 3.4: The comparison of the true variance (black net), the first order expansion (green), the second order expansions without the angle information (blue) and the second order expansions with the angle information (red). The estimation variances in both dimensions are equally low ($\sigma_{jx} = 1$ m, $\sigma_{jy} = 1$ m). The blue and red faces almost overlap with the black net therefore they are difficult to be distinguished. For the symmetric low estimation variances, all three expansions can approximate the true equivalent variance well.

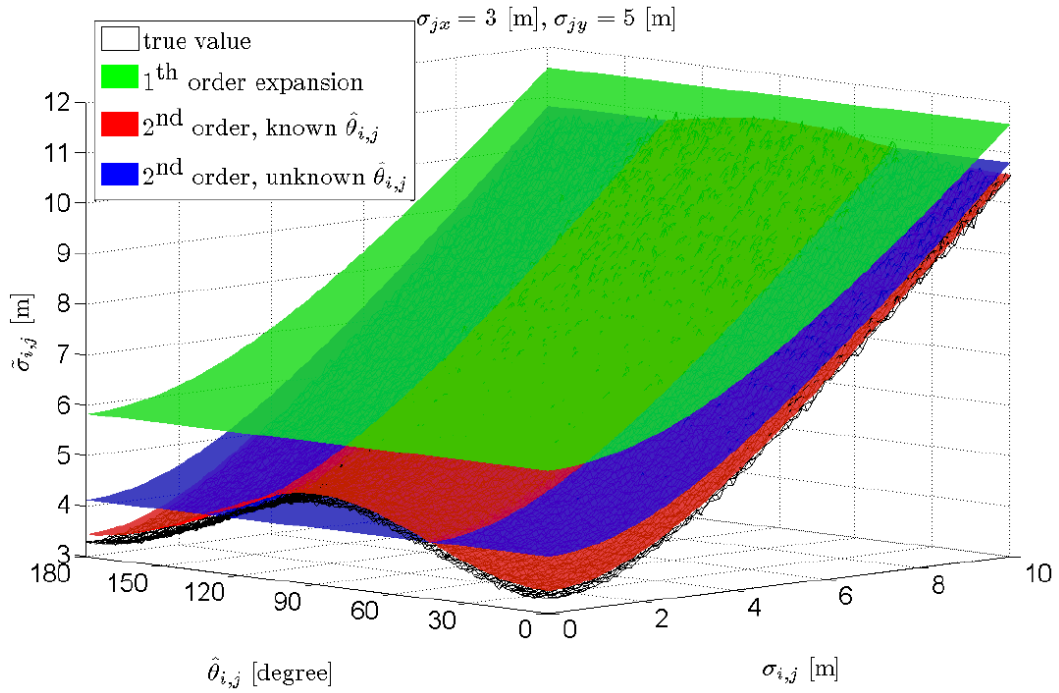

Figure 3.5: The comparison of the true variance (black net), the first order expansion (green), the second order expansions without the angle information (blue) and the second order expansions with the angle information (red). The estimation variances in different dimensions are different ($\sigma_{jx} = 3$ m, $\sigma_{jy} = 5$ m). For the asymmetric estimation variances, the true value is fluctuating according to the observed angle. The red one is also fluctuating and tightly above the true value. The blue value is the average of the true value. The green one is loosely above the true one.

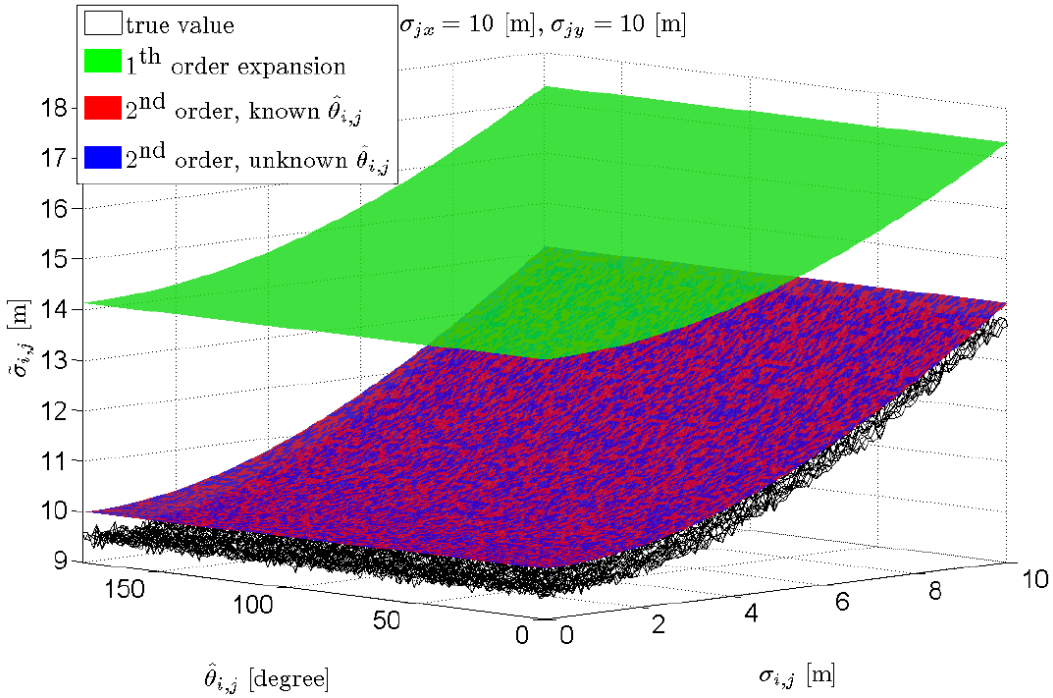

Figure 3.6: The comparison of the true variance (black net), the first order expansion (green), the second order expansions without the angle information (blue) and the second order expansions with the angle information (red). The estimation variances in both dimensions are equally large ($\sigma_{jx} = 10$ m, $\sigma_{jy} = 10$ m). For the symmetric high estimation variances, the first order expansion is too loose. Whereas two second order expansions are exactly overlap and tightly above the true value. In the case, there is a significant benefit of using the second order expansions.

Chapter 4

Cramér-Rao Lower Bound(CRLB) for Ranging and Positioning

In this chapter, we investigate a mathematical tool named Cramér-Rao lower bound (CRLB). The CRLB expresses the lower bound of the variance of any estimation. It was firstly derived by Harald Cramér [27] and Calyampudi Radhakrishna Rao [28]. In the first section, the fundamentals of the CRLB are presented. Then the CRLBs for both non-cooperative and cooperative positioning with independent ranging noise are derived in Section 4.2. We look into the real system deriving the CRLB of delay estimation using the OFDM signal. Then the new positioning CRLBs with the OFDM signals are stated. At the end of this chapter, a local CRLB approximation is introduced with the link evaluation scheme from the previous chapter. For positioning, the CRLB is often used to evaluate the performance of location estimators. In next chapter we propose several novel resource allocation schemes which use the CRLBs introduced in this chapter as a part of the utility functions.

4.1 The Fundamentals of CRLB

In [22] Kay derived several kinds of CRLBs:

For a scalar parameter:

For an unbiased estimator, the parameter α is estimated with the observation g, i.e. $\alpha \approx \hat{\alpha}(g)$. The CRLB theorem states :

$$\mathrm{var}[\hat{\alpha}(g)] \geq \mathrm{CRLB}[\alpha] = \frac{1}{\mathcal{E}\left[|\frac{d}{d\alpha}\ln p(g|\alpha)|^2\right]}. \tag{4.1}$$

An alternative expression states:

$$\text{var}[\hat{\alpha}(g)] \geq \text{CRLB}[\alpha] = \frac{1}{-\mathcal{E}\left[\frac{d^2}{d\alpha^2}\ln p(g|\alpha)\right]}. \tag{4.2}$$

For a scalar parameter and the complex observations with Gaussian noise:

If a scalar parameter α is estimated by m complex observations g_i with Gaussian noise:

$$g_i = \mu_i(\alpha) + n_i, \quad i \in [1, \ldots, m], \quad \mathcal{E}[|n_i|^2] = \sigma^2, \tag{4.3}$$

where $|\cdot|$ denotes the magnitude of a complex number. the CRLB states:

$$\text{var}[\hat{\alpha}(g)] \geq \text{CRLB}[\alpha] = \frac{\sigma^2}{2\sum_{i=1}^{m}|\frac{d}{d\alpha}\mu_i(\alpha)|^2}, \tag{4.4}$$

For multiple parameters:

For multiple parameters $\alpha = [\alpha_1, \ldots, \alpha_N]^T$, the CRLB can be extended as a matrix:

$$\text{CRLB}[\alpha] = J[\alpha]^{-1}, \tag{4.5}$$

where $J[\alpha]$ is called Fischer Information Matrix (FIM). The entity of $J[\alpha]$ is defined as:

$$J[\alpha]_{i,j} = -\mathcal{E}\left[\frac{\partial^2}{\partial\alpha_i\partial\alpha_j}\ln p(g|\alpha)\right]. \tag{4.6}$$

The variance of the parameter estimate is lower bounded by the diagonal element of CRLB matrix:

$$\text{var}\left[\hat{\alpha}_i\right] \geq \text{CRLB}[\alpha]_{(i,i)}. \tag{4.7}$$

For multiple parameters and the observations with Gaussian noise:

If the observation noises are Gaussian distributed:

$$g \sim \mathcal{N}(\mu(\alpha), C(\alpha)) \tag{4.8}$$

then

$$J[\alpha]_{(i,j)} = \Big[\frac{\partial\mu(\alpha)}{\partial\alpha_i}\Big]^T C^{-1}(\alpha)\Big[\frac{\partial\mu(\alpha)}{\partial\alpha_j}\Big] + \frac{1}{2}\text{Trace}\Big[C^{-1}(\alpha)\frac{\partial C(\alpha)}{\partial\alpha_i}C^{-1}(\alpha)\frac{\partial C(\alpha)}{\partial\alpha_j}\Big]. \tag{4.9}$$

4.2 Positioning CRLB with Independent Ranging Noise

We first assume the measurement noise is independent of the location. The positioning CRLBs can be derived as follows:

4.2.1 CRLB of Non-Cooperative Position Estimation

In non-cooperative positioning, a MT only ranges with its neighboring BSs. We assume the terrestrial range ρ_i^k is the distance measurement with location independent Gaussian noise:

$$\rho_i^k = d_i^k + \eta_i^k \quad \eta_i^k \sim \mathcal{N}(0, (\sigma_i^k)^2), \tag{4.10}$$

The marginal log-likelihood function of MT_i states:

$$\begin{aligned}\ln(p(\rho_i^{\mathrm{BS}} \mid \vec{r}_i)) &= \ln\left(\prod_{k=1(i)}^{K_i(i)} \frac{1}{\sqrt{2\pi(\sigma_i^k)^2}} e^{-(d_i^k-\rho_i^k)^2/2(\sigma_i^k)^2}\right) \\ &= \ln\left(\frac{1}{\prod_{k=1(i)}^{K_i(i)}\sqrt{2\pi(\sigma_i^k)^2}}\right) - \sum_{k=1(i)}^{K_i(i)} (d_i^k-\rho_i^k)^2/2(\sigma_i^k)^2, \end{aligned} \tag{4.11}$$

where $\rho_i^{\mathrm{BS}} = [\rho_i^{1(i)} \quad \cdots \quad \rho_i^{K_i(i)}]^T$ is the vector of terrestrial ranging measurements. The FIM of $\vec{r}_i$ (in our case 2-dimensional, but it is in principle straightforward for 3-dimensional extension) is:

$$\begin{aligned} J_{\mathrm{nc}}[\vec{r}_i] &= -\mathcal{E}\left[\frac{\partial^2 \ln\left(p(\rho_i^{\mathrm{BS}} \mid \vec{r}_i)\right)}{\partial(\vec{r}_i)^2}\right] \\ &= \sum_{k=1(i)}^{K_i(i)} \mathcal{E}\left[\frac{\partial^2 (d_i^k-\rho_i^k)^2/2(\sigma_i^k)^2}{\partial(\vec{r}_i)^2}\right] \\ &= \sum_{k=1(i)}^{K_i(i)} 1/(\sigma_i^k)^2 \begin{pmatrix} \mathcal{E}\left[(1-\rho_i^k \frac{(y_i-y^k)^2}{(d_i^k)^3})\right] & \mathcal{E}\left[(\rho_i^k \frac{(x_i-x^k)(y_i-y^k)}{(d_i^k)^3})\right] \\ \mathcal{E}\left[(\rho_i^k \frac{(x_i-x^k)(y_i-y^k)}{(d_i^k)^3})\right] & \mathcal{E}\left[(1-\rho_i^k \frac{(x_i-x^k)^2}{(d_i^k)^3})\right] \end{pmatrix} \\ &= \sum_{k=1(i)}^{K_i(i)} 1/(\sigma_i^k)^2 \begin{pmatrix} \cos^2\theta_i^k & \cos\theta_i^k \sin\theta_i^k \\ \cos\theta_i^k \sin\theta_i^k & \sin^2\theta_i^k \end{pmatrix} \\ &= H_{\mathrm{nc},i}^T C_{\mathrm{nc},i}^{-1} H_{\mathrm{nc},i}, \end{aligned} \tag{4.12}$$

where $\theta_i^k = \mathrm{angle}\left(\vec{e}_i^k\right) = \mathrm{angle}\left(\vec{r}_i - \vec{r}^k\right)$ is the angle of the $BS^k \rightarrow MT_i$ link, $C_{\mathrm{nc},i}$ and $H_{\mathrm{nc},i}$ are as defined in Equation (3.3), (3.2). We can find that $(J_{\mathrm{nc}}[\vec{r}_i])^{-1}$ is the same as the WDOP we defined in Section 3.1. For an M MTs non-cooperative positioning system, the FIM of the global parameter vector ($\vec{r}_{\mathrm{MT}} = [(\vec{r}_i)^T \quad \ldots \quad (\vec{r}_M)^T]^T$) is a block diagonal matrix with the FIM of each MT along the diagonals:

$$J_{\mathrm{nc}}[\vec{r}_{\mathrm{MT}}] = -\mathcal{E}\left[\frac{\partial^2 \ln(p(\rho_{\mathrm{MT}}^{\mathrm{BS}} \mid \vec{r}_{\mathrm{MT}}))}{\partial(\vec{r}_{\mathrm{MT}})^2}\right] = \begin{pmatrix} J_{\mathrm{nc}}[\vec{r}_1] & \cdots & 0 \\ 0 & \ddots & 0 \\ 0 & \cdots & J_{\mathrm{nc}}[\vec{r}_M] \end{pmatrix}, \tag{4.13}$$

where the $\rho_{\mathrm{MT}}^{\mathrm{BS}}$ denotes all the terrestrial ranges from all MTs. The global CRLB matrix can be obtained by inverting $J_{\mathrm{nc}}[\vec{r}_{\mathrm{MT}}]$, which is equivalent to inverting the

diagonal blocks respectively:

$$\mathrm{CRLB}_{\mathrm{nc}}[\vec{r}_{\mathrm{MT}}] = (J_{\mathrm{nc}}[\vec{r}_{\mathrm{MT}}])^{-1} = \begin{pmatrix} (J_{\mathrm{nc}}[\vec{r}_1])^{-1} & \cdots & 0 \\ 0 & \ddots & 0 \\ 0 & \cdots & (J_{\mathrm{nc}}[\vec{r}_M])^{-1} \end{pmatrix}. \tag{4.14}$$

The variances of the estimated coordinates without cooperation are lower bounded by the corresponding diagonal elements of $\mathrm{CRLB}_{\mathrm{nc}}[\vec{r}_{\mathrm{MT}}]$:

$$\mathrm{var}[\hat{\vec{r}}_{\mathrm{MT,nc}}(i)] \geq \mathrm{CRLB}_{\mathrm{nc}}[\vec{r}_{\mathrm{MT}}]_{(i,i)}, \qquad \forall i \in (1, \ldots, M). \tag{4.15}$$

4.2.2 Centralized CRLB of Cooperative Position Estimation

In cooperative positioning, besides the terrestrial ranging (BS-to-MT, Equation (4.10)), MTs also measure the distance from neighboring MTs via peer-to-peer links:

$$\rho_{i,j} = d_{i,j} + \eta_{i,j} \quad \eta_{i,j} \sim \mathcal{N}(0, (\sigma_{i,j})^2), \tag{4.16}$$

where $(\sigma_{i,j})^2$ is the measurement variance of $MT_j \rightarrow MT_i$ link. With this cooperative ranging and the shared (estimated)location from neighbors, MTs are able to enhance their own positioning performance. However, due to the interaction between MTs' estimates, it is complicated to derive the CRLB for a single MT. In [15], Penna et al. also derived a distributed cooperative positioning CRLB. They calculated the FIM for each user based on its own measurements' marginal likelihood function and then constructed the global FIM with all the local ones. In this subsection, we derive the centralized CRLB of cooperative positioning directly from the likelihood of the global measurements to find the theoretic lower bound of the estimator performance. With the assumption that all the ranging measurements are mutual independent and Gaussian distributed, the marginal log-likelihood function of the whole system can be written as:

$$\begin{aligned}
&\ln\left(p(\rho_{\mathrm{MT}} \mid \vec{r}_{\mathrm{MT}})\right) \\
&= \ln\left(\prod_{i=1}^{M} \underbrace{\left(\prod_{k\in\mathbb{B}_i} \frac{1}{\sqrt{2\pi(\sigma_i^k)^2}} e^{-\frac{(d_i^k-\rho_i^k)^2}{2(\sigma_i^k)^2}}\right)}_{\text{terrestrial ranging}} \cdot \underbrace{\left(\prod_{j\in\mathbb{M}_i} \frac{1}{\sqrt{2\pi(\sigma_{i,j})^2}} e^{-\frac{(d_{i,j}-\rho_{i,j})^2}{2(\sigma_{i,j})^2}}\right)}_{\text{cooperative ranging}}\right) \\
&= -\frac{1}{2}\sum_{i=1}^{M}\left(\sum_{k\in\mathbb{B}_i} \ln\left(2\pi(\sigma_i^k)^2\right) + \sum_{j\in\mathbb{M}_i} \ln\left(2\pi(\sigma_{i,j})^2\right)\right) \\
&\quad -\sum_{i=1}^{M}\left(\sum_{k\in\mathbb{B}_i} \frac{(d_i^k-\rho_i^k)^2}{2(\sigma_i^k)^2} + \sum_{j\in\mathbb{M}_i} \frac{(d_{i,j}-\rho_{i,j})^2}{2(\sigma_{i,j})^2}\right),
\end{aligned} \tag{4.17}$$

where ρ_{MT} is a vector containing the ranges (terrestrial and cooperative) of all the MTs. Similarly as Subsection 4.2.1, we further assume the ranging variance does not depend on location. i.e. the first term of Equation (4.17) is a constant with respect to location vector $\vec{r}_{\mathrm{MT}}$. Therefore, the FIM for the whole system can be reformulated as:

$$\begin{aligned}
J[\vec{r}_{\mathrm{MT}}] &= -\mathcal{E}\left[\frac{\partial^2 \ln\left(p(\rho_{\mathrm{MT}} \mid \vec{r}_{\mathrm{MT}})\right)}{\partial(\vec{r}_{\mathrm{MT}})^2}\right] \\
&= \sum_{i=1}^{M} \mathcal{E}\left[\frac{\partial^2\left(\sum_{k\in\mathbb{B}_i}\frac{(d_i^k-\rho_i^k)^2}{2(\sigma_i^k)^2} + \sum_{j\in\mathbb{M}_i}\frac{(d_{i,j}-\rho_{i,j})^2}{2(\sigma_{i,j})^2}\right)}{\partial(\vec{r}_{\mathrm{MT}})^2}\right] \\
&= \sum_{i=1}^{M} \mathcal{E}\left[\frac{\partial^2\sum_{k\in\mathbb{B}_i}\frac{(d_i^k-\rho_i^k)^2}{2(\sigma_i^k)^2}}{\partial(\vec{r}_{\mathrm{MT}})^2}\right] + \sum_{i=1}^{M} \mathcal{E}\left[\frac{\partial^2\sum_{j\in\mathbb{M}_i}\frac{(d_{i,j}-\rho_{i,j})^2}{2(\sigma_{i,j})^2}}{\partial(\vec{r}_{\mathrm{MT}})^2}\right] \\
&= J_{\mathrm{nc}}[\vec{r}_{\mathrm{MT}}] + J_{\mathrm{c}}[\vec{r}_{\mathrm{MT}}],
\end{aligned} \tag{4.18}$$

with $J_{\mathrm{c}}[\vec{r}_{\mathrm{MT}}]$ is the cooperative part defined as:

$$J_{\mathrm{c}}[\vec{r}_{\mathrm{MT}}] \triangleq \sum_{i=1}^{M} \mathcal{E}\left[\frac{\partial^2\sum_{j\in\mathbb{M}_i}\frac{(d_{i,j}-\rho_{i,j})^2}{2(\sigma_{i,j})^2}}{\partial(\vec{r}_{\mathrm{MT}})^2}\right]. \tag{4.19}$$

For a matrix X, we define $Y = \frac{1}{X}$ as the element-wise inverse, i.e. elements in Y are the inverse of the ones in X:

$$Y_{(i,j)} = \frac{1}{X_{(i,j)}}, \quad \forall i, j. \tag{4.20}$$

Expanding Equation (4.19), we can get:

$$\begin{aligned}
J_{\mathrm{c}}[\vec{r}_{\mathrm{MT}}] &= \sum_{i=1}^{M} \mathcal{E}\left[\partial^2 \sum_{j\in\mathbb{M}_i}\frac{(d_{i,j}-\rho_{i,j})^2}{2(\sigma_{i,j})^2}\right]\begin{pmatrix} \frac{1}{\partial\vec{r}_1(\partial\vec{r}_1)^T} & \cdots & \frac{1}{\partial\vec{r}_1(\partial\vec{r}_M)^T} \\ \vdots & \ddots & \vdots \\ \frac{1}{\partial\vec{r}_M(\partial\vec{r}_1)^T} & \cdots & \frac{1}{\partial\vec{r}_M(\partial\vec{r}_M)^T} \end{pmatrix} \\
&\triangleq \begin{pmatrix} J_{\mathrm{c},(1,1)} & \cdots & J_{\mathrm{c},(1,M)} \\ \vdots & \ddots & \vdots \\ J_{\mathrm{c},(M,1)} & \cdots & J_{\mathrm{c},(M,M)} \end{pmatrix},
\end{aligned} \tag{4.21}$$

where $J_{\mathrm{c},(i,j)}$ is a 2x2 matrix $\forall i,j \in (1,\ldots,M)$. The block diagonal element $J_{\mathrm{c},(i,i)}$ can be rewritten as:

$$\begin{aligned} J_{\mathrm{c},(i,i)} &= \overbrace{\sum_{j\in\mathbb{M}_i} \mathcal{E}\left[\frac{\partial^2 (d_{i,j}-\rho_{i,j})^2/2(\sigma_{i,j})^2}{\partial(\vec{r}_i)^2}\right]}^{MT_j \to MT_i \text{ link, measured by } MT_i} + \overbrace{\sum_{\{l|i\in\mathbb{M}_l\}} \mathcal{E}\left[\frac{\partial^2 (d_{l,i}-\rho_{l,i})^2/2(\sigma_{l,i})^2}{\partial(\vec{r}_i)^2}\right]}^{MT_i \to MT_l \text{ link, measured by } MT_l} \\ &= \sum_{\substack{j\in(1,\cdots,M)\\ j\neq i}} (\frac{\delta_{i,j}}{(\sigma_{i,j})^2} + \frac{\delta_{j,i}}{(\sigma_{j,i})^2}) \begin{pmatrix} \cos^2\theta_{i,j} & \cos\theta_{i,j}\sin\theta_{i,j} \\ \cos\theta_{i,j}\sin\theta_{i,j} & \sin^2\theta_{i,j} \end{pmatrix} \\ &= \sum_{\substack{j\in(1,\cdots,M)\\ j\neq i}} c^{-1}_{\mathrm{bi},i,j} \begin{pmatrix} \cos^2\theta_{i,j} & \cos\theta_{i,j}\sin\theta_{i,j} \\ \cos\theta_{i,j}\sin\theta_{i,j} & \sin^2\theta_{i,j} \end{pmatrix} \\ &= H^T_{\mathrm{c},i^-} C^{-1}_{\mathrm{c,bi},i^-} H_{\mathrm{c},i^-}, \end{aligned} \tag{4.22}$$

where $\theta_{i,j} = \text{angle}\,(\vec{e}_{i,j}) = \text{angle}\,(\vec{r}_i - \vec{r}_j)$ is the angle of $MT_j \to MT_i$ link, $\delta_{i,j}$ is the link selection factor:

$$\delta_{i,j} = \begin{cases} 1 & \text{if } MT_j \to MT_i \text{ link is available;} \\ 0 & \text{if } MT_j \to MT_i \text{ link is not available,} \end{cases} \tag{4.23}$$

$c^{-1}_{\mathrm{bi},i,j} \triangleq \frac{\delta_{i,j}}{(\sigma_{i,j})^2} + \frac{\delta_{j,i}}{(\sigma_{j,i})^2}$ for simplicity, $C^{-1}_{\mathrm{c,bi},i^-}$ is the cooperative range weight matrix:

$$C^{-1}_{\mathrm{c,bi},i^-} = \begin{pmatrix} c^{-1}_{\mathrm{bi},i,1} & & & & \\ & \ddots & & 0 & \\ & & c^{-1}_{\mathrm{bi},i,j\neq i} & & \\ & 0 & & \ddots & \\ & & & & c^{-1}_{\mathrm{bi},i,M} \end{pmatrix} \tag{4.24}$$

and $H_{\mathrm{c},i}$ is the cooperative geometry matrix:

$$H_{\mathrm{c},i} = \begin{pmatrix} \frac{(\vec{r}_i-\vec{r}_1)^T}{d_{i,1}} \\ \vdots \\ \frac{(\vec{r}_i-\vec{r}_{j\neq i})^T}{d_{i,j\neq i}} \\ \vdots \\ \frac{(\vec{r}_i-\vec{r}_M)^T}{d_{i,M}} \end{pmatrix} = \begin{pmatrix} (\vec{e}_{i,1})^T \\ \vdots \\ (\vec{e}_{i,j\neq i})^T \\ \vdots \\ (\vec{e}_{i,M})^T \end{pmatrix}. \tag{4.25}$$

Similarly, the non-block-diagonal elements($\forall J_{c,(i,j)}$ with $i \neq j$) are symmetric and can be derived as:

$$\begin{aligned} J_{c,(i,j)} = J_{c,(j,i)} &= \overbrace{\delta_{i,j} \cdot \mathcal{E}\left[\frac{\partial^2 (d_{i,j} - \rho_{i,j})^2 / 2(\sigma_{i,j})^2}{\partial \vec{r}_j \partial \vec{r}_i}\right]}^{MT_j \to MT_i \text{ link, measured by } MT_i} + \overbrace{\delta_{j,i} \cdot \mathcal{E}\left[\frac{\partial^2 (d_{j,i} - \rho_{j,i})^2 / 2(\sigma_{j,i})^2}{\partial \vec{r}_j \partial \vec{r}_i}\right]}^{MT_i \to MT_j \text{ link, measured by } MT_j} \\ &= -c_{\mathrm{bi},i,j}^{-1} \begin{pmatrix} \cos^2\theta_{i,j} & \cos\theta_{i,j}\sin\theta_{i,j} \\ \cos\theta_{i,j}\sin\theta_{i,j} & \sin^2\theta_{i,j} \end{pmatrix} \\ &= -\vec{e}_{i,j} \cdot c_{\mathrm{bi},i,j}^{-1} \cdot \vec{e}_{i,j}^{T}. \end{aligned} \tag{4.26}$$

If we assume an MT is considered as a neighbor only if both of the bi-directional links are available (mutual neighbor), i.e.:

$$i \in \mathbb{M}_j \Leftrightarrow {}^1 j \in \mathbb{M}_i, \quad \forall i, j \in (1, \cdots, M) \text{ and } i \neq j, \tag{4.27}$$

It is reasonable for the peer-to-peer links in the mobile radio networks unlike in GNSS systems, and necessarily to be true for RTL measurement. Then Equation (4.22) can be simplified as:

$$\begin{aligned} J_{\mathrm{c},(i,i)} &= \sum_{j \in \mathbb{M}_i} \mathcal{E}\left[\frac{\partial^2 \left((d_{i,j} - \rho_{i,j})^2 / 2(\sigma_{i,j})^2 + (d_{j,i} - \rho_{j,i})^2 / 2(\sigma_{j,i})^2\right)}{\partial (\vec{r}_i)^2}\right] \\ &= \sum_{j \in \mathbb{M}_i} \left(\frac{1}{(\sigma_{i,j})^2} + \frac{1}{(\sigma_{j,i})^2}\right) \begin{pmatrix} \cos^2\theta_{i,j} & \cos\theta_{i,j}\sin\theta_{i,j} \\ \cos\theta_{i,j}\sin\theta_{i,j} & \sin^2\theta_{i,j} \end{pmatrix} \\ &= \tilde{H}_{\mathrm{c},i}^{T} \tilde{C}_{\mathrm{c,bi},i}^{-1} \tilde{H}_{\mathrm{c},i}, \end{aligned} \tag{4.28}$$

where

$$\tilde{C}_{\mathrm{c,bi}i}^{-1} = \begin{pmatrix} \frac{1}{(\sigma_{i,1(i)})^2} + \frac{1}{(\sigma_{1(i),i})^2} & \cdots & 0 \\ 0 & \ddots & 0 \\ 0 & \cdots & \frac{1}{(\sigma_{i,M_i(i)})^2} + \frac{1}{(\sigma_{M_i(i),i})^2} \end{pmatrix}, \tag{4.29}$$

and

$$\tilde{H}_{\mathrm{c},i} = \begin{pmatrix} \frac{(\vec{r}_i - \vec{r}_{1(i)})^T}{d_{i,1(i)}} \\ \vdots \\ \frac{(\vec{r}_i - \vec{r}_{M_i(i)})^T}{d_{i,M_i(i)}} \end{pmatrix} = \begin{pmatrix} (\vec{e}_{i,1(i)})^T \\ \vdots \\ (\vec{e}_{i,M_i(i)})^T \end{pmatrix}. \tag{4.30}$$

Equation (4.26) can be rewritten as:

$$J_{c,(i,j)} = J_{c,(j,i)} = \begin{cases} -\vec{e}_{i,j} \cdot \left(\frac{1}{(\sigma_{i,j})^2} + \frac{1}{(\sigma_{j,i})^2}\right) \cdot (\vec{e}_{i,j})^T & \text{if } j \in \mathbb{M}_i \\ 0 & \text{if } j \notin \mathbb{M}_i \end{cases} \tag{4.31}$$

[1] $\Leftrightarrow$ is read as 'is equivalent to'.

The cooperative contribution can be obtained by inserting Equations (4.22), (4.26) (or (4.28), (4.31)) into Equation (4.21), and then we can get the overall FIM $J[\vec{r}_{\mathrm{MT}}]$ by Equation (4.18). By inverting $J[\vec{r}_{\mathrm{MT}}]$, we can have the global CRLB matrix for a cooperative positioning system:

$$\mathrm{CRLB_c}[\vec{r}_{\mathrm{MT}}] = J[\vec{r}_{\mathrm{MT}}]^{-1}. \tag{4.32}$$

The variances of estimate coordinates with cooperation are lower bounded by the corresponding diagonal elements of $\mathrm{CRLB}_{[}\vec{r}_{\mathrm{MT}}]$:

$$\mathrm{var}[\hat{\vec{r}}_{\mathrm{MT,c}}(i)] \geq \mathrm{CRLB}[\vec{r}_{\mathrm{MT}}]_{(i,i)}, \qquad \forall i \in (1, \ldots, M). \tag{4.33}$$

For bi-directional peer-to peer links ($MT_j \rightarrow MT_i$ and $MT_i \rightarrow MT_j$), the measurement variances are normally not identical:

$$(\sigma_{i,j})^2 \nLeftrightarrow (\sigma_{j,i})^2, \tag{4.34}$$

because of the different channel state information(CSI) and the adaptive resource allocation scheme. The CRLBs for non-cooperative and cooperative positioning as well as the simulated positioning estimation error are shown in Figure 4.1. We can see for non-cooperative positioning, the estimation error can achieve the CRLB and is quite stable. For cooperative positioning, the estimation accuracy is also close to the bound. The non-cooperative positioning performances better than the cooperative case because the bandwidth per MT for the latter one is only a half of the former one's, which makes it an unfair comparison.

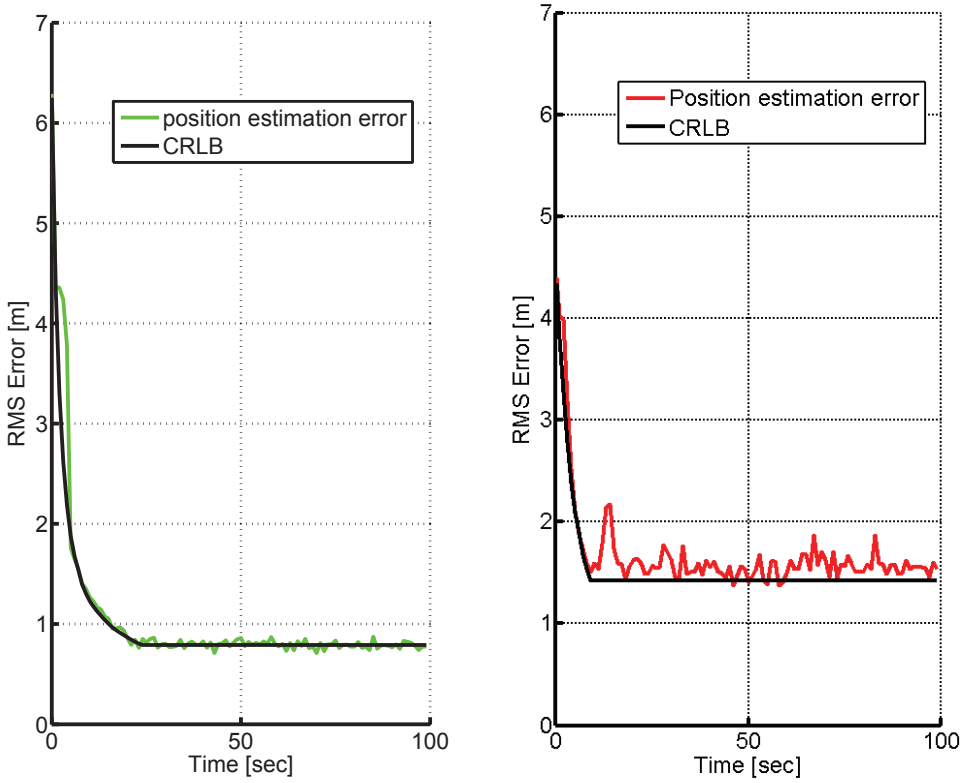

(a) non-cooper.

(b) cooper.

Figure 4.1: The positioning CRLB and the simulated positioning estimations. For cooperative positioning, two MTs are involved. It is the average of 100 simulations

4.2.3 Approximate the Local Cooperative Positioning CRLB

From the previous derivation, it is clear that for cooperative positioning, the global FIM is normally not a block diagonal matrix. When calculating the global CRLB matrix, by the inverting operation, the entities interact with each other. That means the estimate error of one MT can directly affect the neighboring MTs who use this estimate as their reference. Furthermore, this error may even affect some non-neighboring MTs through some intermediate MTs. Therefore, calculating the positioning CRLB for a specific MT is difficult. On the other hand, for a distributed system there is no central unit collecting the global information. In this condition, how can a MT know its own estimate accuracy? Instead of using the global CRLB matrix, we present an approach to approximate the lower bound of its own estimate variance only by local information. If the neighbor's estimate variance is known, recalling Section 3.3, the link evaluation scheme we introduced allows us

transferring the neighbor's location estimation inaccuracy to an equivalent ranging variance. It is like assuming the neighbor's estimate is true, but the ranging measurement is less reliable. With this transformation, we are able to calculate an equivalent non-cooperative CRLB just by replacing the true ranging variances by the equivalent ones. At the end of each time step, besides the location estimate, a MT also broadcasts its own local CRLB approximation so that others can use it as its position estimate variance to evaluate this link's quality. Sequentially, each MT can approximate its positioning CRLB and the extra communication effort is negligible (only one or two more values to share). In Figure 4.2 - 4.4 the (non-)cooperative positioning CRLB and the local cooperative CRLB approximation snapshots are compared. For this simulation, the second order expansion with the angle information is used. The standard deviation of all the links are set to be the same (64 m) and the neighbors'initial approximated CRLBs are set to infinity. We can see that the approximated CRLB is close to the true one. Also it is shown that the CRLB decreases when there are more cooperative nodes. Figure 4.5 shows the iterative approximation procedure averaging from 1000 simulations. It can be seen that the approximated local CRLB converges to a level which slightly higher than the true CRLB in a few iterations. Recalling Section 3.3, the second order expansion with angle information is slightly higher than the true equivalent variance. It could be the explanation why the local CRLB approximation is slightly higher than the true one.

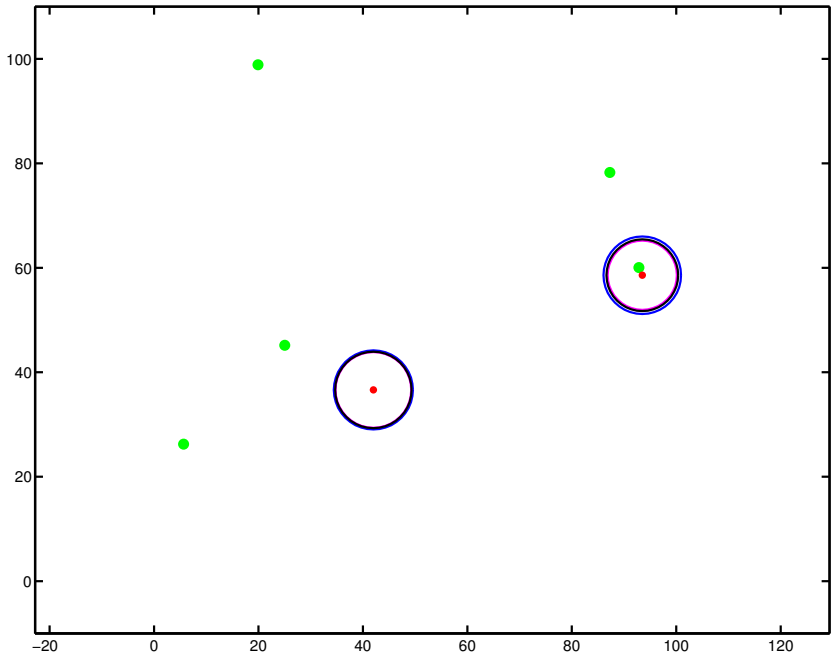

Figure 4.2: The comparison of the non-cooperative positioning CRLB (blue circle), the cooperative CRLB (magenta circle) and the local cooperative CRLB (black circle) approximation in 5 BSs (green dot) and 2 MTs (red dot) case. In this case the MT network is not dense, therefor, the cooperative gain is not significant. The three CRLBs are almost overlapping and difficult to distinguished.

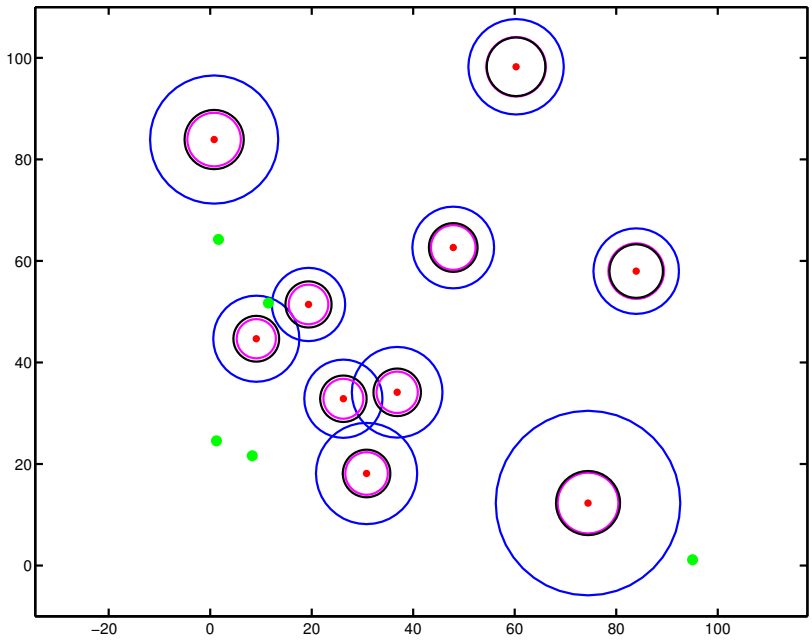

Figure 4.3: The comparison of the non-cooperative positioning CRLB (blue circle), the cooperative CRLB (magenta circle) and the local cooperative CRLB (black circle) approximation in 5 BSs (green dot) and 10 MTs (red dot) case. We can observe a significant gain from cooperation. The local approximated CRLBs are almost overlapping with the true cooperative ones. It shows the approximation scheme perform well.

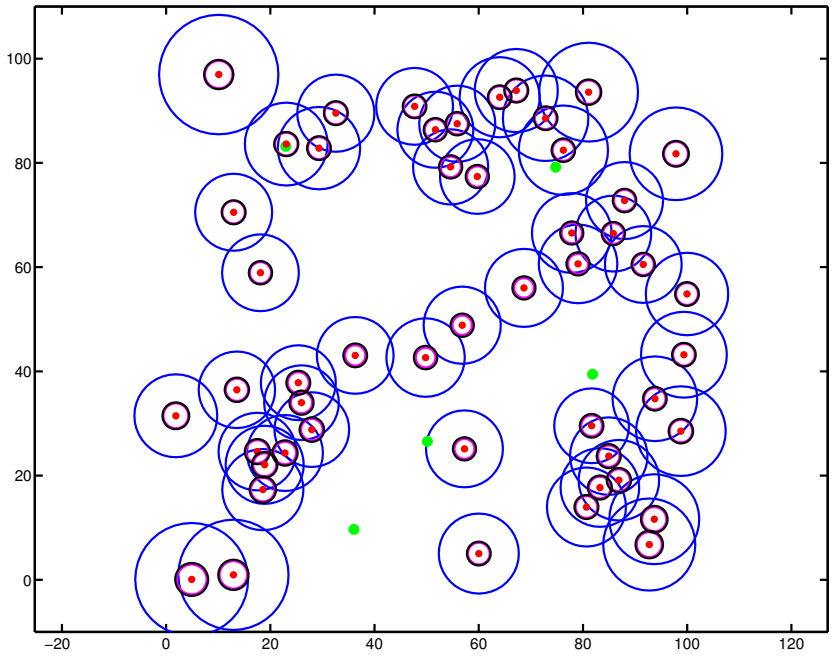

Figure 4.4: The comparison of the non-cooperative positioning CRLB (blue circle), the cooperative CRLB (magenta circle) and the local cooperative CRLB (black circle) approximation in 5 BSs (green dot) and 50 MTs (red dot) case. The gain of cooperation is more significant because of the dense MT network. The local approximated CRLBs almost overlap with the true cooperative ones. It shows the approximation scheme perform well.

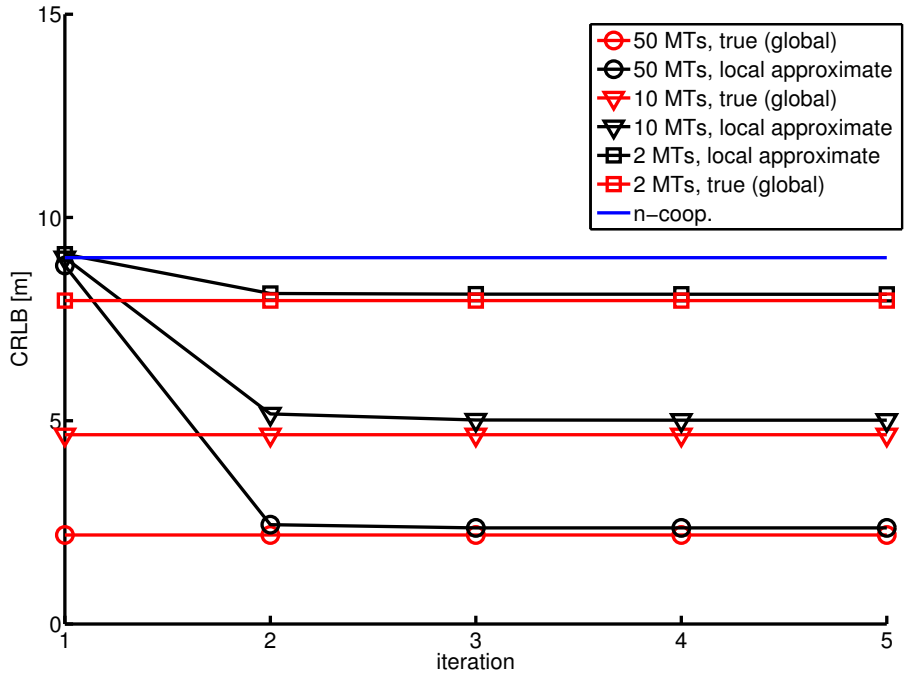

Figure 4.5: The comparison of the (non-) cooperative positioning CRLB and the local cooperative CRLB approximation

From the simulation results we can see that the cooperative CRLB can be well approximated by the local approximation scheme we proposed.

4.3 Positioning CRLB with OFDM signal

OFDM is one of the candidate techniques for the next generation mobile radio system due to some key advantages like the spectrum efficiency, the orthogonality, the resource flexibility, etc. In this section, we look into a OFDM cooperative positioning system. We first introduce the CRLB of delay estimation (TOA masurement). Then use it as the measurement variance to recalculate the (non-)cooperative positioning CRLB as the bound of the real system performance.

4.3.1 Ranging CRLB without Pathloss Dependency

An OFDM signal is formulated as [29]:

$$s(t) = \frac{1}{\sqrt{N}} \sum_{n=\lfloor -\frac{N-1}{2} \rfloor}^{\lfloor \frac{N-1}{2} \rfloor} S_n e^{j2\pi n f_{\text{sc}} t} \tag{4.35}$$

f_{sc} is the subcarrier spacing, N is the number of subcariers and S_n is the information symbol carried by each subcarrier. Dammann derived the CRLB of the delay estimation in [29] which states:

$$\begin{aligned}\text{var}[\hat{\tau}] \geq \text{CRLB}[\tau] =& \frac{1}{8\pi^2 f_{\text{sc}}^2 \sum_{n=\lfloor -\frac{N-1}{2} \rfloor}^{\lfloor \frac{N-1}{2} \rfloor} n^2 |S_n|^2/\sigma_0^2} \\ =& \frac{1}{8\pi^2 f_{\text{sc}}^2 \sum_{n=\lfloor -\frac{N-1}{2} \rfloor}^{\lfloor \frac{N-1}{2} \rfloor} n^2 \text{SNR}_n}\end{aligned} \tag{4.36}$$

τ is the propagation delay, σ_0^2 is the variance of thermal noise. The CRLB of ranging is:

$$\text{var}[\hat{\rho}] \geq \text{CRLB}[\rho] = \frac{c^2}{8\pi^2 f_{\text{sc}}^2 \sum_{n=-\frac{N-1}{2}}^{\frac{N-1}{2}} n^2 \text{SNR}_n}. \tag{4.37}$$

If the n^{th} subcarrier is used, $|S_n|^2$ is the transmit power of that subcarrier. Whereas if the n^{th} subcarrier is not used, then $|S_n|^2 = 0$. From Equation (4.37) we can see for the given bandwidth and the constant subcarrier spacing, $\text{var}[\hat{\tau}]$ can be reduced by

1. Increasing the SNR;
2. Increasing the number of used subcarriers $\left(\left|\{n|_{|S_n|^2 \neq 0}\}\right|\right)$;
3. Using the edge subcarriers (ones with higher index) instead of the central ones.

Moreover, the SNR (dB) of a single subcarrier can be formulated according to the pathloss (PL) and thermal noise ($N_{\text{th,dBm}}$) [30]:

$$\text{PL}_{\text{dB}} = 10\lg(d^2) + 20\lg(f_c) + 20\lg\frac{4\pi}{c}, \tag{4.38}$$

$$N_{\text{th,dBm}} = -174\text{dBm/Hz} + 10\lg(f_{\text{sc}}) + 7\text{dB}, \quad \text{(the rule of thumb)} \tag{4.39}$$

$$\text{SNR}_{n,\text{dB}} = P_{\text{tx},n} - \text{PL}_{\text{dB}} - N_{\text{th,dBm}}, \tag{4.40}$$

where $P_{\text{tx},n}$ is the transmit power of subcarrier n, f_c is the carrier frequency. Normally the value of the carrier frequency is much larger than the value of the bandwidth, i.e. $f_c \gg N f_{\text{sc}}$. Therefore, the subcarriers can be assumed to experience the same pathloss. The SNR is inverse proportional to d^2:

$$\text{SNR} \propto \frac{1}{d^2}. \tag{4.41}$$

According to some recent researches [31], the CRLB of TOA estimation with OFDM signal is achievable especially when the SNR is not too low. It is reasonable to assume there is a ranging estimator which can always achieve the CRLB within

certain communication range. By this assumption, we are able to focus on the main issues while avoiding an investigation of the details of ranging technique. We model the ranging measurement as follow:

$$\rho = d + \eta, \quad \eta \sim \mathcal{N}(0, \sigma^2_{\text{ofdm}}), \quad \text{if } d \leq R \tag{4.42}$$

where $\sigma^2_{\text{ofdm}} = \text{CRLB}[\rho]$. For writing simplicity, in the remaining part of the thesis, all the variables are referring to the OFDM system without explicitly specified (e.g. $\sigma^2 \equiv \sigma^2_{\text{ofdm}}$), unless stated otherwise.

4.3.2 Ranging CRLB with Pathloss Dependency

If we take the dependency between pathloss and delay into account, for the same time domain transmit signal as Equation (4.35), the sampled received signal is:

$$r(iT - \tau) = \frac{1}{\sqrt{N}} \sum_{n=-\frac{N-1}{2}}^{\frac{N-1}{2}} \vartheta(\tau) S_n e^{j2\pi n f_{\text{sc}}(iT-\tau)}, \tag{4.43}$$

where ϑ is the attenuation factor N is the number of subcarriers, τ is the propagation delay and $T = \frac{1}{N f_{\text{sc}}}$ is the sampling period. As shown in Equation 4.4, we need to calculate the derivative to get the CRLB.

$$\frac{d}{d\tau} r(iT - \tau) = \frac{1}{\sqrt{N}} \sum_{n=\lfloor -\frac{N-1}{2} \rfloor}^{\lfloor \frac{N-1}{2} \rfloor} \left(\frac{d\vartheta}{d\tau} S_n + \vartheta S_n (-j2\pi n f_{\text{sc}}) \right) e^{j2\pi n f_{\text{sc}}(iT-\tau)}. \tag{4.44}$$

We can formulate $\sum_{i=0}^{N-1} |\frac{d}{d\tau} r(iT-\tau)|^2$ as:

$$
\begin{aligned}
&\sum_{i=0}^{N-1} |\frac{d}{d\tau} r(iT-\tau)|^2 \\
=&\sum_{i=0}^{N-1} \frac{d}{d\tau} r(iT-\tau) \left(\frac{d}{d\tau} r(iT-\tau)\right)^* \\
=&\frac{1}{N} \sum_{i=0}^{N-1} \sum_{n,m=\lfloor -\frac{N-1}{2} \rfloor}^{\lfloor \frac{N-1}{2} \rfloor} \left(\frac{d\vartheta}{d\tau} S_n + \vartheta S_n(-j2\pi n f_{\mathrm{sc}})\right) e^{j2\pi n f_{\mathrm{sc}}(iT-\tau)} \\
&\cdot \left(\frac{d\vartheta}{d\tau} S_m + \vartheta S_m(-j2\pi m f_{\mathrm{sc}})\right)^* e^{-j2\pi m f_{\mathrm{sc}}(iT-\tau)} \\
=&\sum_{n,m=\lfloor -\frac{N-1}{2} \rfloor}^{\lfloor \frac{N-1}{2} \rfloor} \left(\frac{d\vartheta}{d\tau} S_n + \vartheta S_n(-j2\pi n f_{\mathrm{sc}})\right) \left(\frac{d\vartheta}{d\tau} S_m^* + \vartheta S_m^*(j2\pi m f_{\mathrm{sc}})\right) \\
&\cdot \underbrace{\sum_{i=0}^{N-1} e^{j2\pi(n-m) f_{\mathrm{sc}}(iT-\tau)}}_{=N\delta(n-m)} \\
=&\sum_{n=\lfloor -\frac{N-1}{2} \rfloor}^{\lfloor \frac{N-1}{2} \rfloor} S_n S_n^* \left(\frac{d\vartheta}{d\tau}\right)^2 + \underbrace{j2\pi n f_{\mathrm{sc}} \vartheta \left(S_n \frac{d\vartheta}{d\tau} S_n^* - S_n \frac{d\vartheta}{d\tau} S_n^*\right)}_{=0} + 4\pi^2 n^2 f_{\mathrm{sc}}^2 S_n S_n^* \vartheta^2 \\
=&\left(\frac{d\vartheta}{d\tau}\right)^2 \sum_{n=\lfloor -\frac{N-1}{2} \rfloor}^{\lfloor \frac{N-1}{2} \rfloor} |S_n|^2 + 4\pi^2 f_{\mathrm{sc}}^2 \vartheta^2 \sum_{n=\lfloor -\frac{N-1}{2} \rfloor}^{\lfloor \frac{N-1}{2} \rfloor} n^2 |S_n|^2. \qquad (4.45)
\end{aligned}
$$

Based on Equation (4.4), CRLB$[\tau]$ is:

$$
\begin{aligned}
\mathrm{CRLB}[\tau] &= \frac{\sigma_0^2}{2\sum_{i=0}^{N-1} |\frac{d}{d\tau} r(iT-\tau)|^2} \\
&= \frac{\sigma_{\mathrm{No}}^2}{2\left(\frac{d\vartheta}{d\tau}\right)^2 \sum_{n=-\frac{N-1}{2}}^{\frac{N-1}{2}} |S_n|^2 + 8\pi^2 f_{\mathrm{sc}}^2 \vartheta^2 \sum_{n=-\frac{N-1}{2}}^{\frac{N-1}{2}} n^2 |S_n|^2}. \qquad (4.46)
\end{aligned}
$$

ϑ can be obtained from the pathloss (PL):

$$
\begin{aligned}
\mathrm{PL_{dB}} &= 10\lg(d^2) + 20\lg(f_c) + 20\lg\frac{4\pi}{c}, \\
\mathrm{PL} &= 10^{\frac{\mathrm{PL_{dB}}}{10}}. \qquad (4.47)
\end{aligned}
$$

ϑ states:

$$
\vartheta = \frac{1}{\sqrt{\mathrm{PL}}} = \frac{1}{4\pi\tau f_c}, \qquad (4.48)
$$

and

$$\left(\frac{d\vartheta}{d\tau}\right)^2 = \frac{1}{16\pi^2 f_c^2 \tau^4}. \tag{4.49}$$

Then CRLB[τ] can be reformulated as:

$$\text{CRLB}[\tau] = \frac{\sigma_0^2}{\frac{1}{8\pi^2 f_c^2 \tau^4} \sum_{n=\left\lfloor -\frac{N-1}{2} \right\rfloor}^{\left\lfloor \frac{N-1}{2} \right\rfloor} |S_n|^2 + \frac{f_{sc}^2}{2 f_c^2 c^2 \tau^2} \sum_{n=\left\lfloor -\frac{N-1}{2} \right\rfloor}^{\left\lfloor \frac{N-1}{2} \right\rfloor} n^2 |S_n|^2}. \tag{4.50}$$

The ranging variance is lower bounded by:

$$\begin{aligned} \text{var}[\hat{\rho}] &\geq \text{CRLB}[\rho] \\ &= \text{CRLB}[\tau] c^2 \\ &= \frac{\sigma_0^2 c^2}{\frac{1}{8\pi^2 f_c^2 \tau^4} \sum_{n=\left\lfloor -\frac{N-1}{2} \right\rfloor}^{\left\lfloor \frac{N-1}{2} \right\rfloor} |S_n|^2 + \frac{f_{sc}^2}{2 f_c^2 c^2 \tau^2} \sum_{n=\left\lfloor -\frac{N-1}{2} \right\rfloor}^{\left\lfloor \frac{N-1}{2} \right\rfloor} n^2 |S_n|^2}. \end{aligned} \tag{4.51}$$

Compared with the result from the last subsection, there is one more term added in the denominator: $\frac{1}{8\pi^2 f_c^2 \tau^4} \sum_{n=\left\lfloor -\frac{N-1}{2} \right\rfloor}^{\left\lfloor \frac{N-1}{2} \right\rfloor} |S_n|^2$. The physical meaning of this is after having a rough estimation, we also take the RSS into account to correct the TOA estimation. Similarly as in the previous subsection, we assume an optimal estimator:

$$\rho = d + \eta, \quad \eta \sim \mathcal{N}(0, \sigma^2(d)), \quad \text{if } d \leq R, \tag{4.52}$$

where $\sigma^2(d) = \text{CRLB}[\rho]$. The CRLBs for delay estimation is shown in Figure 4.6. We can find out that for a short distance ranging, exploring the RSS-TOA dependency to correct the TOA estimation can offer a significant gain. Whereas when the neighbor is far, this dependency is less helpful and the accuracy of this TOA-RSS hybrid metric is almost the same as to only use the TOA.

4.3.3 Positioning CRLB without Pathloss Dependency

If the position - pathloss dependency is not considered, the SNR is considered as known (e.g. through channel estimation). Therefore, the covariance matrix is not delay dependent. For both non-cooperative and cooperative positioning with the OFDM signals, the CRLB is similar as in Subsection 4.2.1 (non-cooperative) and Subsection 4.2.2 (cooperative), just replacing the ranging variance by its CRLB (Equation (4.37)).

4.3.4 Positioning CRLB with Pathloss Dependency

Because the ranging variance depends on the true (GLOS) distance, the assumption of parameter-independent covariance matrix from Section 4.2 does not hold anymore. Therefore, new CRLBs for (non-) cooperative positioning need to be derived.

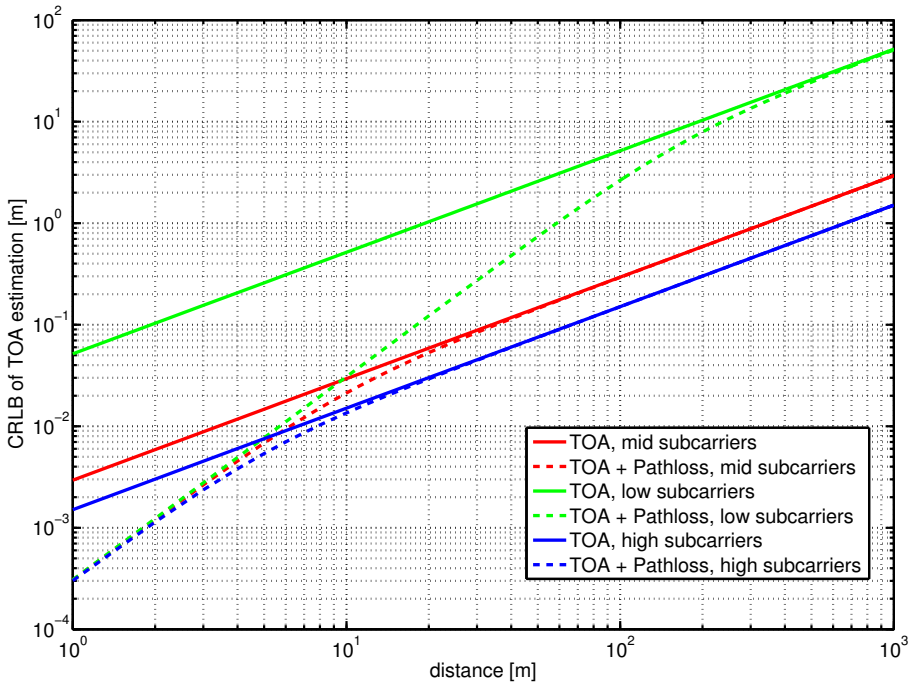

Figure 4.6: CRLB for TOA estimation with(out) the RSS-TOA dependency. fifty subcarriers are used for each time. In order to show the impact of the subcairrer indices, we use the bandwidth $0 \sim B$ instead of the baseband ($-\frac{1}{2}B \sim \frac{1}{2}B$) where B is the bandwidth. Three groups of subcarriers (0-50, 475-524 and 950-1000) are compared. We can see that using the subcarriers with higher indices improves the performance. For each subcarrier group, a crucial distance can be found. If the distance is smaller than the crucial one, the gain from using the RSS additionally is significant. Whereas when the distance is larger than the crucial one, the RSS gain can be neglected.

Non-Cooperative Positioning

For non-cooperative positioning, MT_i measures the distance to BS^k. The ranging variance depends on $\vec{r}_i$ and $\vec{r}^{\,k}$ is constant and known. The marginal likelihood function of MT_i (Equation 4.11) can be modified as:

$$\begin{aligned}&\ln\left(p\left(\rho_i^{\mathrm{BS}} \mid \vec{r}_i\right)\right)\\ =&\ln\left(\frac{1}{(2\pi)^{\frac{K_i}{2}}\det^{\frac{1}{2}}\left[C_{\mathrm{nc},i}(\vec{r}_i)\right]}\cdot\exp\left[-\frac{1}{2}\left(\rho_i^{\mathrm{BS}}-d_i^{\mathrm{BS}}\right)^T\cdot C_{\mathrm{nc},i}^{-1}(\vec{r}_i)\cdot\left(\rho_i^{\mathrm{BS}}-d_i^{\mathrm{BS}}\right)\right]\right),\end{aligned} \tag{4.53}$$

where d_i^{BS} is the vector of the true (GLOS) distances of all the terrestrial links. As a multi-parameter estimator with gaussian noise, the covariance matrix is parameter-dependent. The FIM can be formulated according to Equation (4.9):

$$\begin{aligned}J_{\mathrm{nc}}[\vec{r}_i] =&H_{\mathrm{nc},i}^T C_{\mathrm{nc},i}^{-1} H_{\mathrm{nc},i}\\ &+\frac{1}{2}\begin{pmatrix}\mathrm{Trace}\left[C_{\mathrm{nc},i}^{-1}\frac{\partial C_{\mathrm{nc},i}}{\partial x_i}C_{\mathrm{nc},i}^{-1}\frac{\partial C_{\mathrm{nc},i}}{\partial x_i}\right] & \mathrm{Trace}\left[C_{\mathrm{nc},i}^{-1}\frac{\partial C_{\mathrm{nc},i}}{\partial x_i}C_{\mathrm{nc},i}^{-1}\frac{\partial C_{\mathrm{nc},i}}{\partial y_i}\right]\\ \mathrm{Trace}\left[C_{\mathrm{nc},i}^{-1}\frac{\partial C_{\mathrm{nc},i}}{\partial y_i}C_{\mathrm{nc},i}^{-1}\frac{\partial C_{\mathrm{nc},i}}{\partial x_i}\right] & \mathrm{Trace}\left[C_{\mathrm{nc},i}^{-1}\frac{\partial C_{\mathrm{nc},i}}{\partial y_i}C_{\mathrm{nc},i}^{-1}\frac{\partial C_{\mathrm{nc},i}}{\partial y_i}\right]\end{pmatrix}.\end{aligned} \tag{4.54}$$

Expanding the upper-left part of the second term:

$$\mathrm{Trace}\left[C_{\mathrm{nc},i}^{-1}\frac{\partial C_{\mathrm{nc},i}}{\partial x_i}C_{\mathrm{nc},i}^{-1}\frac{\partial C_{\mathrm{nc},i}}{\partial x_i}\right]=\sum_{k\in\mathbb{B}_i}\frac{1}{(\sigma_i^k)^2}\frac{\partial(\sigma_i^k)^2}{\partial x_i}\frac{1}{(\sigma_i^k)^2}\frac{\partial(\sigma_i^k)^2}{\partial x_i} \tag{4.55}$$

Using $\mathrm{CRLB}[\rho_i^k]$ in Equation (4.51) to replace σ_i^k, then $\frac{\partial(\sigma_i^k)^2}{\partial x_i}$ becomes:

$$\frac{\partial(\sigma_i^k)^2}{\partial x_i}=\frac{c^2(\sigma_i^k)^4(x_i-x^k)}{2\pi^2 f_c^2(d_i^k)^4}\left(\frac{1}{(d_i^k)^2}\sum_{n\in\mathbb{N}_i^k}\frac{|S_n|^2}{\sigma_0^2}+\frac{2\pi^2 f_{\mathrm{sc}}^2}{c^2}\sum_{n\in\mathbb{N}_i^k}n^2\frac{|S_n|^2}{\sigma_0^2}\right). \tag{4.56}$$

where $\mathbb{N}_i^k$ is the index set of subcarriers used by the $MT_i \to BS^k$ link. Then

$$\frac{1}{(\sigma_i^k)^2}\frac{\partial(\sigma_i^k)^2}{\partial x_i}=\frac{4(x_i-x^k)}{(d_i^k)^2}\left(\frac{\overbrace{c^2\sum_{n\in\mathbb{N}_i^k}|S_n|^2}^{\triangleq A_i^k}+\overbrace{2(d_i^k)^2\pi^2 f_{\mathrm{sc}}^2\sum_{n\in\mathbb{N}_i^k}n^2|S_n|^2}^{\triangleq B_i^k}}{c^2\sum_{n\in\mathbb{N}_i^k}|S_n|^2+4(d_i^k)^2\pi^2 f_{\mathrm{sc}}^2\sum_{n\in\mathbb{N}_i^k}n^2|S_n|^2}\right). \tag{4.57}$$

Then the term $\frac{1}{(\sigma_i^k)^2}\frac{\partial(\sigma_i^k)^2}{\partial x_i}\frac{1}{(\sigma_i^k)^2}\frac{\partial(\sigma_i^k)^2}{\partial x_i}$ becomes:

$$\begin{aligned}\frac{1}{(\sigma_i^k)^2}\frac{\partial(\sigma_i^k)^2}{\partial x_i}\frac{1}{(\sigma_i^k)^2}\frac{\partial(\sigma_i^k)^2}{\partial x_i}=&\frac{16(x_i-x^k)^2}{(d_i^k)^4}\left(\frac{A_i^k+B_i^k}{A_i^k+2B_i^k}\right)^2\\ =&\frac{16}{(d_i^k)^2}\left(\frac{A_i^k+B_i^k}{A_i^k+2B_i^k}\right)^2\cdot\cos^2\theta_i^k.\end{aligned} \tag{4.58}$$

At the end, the whole second term of Equation (4.54) can be similarly derived and the $J[\vec{r}_i]$ states:

$$\begin{aligned} J_{\text{nc}}[\vec{r}_i] =& H_{\text{nc},i}^T C_{\text{nc},i}^{-1} H_{\text{nc},i} + \sum_{k\in\mathbb{B}_i} \frac{8}{(d_i^k)^2}\left(\frac{A_i^k + B_i^k}{A_i^k + 2B_i^k}\right)^2 \cdot \begin{pmatrix} \cos^2\theta_i^k & \cos\theta_i^k \sin\theta_i^k \\ \cos\theta_i^k \sin\theta_i^k & \sin^2\theta_i^k \end{pmatrix} \\ =& \sum_{k\in\mathbb{B}_i} \left(\frac{1}{(\sigma_i^k)^2} + \frac{8}{(d_i^k)^2}\left(\frac{A_i^k + B_i^k}{A_i^k + 2B_i^k}\right)^2\right) \cdot \begin{pmatrix} \cos^2\theta_i^k & \cos\theta_i^k \sin\theta_i^k \\ \cos\theta_i^k \sin\theta_i^k & \sin^2\theta_i^k \end{pmatrix}. \end{aligned} \tag{4.59}$$

The global FIM is again a block diagonal matrix:

$$J_{\text{nc}}[\vec{r}_{\text{MT}}] = \begin{pmatrix} J_{\text{nc}}[\vec{r}_1] & \cdots & 0 \\ 0 & \ddots & 0 \\ 0 & \cdots & J_{\text{nc}}[\vec{r}_M] \end{pmatrix}. \tag{4.60}$$

Cooperative Positioning

For cooperative positioning, similarly as we derived in Subsection 4.2.2 (Equation (4.18), (4.21)):

$$\begin{aligned} J_{[}\vec{r}_{\text{MT}}] &= J_{\text{nc}}[\vec{r}_{\text{MT}}] + J_{\text{c}}[\vec{r}_{\text{MT}}], \\ J_{\text{c}}[\vec{r}_{\text{MT}}] &\triangleq \begin{pmatrix} J_{\text{c},(1,1)} & \cdots & J_{\text{c},(1,M)} \\ \vdots & \ddots & \vdots \\ J_{\text{c},(M,1)} & \cdots & J_{\text{c},(M,M)} \end{pmatrix}. \end{aligned} \tag{4.61}$$

The difference is that $(\sigma_{i,j})^2$ is replaced by the CRLB$[\rho_{i,j}]$ and it depends on both $\vec{r}_i$ and $\vec{r}_j$. After the derivation similar as the non-cooperative case (Equation (4.53) - (4.60)), the non-cooperative contribution $J_{\text{nc}}[\vec{r}_{\text{MT}}]$ is the same as non-cooperative FIM (Equation (4.60)). For the cooperative contribution, first we define $A_{i,j}$ and $B_{i,j}$ similarly as in Equation (4.57):

$$\begin{aligned} A_{i,j} &\triangleq c^2 \sum_{n\in\mathbb{N}_{i,j}} |S_n|^2 \\ B_{i,j} &\triangleq 2(d_{i,j})^2 \pi^2 f_{\text{sc}}^2 \sum_{n\in\mathbb{N}_{i,j}} n^2 |S_n|^2 \end{aligned} \tag{4.62}$$

where $\mathbb{N}_{i,j}$ denotes the indices set of subcarriers used by the $MT_j \to MT_i$ link. For non-diagonal entity $J_{\mathrm{c},(i,j)}$ where $i \neq j$:

$$
\begin{aligned}
&J_{\mathrm{c},(i,j)} \\
&\quad = -\left(\delta_{i,j}\left(\frac{8}{(d_{i,j})^2}\left(\frac{A_{i,j}+B_{i,j}}{A_{i,j}+2B_{i,j}}\right)^2+\frac{1}{(\sigma_{i,j})^2}\right)\right. \\
&\qquad \left.+\,\delta_{j,i}\left(\frac{8}{(d_{j,i})^2}\left(\frac{A_{j,i}+B_{j,i}}{A_{j,i}+2B_{j,i}}\right)^2+\frac{1}{(\sigma_{j,i})^2}\right)\right)\cdot\begin{pmatrix}\cos^2\theta_{i,j} & \cos\theta_{i,j}\sin\theta_{i,j}\\ \cos\theta_{i,j}\sin\theta_{i,j} & \sin^2\theta_{i,j}\end{pmatrix}.
\end{aligned}
\tag{4.63}
$$

For block diagonal entity $J_{\mathrm{c},(i,i)}$:

$$
\begin{aligned}
J_{\mathrm{c},(i,i)} = &\sum_{\substack{j=1\\(j\neq i)}}^{M}\left(\delta_{i,j}\left(\frac{8}{(d_{i,j})^2}\left(\frac{A_{i,j}+B_{i,j}}{A_{i,j}+2B_{i,j}}\right)^2+\frac{1}{(\sigma_{i,j})^2}\right)\right.\\
&\left.+\,\delta_{j,i}\left(\frac{8}{(d_{j,i})^2}\left(\frac{A_{j,i}+B_{j,i}}{A_{j,i}+2B_{j,i}}\right)^2+\frac{1}{(\sigma_{j,i})^2}\right)\right)\cdot\begin{pmatrix}\cos^2\theta_{i,j} & \cos\theta_{i,j}\sin\theta_{i,j}\\ \cos\theta_{i,j}\sin\theta_{i,j} & \sin^2\theta_{i,j}\end{pmatrix}.
\end{aligned}
\tag{4.64}
$$

So far, we have derived the (non-) cooperative positioning CRLB considering the location-pathloss dependency. Compared with the result without this dependency, in general one more term $\frac{8}{d^2}\left(\frac{A+B}{A+2B}\right)^2$ is added to the inverse of the ranging variance. It can be considered as the lower bound of the inaccuracy of a position estimator with the TOA measurement adjusted by RSS.

4.3.5 Approximate the Pathloss Dependent Positioning CRLB

Looking into the ranging CRLB with the pathloss-location dependency in Equation (4.51) we can see when d increases, the first term of the denominator $\left(\frac{\sigma_0^2c^2}{\frac{1}{8\pi^2f_c^2\tau^4}\sum_{n=\lfloor-\frac{N-1}{2}\rfloor}^{\lfloor\frac{N-1}{2}\rfloor}|S_n|^2}\right)$ decreases much more rapidly than the second term $\left(\frac{f_{\mathrm{sc}}^2}{2f_c^2c^2\tau^2}\sum_{n=\lfloor-\frac{N-1}{2}\rfloor}^{\lfloor\frac{N-1}{2}\rfloor}n^2|S_n|^2\right)$. Therefore, in case of long distance, the first term can be ignored. Then for non-cooperative positioning, Equation (4.54) can be simplified as:

$$
\begin{aligned}
J[\vec{r}_i] \approx & H_{\mathrm{nc},i}^T C_{\mathrm{nc},i}^{-1} H_{\mathrm{nc},i} + \sum_{k\in\mathbb{B}_i}\begin{pmatrix}\frac{2(x_i-x^k)^2}{(d_i^k)^4} & \frac{2(x_i-x^k)(y_i-y^k)}{(d_i^k)^4}\\ \frac{2(x_i-x^k)(y_i-y^k)}{(d_i^k)^4} & \frac{2(y_i-y^k)^2}{(d_i^k)^4}\end{pmatrix}\\
= &\sum_{k\in\mathbb{B}_i}\left(\frac{1}{(\sigma_i^k)^2}+\frac{2}{(d_i^k)^2}\right)\begin{pmatrix}\cos^2\theta_i^k & \cos\theta_i^k\sin\theta_i^k\\ \cos\theta_i^k\sin\theta_i^k & \sin^2\theta_i^k\end{pmatrix}.
\end{aligned}
\tag{4.65}
$$

Similarly for the cooperative case,

$$J_{\substack{c,(i,j)\\ j\neq i}} \approx -\left(\delta_{i,j}\left(\frac{2}{(d_{i,j})^2}+\frac{1}{(\sigma_{i,j})^2}\right)+\delta_{j,i}\left(\frac{2}{(d_{j,i})^2}+\frac{1}{(\sigma_{j,i})^2}\right)\right) \cdot \begin{pmatrix} \cos^2\theta_{i,j} & \cos\theta_{i,j}\sin\theta_{i,j} \\ \cos\theta_{i,j}\sin\theta_{i,j} & \sin^2\theta_{i,j} \end{pmatrix}, \tag{4.66}$$

and

$$J_{c,(i,i)} \approx \sum_{\substack{j=1\\ (j\neq i)}}^{M}\left(\delta_{i,j}\left(\frac{2}{(d_{i,j})^2}+\frac{1}{(\sigma_{i,j})^2}\right)+\delta_{j,i}\left(\frac{2}{(d_{j,i})^2}+\frac{1}{(\sigma_{j,i})^2}\right)\right) \cdot \begin{pmatrix} \cos^2\theta_{i,j} & \cos\theta_{i,j}\sin\theta_{i,j} \\ \cos\theta_{i,j}\sin\theta_{i,j} & \sin^2\theta_{i,j} \end{pmatrix}. \tag{4.67}$$

The same result can be also obtained by using $\lim_{d\to\infty}\left(\frac{A+B}{A+2B}\right)^2$ to approximate $\left(\frac{A+B}{A+2B}\right)^2$ in Equation (4.59), (4.63) and (4.64).

Chapter 5

Resource Allocation Scheme for Cooperative Positioning

Most of the previous research in cooperative positioning assume the ranging variances for all the links are identical or only depend on distance. However, from the derivation in Chapter 4 we can see that for a real OFDM signal, this variance also depends on the transmit power, carrier frequency, bandwidth, the number and indices of used subcarriers ($|S_n|^2 \neq 0$), etc. All of these can be considered as the resources. Using different resources may lead to a quite different performance. The resource independent variance assumption from the previous research only holds when we consider a Time Division Multiple Access (TDMA) system, where all the links use the same spectrum resource within a specific time slot sequentially. In dense networks, the overall processing delay (T_{pro}) of such a system is proportional to the total number of the links L and increases quadratically with the number of MTs:

$$T_{\text{pro}} \propto L \sim O(M^2). \tag{5.1}$$

In a static scenario, a high accuracy can be guaranteed because the delay will not cause any additional uncertainty. However, if a system is dynamic, MTs use the neighbors' old estimates as the references which are less reliable when the delay increases. To avoid this effect, we divide the spectrum resource into small parts to serve multiple links simultaneously (similar as the Frequency Division Multiple Access (FDMA) technique in communications). As already mentioned before, for a real wireless system, the resources are limited. In order to improve the overall performance, a resource optimization scheme is required. Because of the high diversity and the interaction due to the cooperation, it is difficult to get a global optimal solution. Alternatively, we can use some suboptimal approaches like the greedy algorithm. Moreover, recently the usage of game theory in wireless communication has been discussed, especially for a distributed system [32], [33]. Inspired by that, several resource allocation games are proposed for our distributed cooperative positioning system. In this chapter, we mainly consider the problem of allocating the subcarriers. Although the precise definition of resource allocation may also include

distributing power, time slot, etc.

In this chapter, firstly a global greedy algorithm is introduced, which directly works with the global positioning CRLB. Then a partial decentralized approach inspired by the bidding game is raised to reduce the computational complexity. These two schemes will be compared with a centralized random allocation scheme (i.e. at each time step, certain amount of resources are allocated to a random link). At the end, we look into the purely decentralized case. First we introduce the non-cooperative game from the Nash equilibrium. Then we design a non-selfish utility function for our decentralized resource allocation game to reduce the interference.

5.1 Centralized Greedy Allocation Scheme

From the previous chapter, we already obtained (or at least estimated) a global positioning CRLB matrix ($2M \times 2M$):

$$\mathrm{CRLB}[\vec{r}_{\mathrm{MT}}] = \begin{pmatrix} G_{(1,1)} & \cdots & G_{(1,M)} \\ \vdots & \ddots & \vdots \\ G_{(M,1)} & \cdots & G_{(M,M)} \end{pmatrix}. \tag{5.2}$$

The trace of each block diagonal submatrix ($\mathrm{Trace}[G_{(i,i)}]$) is the lower bound of the position variance in distance for each MT. The mean of these traces denotes the average performance of all the MTs, which refers to the system's efficiency. Whereas the variance of them shows the performance fluctuations of different MTs which measures the system's fairness. These two values are used in the cost function (f_{cost}) for the centralized resource optimization scheme to achieve an efficiency-fairness tradeoff:

$$\text{efficiency:} \quad E = \frac{1}{M} \sum_{i=1}^{M} \mathrm{Trace}[G_{(i,i)}] \tag{5.3}$$

$$\text{fairness:} \quad F = \frac{1}{M-1} \sum_{i=1}^{M} (\mathrm{Trace}[G_{(i,i)}] - E)^2 \tag{5.4}$$

$$f_{\mathrm{cost}} = \nu_{\mathrm{c}} \cdot E^2 + (1 - \nu_{\mathrm{c}}) \cdot F \tag{5.5}$$

where $\nu_{\mathrm{c}} \in [0, 1]$ is the tradeoff factor. When $\nu_{\mathrm{c}} = 1$ the system is purely efficiency oriented whereas $\nu_{\mathrm{c}} = 0$ means the system only cares about the fairness. The resource allocation problem can be formulated as:

$$\mathrm{SC}_{\mathrm{MT,opt}} = \arg\min_{\mathrm{SC}_{\mathrm{MT}}} f_{\mathrm{cost}} \qquad \text{with the resource constraints} \tag{5.6}$$

where $\mathrm{SC}_{\mathrm{MT,opt}}$ is the optimal resource allocation strategy. The global CRLB matrix is obtained from the inverse of the global FIM, whose dimension increases with the

number of MTs (M). It is difficult to get a real global optimal solution when M is high. Alternatively, the greedy algorithm is used which tries to optimize the subproblems stepwise. Each time we take one piece of resources (could be a group of subcarriers), try to add them to each link, calculate a potential cost function and at the end assign it to the one with the lowest cost. Even with this scheme, the complexity is quite high. The computational complexity of allocating N_{res} pieces of resource is $O(M^5 N_{\text{res}})$ (assuming the complexity of inverting a $N \times N$ matrix is $O(N^3)$), which will dramatically grow when the network density increases. Besides, as a centralized approach, a central unit with very high computation capacity is required.

5.2 Partial Decentralized Allocation Bidding Game

The resource allocation problem can also be analogically considered as a bidding game. A central resource pool contains all the free resources and works as a coordinator. Each candidate MT acts as a player of this game. At each time step, the resource pool chooses some resources and the players bid for it. The resource will be assigned to the player who offers the highest price. In our case, the price from each player is designed to denote how much improvement it will get with this these additional resources.

We derived an approximation of local positioning CRLB in Subsection 4.2.3 and the positioning CRLB with the OFDM signals in Section 4.3. An MT (MT_i) can add the potential new resources to each of its links and calculate the approximated local positioning CRLBs. The MT takes the smallest one and names it $\text{CRLB}[\vec{r}_i]_{\text{loc,new}}$. The potential improvement can be obtained by subtracting $\text{CRLB}[\vec{r}_i]_{\text{loc,new}}$ from the current local CRLB approximation ($\text{CRLB}[\vec{r}_i]_{\text{loc,cur}}$). The value of this improvement are transmitted to the central resource pool as the bidding price of MT_i:

$$\text{Price}_i = \text{CRLB}[\vec{r}_i]_{\text{loc,cur}} - \text{CRLB}[\vec{r}_i]_{\text{loc,new}}. \tag{5.7}$$

The resource pool compares the prices from all the MTs and gives this resource to the one with the highest price. This resource will be used for this specific link.

The local CRLB matrix is the inverse of the local FIM (only 2×2). For a dense network the complexity of it can be neglected. Unlike the centralized greedy approach, for the bidding game the computations take place at both the MTs and the central unit. The MT's complexity linearly depends on the number of neighbors ($O((M_i + K^i)N_{\text{res}})$). The central unit's complexity depends on the number of MTs ($O(MN_{\text{res}})$). For dense network, the overall complexity is $O(M^2 N_{\text{res}})$.

5.3 Decentralized Resource Allocation Game

For a purely decentralized system, each MT chooses the resources by itself. It is difficult to find an allocation scheme which works individually, meanwhile achieves

the global optimal performance. A more severe problem is the interference. As there is no central coordinator available, a MT is not aware of which resources are used by others. Therefore, the subcarriers may be reused by multiple links, which leads to interference. The SNR will be replaced by the SINR (Signal-to-Interference-and-Noise Ratio). Consequently, the ranging accuracy will decrease. It is a common feature of decentralized systems, sometimes referred to as the *Price of Anarchy* [34].

To reduce this effect, we assume the system works with a random access protocol. Each MT transmit and to listen the positioning signals only within a certain time window. Instead of designing a specific protocol, we only consider the effect of random access in a statistic sense. i.e. If there are two links sharing the same subcarrier, We assume the chance of having interference is p_{intf}. It is like exploring the diversity in time domain. When $p_{\text{intf}} = 0$, the subcarriers are used by links sequentially, like in a TDMA system. Whereas when $p_{\text{intf}} = 1$, all the links measure simultaneously. With this random access assumption, the interference can be reduced with the cost of increasing the processing delay.

5.3.1 Non-Cooperative Allocation Game

Game theory is a mathematical tool to analyze the rational behaviors of human in a competitive environment. It has been applied to predict politics and economy and to make decision in those areas. There are many types of game in the game theory. The most commonly used one is called the non-cooperative game. The idea of the non-cooperative game theory is as follow:

There are several players in a competitive game known as agents. The agents cannot communicate with each other. An agent (say the i^{th} one: a_i) has some candidate strategies $\lambda_{m(i)}$[1]$\in \Lambda_i, m = 1, 2, \ldots$, where Λ_i is the strategies set for a_i. An utility function $u_{m(i)}$ can be formulated based on the strategies chosen by a_i and the others which evaluates the benefit (can also be the cost, penalty, etc. depending on the type of the game) of this choice. A rational agent will be aware of others' potential strategies and the corresponding effects to itself. The goal of each agent is to optimize its utility function by applying a specific strategy.

The game theory normally cannot find a global optimum. Instead, it looks for a stable state known as the *equilibrium*. The most famous one is called *Nash equilibrium* (NE, named after John Forbes Nash), which states [35]:

Definition 1 (Nash Equilibrium) *For a beneficial utility function (the larger the better), the joint strategies $(\lambda_{\bar{m}(1)}, \lambda_{\bar{m}(2)}, \cdots)$ is a NE, if no agent can get further improvement (e.g. increasing the utility) by exploring its own strategy diversity, i.e.:*

$$\forall ag_i : u_{\bar{m}(i)} \geq u_{m(i)} \quad \forall \lambda_{m(i)} \in \Lambda_i$$

In [35] Nash proved that for any finite non-cooperative game, at least one NE point exists. A common example of the non-cooperative game is the *prisoner's dilemma*

[1] This notation conflicts with the notation for the MT_i's m^{th} neighboring MT and is used restrictively in this section.

a_1 \ a_2	confess	silent
confess	(3,3)	(0,12)
silent	(12,0)	(1,1)

Table 5.1: Prisoner's dilemma

a_1 \ a_2	null	sc_1	sc_2	sc_1, sc_2
null	(0,0)	(0,1)	(0,1)	(0,2)
sc_1	(1,0)	(0.1,0.1)	(1,1)	(0.1, 1.1)
sc_2	(1,0)	(1,1)	(0.1,0.1)	(0.1,1.1)
sc_1, sc_2	(2,0)	(1.1,0.1)	(1.1, 0.1)	(0.2,0.2)

Table 5.2: Non-cooperative resource allocation game

[36]: Assuming two men (ag_1, ag_2) are arrested without evidence. They cannot communicate to each other, but both of them can decide to confess ($\lambda_{1(i)} = \text{confess}$) or to keep silent ($\lambda_{2(i)} = \text{silent}$). If both confess, they will be prisoned for three months ($u_{\text{confess}(1)} = u_{\text{confess}(2)} = 3$ months). If both of them keep silent, they will be set free after one month ($u_{\text{silent}(1)} = u_{\text{silent}(2)} = 1$ month). However, if one man (say ag_1) confesses and the other keeps silent, the former will be released immediately as a reward ($u_{\text{confess}(1)} = 0$ months) whereas the latter one will be sentenced to one year ($u_{\text{silent}(2)} = 12$ months), and vice versa. The strategies and utilities are shown in Table 5.1, where the joint utilities of strategies pair $(\lambda_{m(1)}, \lambda_{n(2)})$ is denoted as $(u_{m(1)}, u_{n(2)})$. The utility function represents the penalty. The goal of an agent is to minimize its own utility. From Table 5.1 we can find no matter what the other decides, the rational reaction for an agent is to confess. Therefore, the only NE for this game is both of them confessing (utilities (3,3)). It is clear that the global optimum is achieved when both of them keep silent (utilities (1,1)). However, without communications, none of the individuals has the motivation to keep silent.

Now come back to our problem: For a decentralized cooperative positioning system, MTs are considered as agents and the strategies set includes adding new subcarriers or not, which subcarriers to add, etc. First we investigate a simple case: Assuming two MTs are going to share two subcarriers (sc_1 and sc_2). The strategies for each MT should contain not adding a new subcarrier (null), adding one subcarrier (sc_1 or sc_2) and adding both (sc_1, sc_2). We further assume if a subcarrier is used exclusively, it will contribute to the utility for one unit, but if a subcarrier is shared with both MTs, due to the interference, it only brings 0.1 unit contribution to each utility. Similarly as the prisoner's dilemma, a table of strategies and utility can be shown in Table 5.2. The only NE is obtained when both of the agents use both of the subcarriers. If there is no cooperative agreement, an agent will always behave selfishly and tries to occupy both of the subcarriers, even though 80% of

the other joint allocation strategies achieve higher global utilities (except the three along the diagonal). The result can be extended to the scenario with more MTs and subcarriers. With non-cooperative resource allocation game, all MTs are trying to occupy as many subcarriers as possible. As the consequence, the interference will be dominant which may lead to a poor performance.

5.3.2 Resource Allocation Game with Cooperative Behavior

In the previous subsection, a non-cooperative allocation game was introduced, where the price of anarchy problem may be severe. To avoid this, an allocation game with the cooperative behavior is proposed. In this game, a MT is not a greedy agent anymore. It will be satisfied when its targeting estimation accuracy is achieved. Meanwhile, it evaluates the probability to have interference based on the number of used subcarriers, and jointly chooses its resource allocation strategy.

We assume there are N subcarriers and M MTs. for MT_i the current number of subcarriers is defined as $n_{\mathrm{sc},i}$, the targeting accuracy as ϱ_i and the current local CRLB approximate as $\mathrm{CRLB}[\vec{r}_i]_{\mathrm{loc,cur}}$. the relative need of improvement Δ_i is:

$$\Delta_i = \frac{\mathrm{CRLB}_{[\vec{r}_i]\mathrm{loc,cur}} - (\varrho_i \cdot \gamma)^2}{\varrho_i^2}, \tag{5.8}$$

γ is the redundancy factor due to the fact that the CRLB may be not achievable by a suboptimal positioning algorithm. Instead of using a deterministic strategy, we use a statistic one. If $\Delta_i > 0$ which means MT_i is not satisfied with the current accuracy. We design $p_{i,\mathrm{get}}$ as the probability of MT_i getting some new subcarriers. $p_{i,\mathrm{get}}$ depends on the required improvement and the guessed interference condition. Whereas if $\Delta_i < 0$ which means the accuracy is more than enough. In order to reduce the potential interference for others, MT_i is willing to release some subcarriers with the probability $p_{i,\mathrm{release}}$.

Assuming all the other MTs have the same number of subcarriers randomly chosen from all the subcarriers. For MT_i, the probability that a single subcarrier is interfered by a specific neighbor (MT_j)'s ranging signal is:

$$p_{i,j,\mathrm{one}} = \frac{\binom{n_{\mathrm{sc},i}-1}{N-1}}{\binom{n_{\mathrm{sc},i}}{N}} \cdot p_{\mathrm{intf}}. \tag{5.9}$$

The probability that a single subcarrier is interfered reads:

$$\begin{aligned} p_{i,\mathrm{one}} =& 1 - (1 - \frac{\binom{n_{\mathrm{sc},i}-1}{N-1}}{\binom{n_{\mathrm{sc},i}}{N}} \cdot p_{\mathrm{intf}})^{(M-1)} \\ =& 1 - (1 - \frac{n_{\mathrm{sc},i}}{N} \cdot p_{\mathrm{intf}})^{(M-1)}. \end{aligned} \tag{5.10}$$

We define a percentage factor $\zeta \in [0, 1]$. Then the probability that less than $\zeta n_{\mathrm{sc},i}$

subcarriers get interference follows the Bernoulli distribution:

$$p_\zeta = \sum_{k=0}^{\lceil n_{\mathrm{sc},i}\cdot\zeta\rceil} \binom{k}{n_{\mathrm{sc},i}} p_{i,\mathrm{one}}^{k}(1-p_{i,\mathrm{one}})^{(n_{\mathrm{sc},i}-k)}. \tag{5.11}$$

If $\Delta_i > 0$, probability of getting some new resources should be constructed in a way that it monotonically increases with respect to both Δ_i and p_ζ. Moreover, it should not exceed the interval of [0,1].We propose a function which fulfill the above constraints:

$$p_{i,\mathrm{get}} = \nu_{\mathrm{dc}} \cdot e^{-\frac{1}{\Delta_i}} + (1-\nu_{\mathrm{dc}})p_\zeta, \tag{5.12}$$

where $\nu_{\mathrm{dc}} \in [0,1]$ is a control factor to control the tradeoff between accuracy improvement and interference avoidance. If $\Delta_i < 0$, the probability of releasing some occupied resources should be designed in a way that it monotonically decreases with respect of both Δ_i and p_ζ. It should also be constrained by the interval $[0,1]$. Similarly, we design the function as follow:

$$p_{i,\mathrm{release}} = \nu_{\mathrm{dc}} \cdot e^{\frac{1}{\Delta_i}} + (1-\nu_{\mathrm{dc}})(1-p_\zeta). \tag{5.13}$$

By this strategy, the overall number of used subcarriers is controlled by both current accuracy and chance of interference, which on some levels improves the performance. Figure 5.1 shows how the probability of getting or releasing subcarriers depends on the current local CRLB approximation and the number of subcarriers a MT already has.

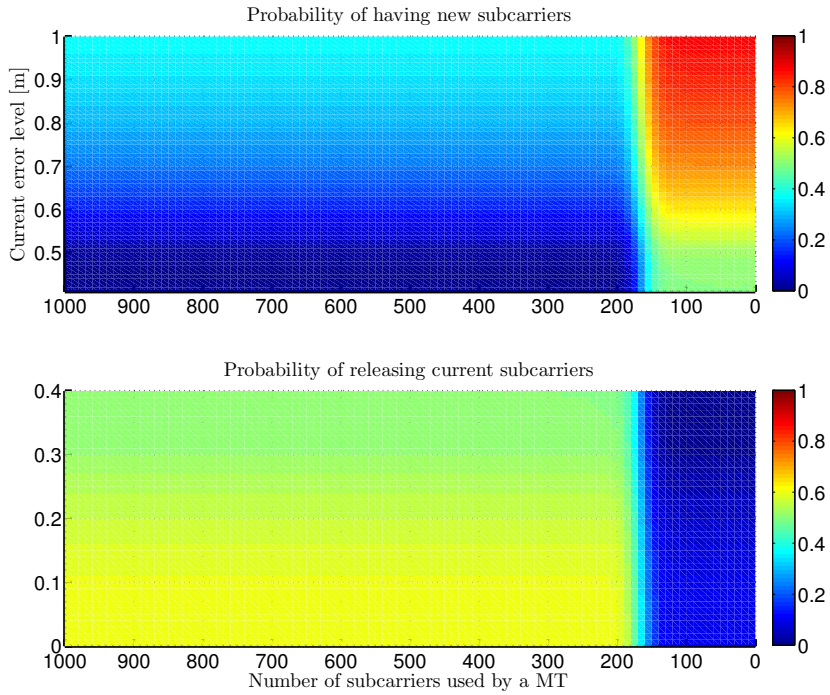

Figure 5.1: The probability of getting some new subcarriers (upper) and the probability of releasing some current subcarriers (lower). $M = 5$, $N = 1000$, $\varrho_i = 0.5$ m, $p_{\text{intf}} = 1$, $\zeta = 0.5$ and $\gamma = 0.8$

Chapter 6

Simulation

In this chapter, some scenarios are set. The simulation results with the previously presented schemes are shown. At the end of each scenario, the analysis is presented.

6.1 Scenario 1

In Scenario 1, we use the deterministic maps to compare the resource allocation solutions from different allocation schemes. three BSs and two MTs are located in the maps. We change the location of one BS to see the impact to the allocation solution (Figure 6.1 and 6.4). We used an OFDM system for positioning which has the total bandwidth of 20 MHz (0MHz∼20MHz). The subcarrier spacing is set to 10 KHz and the carrier frequency is set to 5.2 GHz. Each used subcarrier transmits the signal with the power of -30dBm. Only the TOA measurements are considered. The allocation solutions are shown in Figure 6.2, 6.3, 6.5 and 6.6.

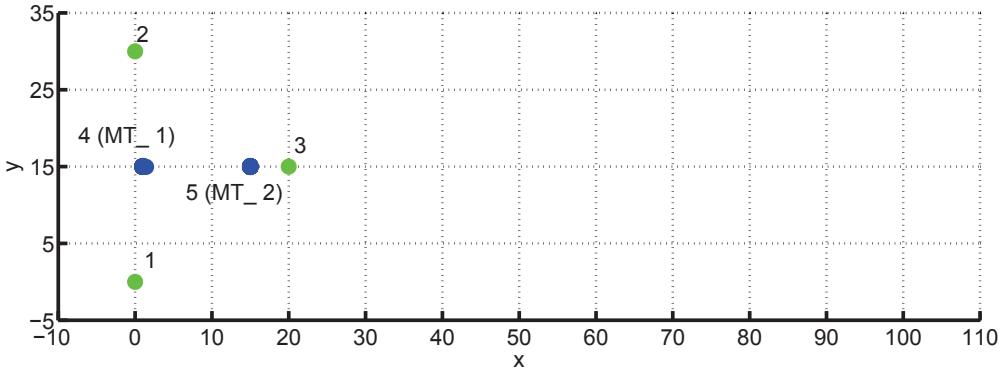

Figure 6.1: The map setup of Scenario 1. The green dots are the true positions of BSs and the blue ones are the MTs. In this case, the third BS is close to the MTs.

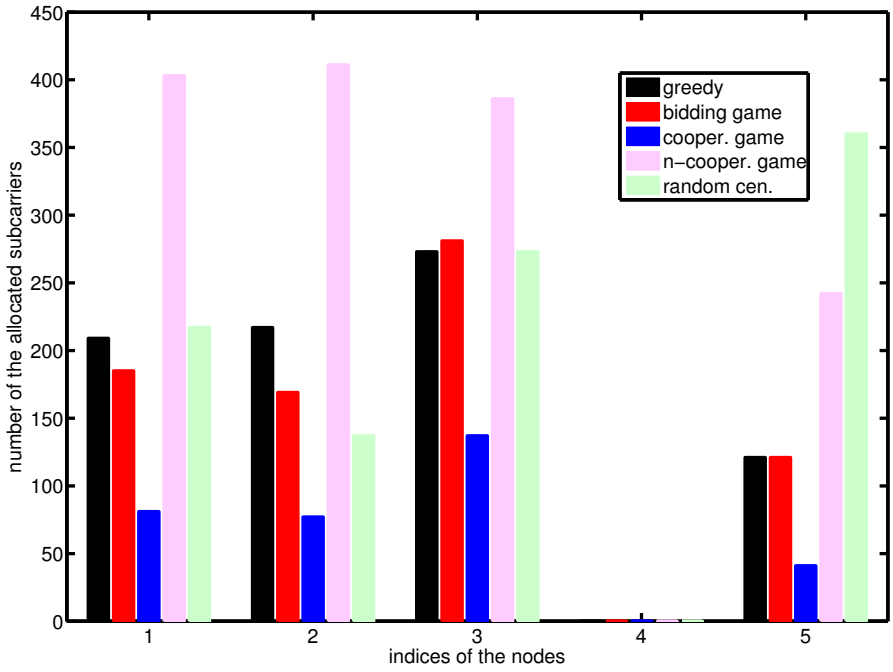

Figure 6.2: Comparison of the resource allocation solutions for MT_1 from different resource allocation schemes in Scenario 1 when the third BS is nearby.

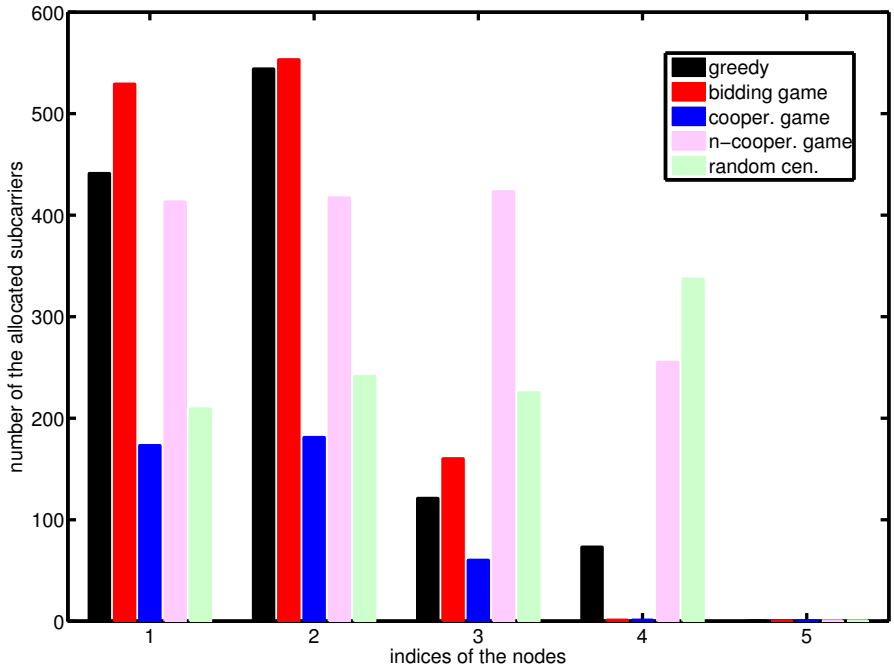

Figure 6.3: Comparison of the resource allocation solutions for MT_2 from different resource allocation schemes in Scenario 1 when the third BS is nearby.

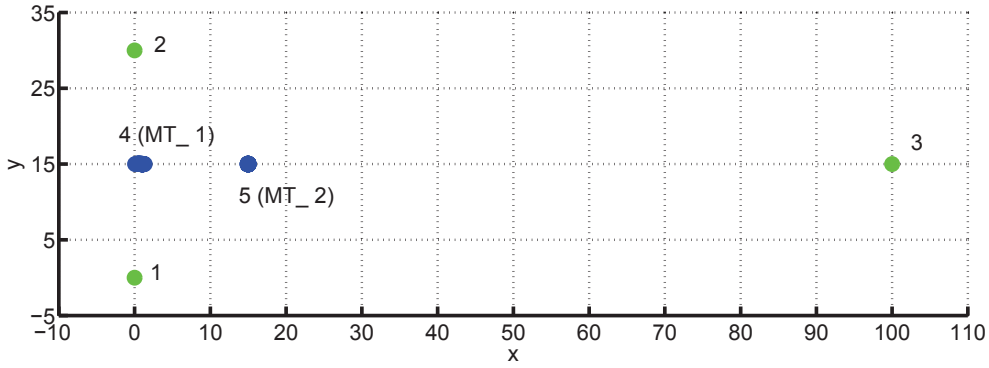

Figure 6.4: The map setup of scenario 1. The green dots are the true positions of BSs and the blue ones are the MTs. In this case, the third BS is far from the MTs.

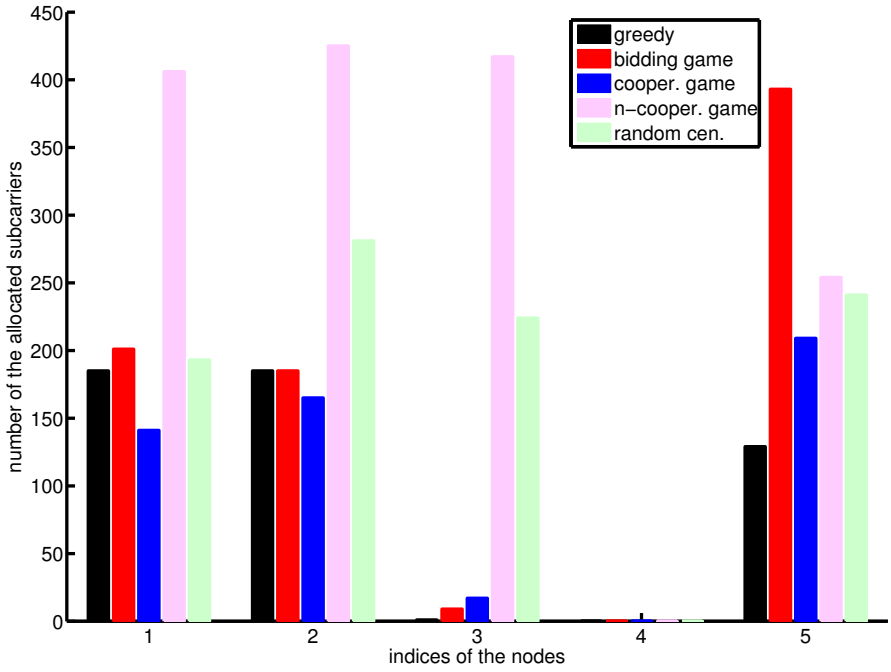

Figure 6.5: Comparison of the resource allocation solutions for MT_1 from different resource allocation schemes in Scenario 1 when the third BS is far away.

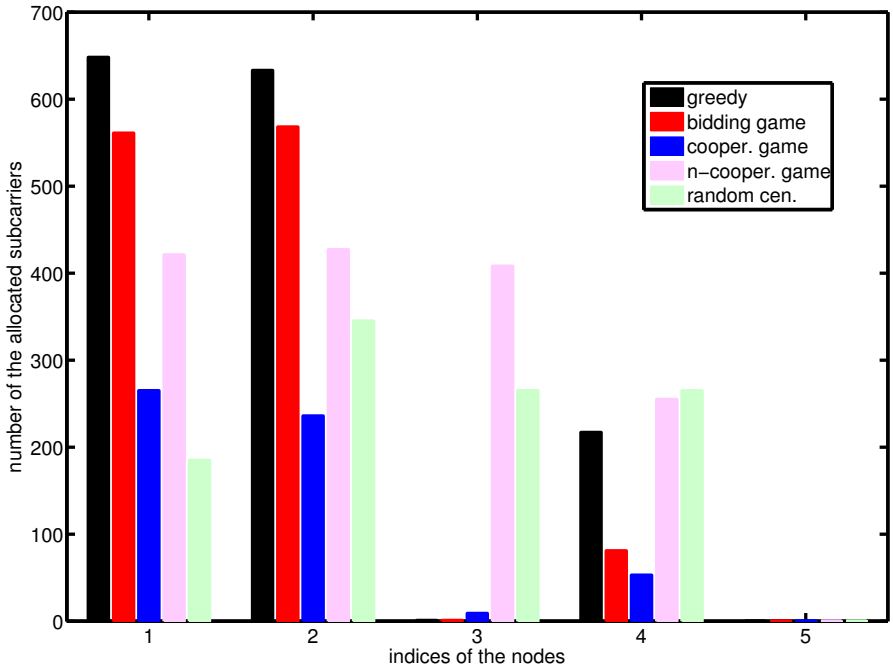

Figure 6.6: Comparison of the resource allocation solutions for MT_2 from different resource allocation schemes in Scenario 1 when the third BS is far away.

From the simulation results we can see, if the BS is close (Figure 6.1), the MTs will use the BS-MT links instead of the peer-to-peer links (Figure 6.2 and 6.3). Because the location inaccuracy of a neighboring MT is taken into account. Whereas when a BS is far (Figure 6.4), the MTs will focus on the peer-to-peer links instead of the long distance BS-MT link (Figure 6.5 and 6.6). Because the SNR is attenuated due to the long propagation distance which decreasing the measurement reliability. Moreover, when a BS is far, we can observe that the MT_1 put more effort on the peer-to-peer link than the MT_2. It is because of the geometric. For MT_1, a reference point on the right can significantly decease the estimation uncertainty at x dimension. Whereas for MT_2, an additional MT on the left will not offer big gain because there have already been two BSs on the left. In general, we can find that the three allocation schemes we proposed make similar allocating decisions.

6.2 Scenario 2

In Scenario 2, thirteen BSs are located uniformly in a 60 m $\times$ 60 m map, two MTs are located at the predefined positions. All the BSs and the MTs are stationary. We used a similar OFDM system as in Scenario 1, expect the total bandwidth is 2 MHz

(0MHz-2MHz). We use GN for this scenario. The map setup can be found in Figure 6.7 and the simulation results (RMS (root mean square) error) with different resource allocation schemes are shown in Figure 6.8. The resource allocation solutions can be found in Figure 6.9 and 6.10.

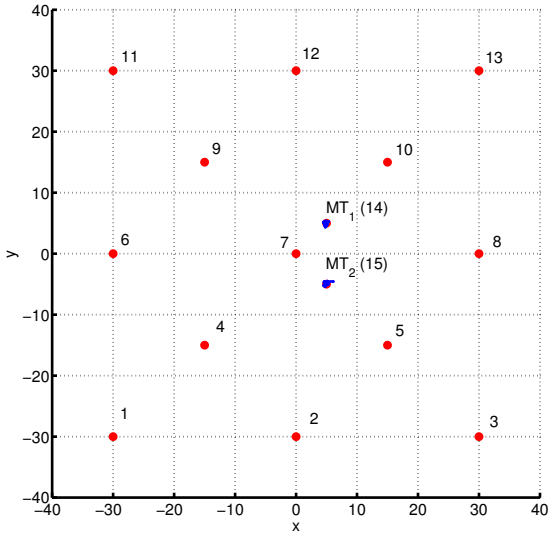

Figure 6.7: The map setup of scenario 2. The red dots are the true positions for both the BSs and the MTs. The blue traces are the connected estimations for MTs

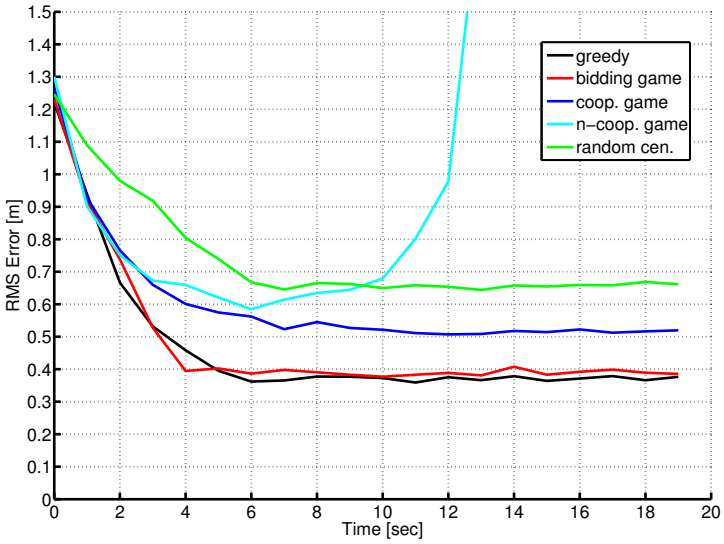

Figure 6.8: The comparison of different resource allocation schemes in Scenario 2

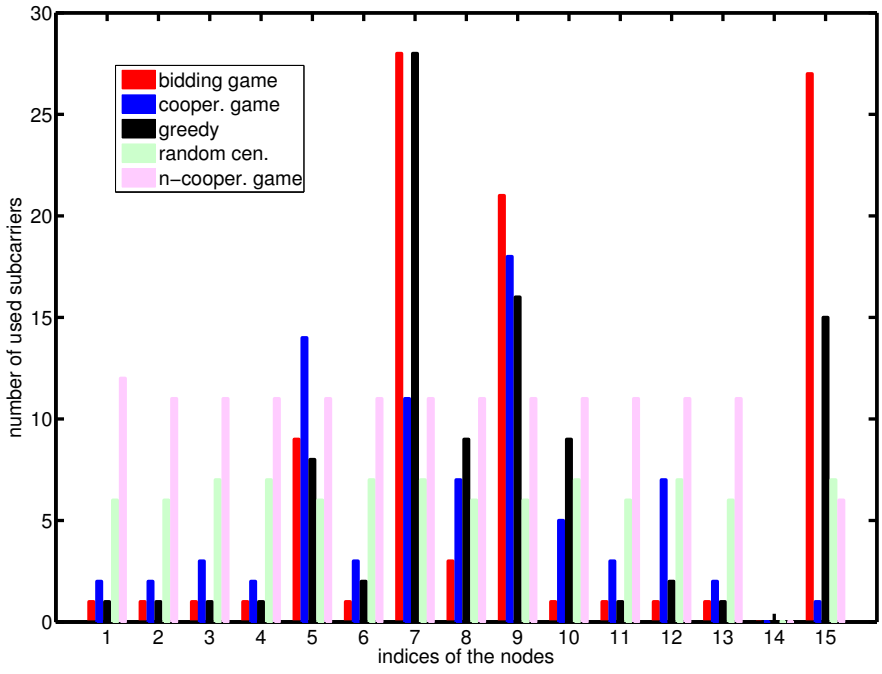

Figure 6.9: Comparison of the resource allocation solutions for MT_1 from different resource allocation schemes in Scenario 2.

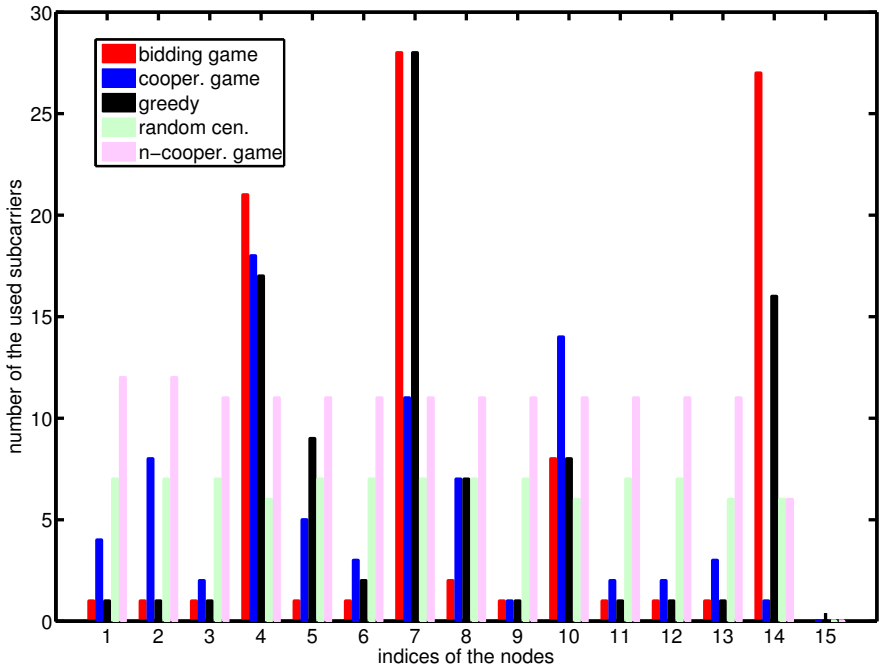

Figure 6.10: Comparison of the resource allocation solutions for MT_2 from different resource allocation schemes in Scenario 2.

From Figure 6.8, we can see that in this specific scenario, the resource allocation schemes works well. The result of bidding game is close to the centralized greedy algorithm. The greedy algorithm has a much higher complexity: $O(M^5 N_{\text{res}})$ (Section 5.1), whereas the bidding game has a relatively low complexity: $O(MN_{\text{res}})$ for the central unit and $O(MN_{\text{res}})$ for each MT. Therefore, we can conclude that the bidding game is more suitable for a real system. The cooperative game performs worse than the greedy scheme and the bidding game but better than the random centralized approach and the non-cooperative game. For a decentralized approach, we find the performance of cooperative game is quite good. For the non-cooperative game, each MT always tries to increase its number of subcarriers. Therefore, after ten iterations, the interference is dominant which makes the error increasing rapidly. From Figure 6.9 and 6.10 we can see that for the random centralized scheme and the non-cooperative game, the resource are allocated randomly. For the other three, only the links with short distance are chosen. More specifically the allocation solutions from bidding game and greedy scheme are similar. The biggest different between the cooperative game and the other two is that for the cooperative game, the resources will not be spent on the peer-to-peer links.

6.3 Scenario 3

We set a more general scenario in this section. We use a similar map as in Scenario 2, except that there are 5 MTs in the map, initialized with random locations. The MTs can be stationary or moving. For the moving cases, the RWP mobility model is used to move the MTs in the centering 50 m $\times$ 50 m area. For the OFDM system, the bandwidth is increased to 10MHz (0MHz$\sim$10MHz). The scenario setup can be find in Figure 6.11.

In this scenario, we firstly compare the performances of different prediction mobility models for the PF. The MTs move with several velocities (0.1 m/s, 1.0 m/s and 2.0 m/s). The MLF_LT model will be compared with the WNA with different acceleration variances (0.2, 0.5, 1.0 and 2.0 m^2/s^4). The RMS error can be found in Figure 6.12 - 6.14. Then we look into the simulation results with different resource allocation schemes (Figure 6.15 - 6.21).

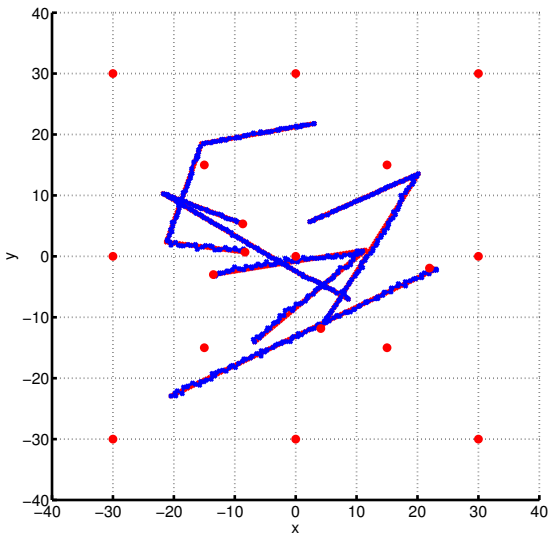

Figure 6.11: The map setup of scenario 3 with the RWP (v = 1.0 m/s). The red dots are the true positions for both the BSs and the MTs. The blue traces are the connected estimations for MTs. The red lines (mostly overlapped by the blue ones) connect the true position in time, which show the true tracks.

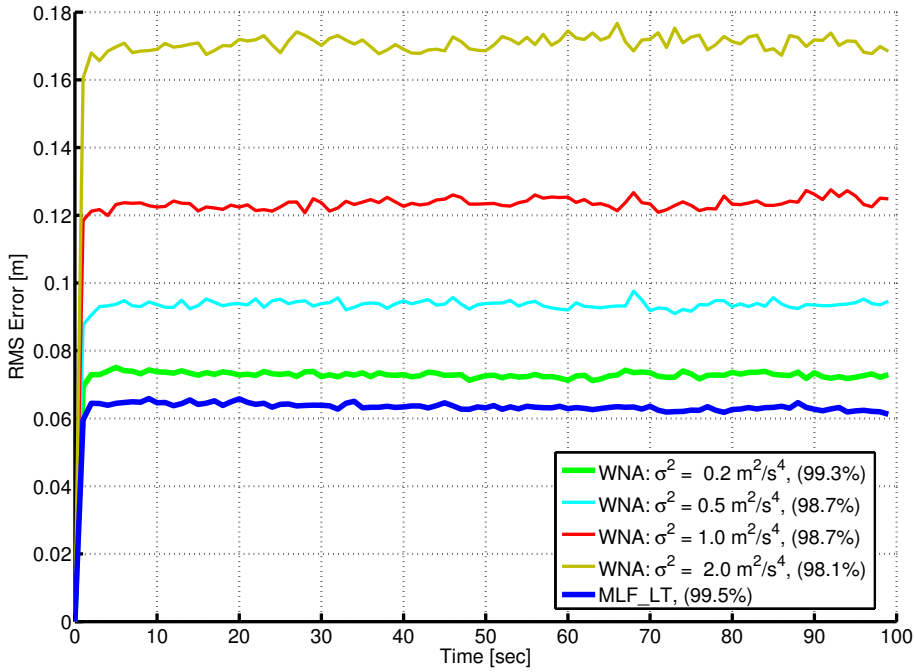

Figure 6.12: RMS error comparisons of WNA and MLF_LT. There are 13 BSs and 5 MTs in the map. MTs move with the RWP model (v = 0.1 m/s). The percentage in the legends show the probability of successful tracking. In this case the optimal parameter for WNA is $\sigma^2 = 0.2\text{m}^2/\text{s}^4$.

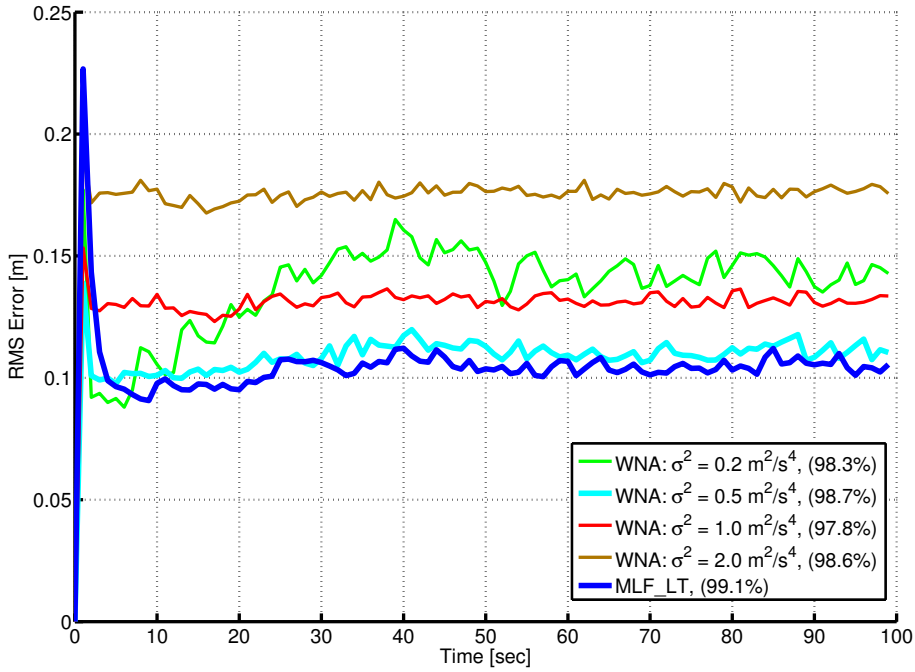

Figure 6.13: RMS error comparisons of WNA and MLF_LT. There are 13 BSs and 5 MTs in the map. MTs move with the RWP model (v = 1.0 m/s). The percentage in the legends show the probability of successful tracking. In this case the optimal parameter for WNA is $\sigma^2 = 0.5\mathrm{m}^2/\mathrm{s}^4$.

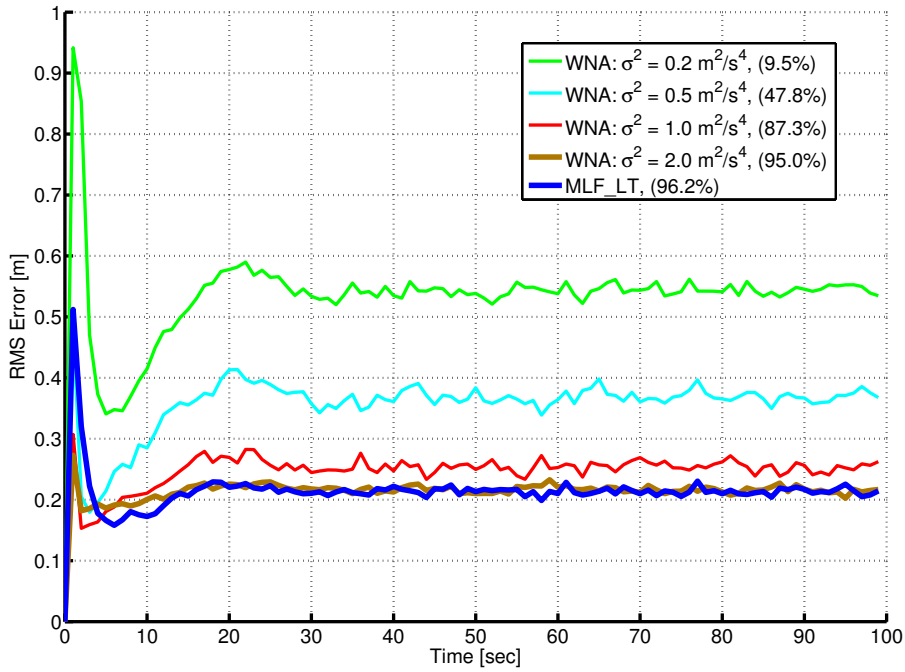

Figure 6.14: RMS error comparisons of WNA and MLF_LT. There are 13 BSs and 5 MTs in the map. MTs move with the RWP model (v = 2.0 m/s). The percentage in the legends show the probability of successful tracking. In this case the optimal parameter for WNA is $\sigma^2 = 2.0\text{m}^2/\text{s}^4$.

We can see that the performance of WNA is sensitive to the chosen parameter (acceleration variance). The MLF_LT mobility uses the same group of parameters for all the cases ($\mu_f = 0$, $\ell_f = 0.7$, $a_v = 1.0$ and $b_v = 2.0$). In all the three cases, MLF_LT performs better or at least as well as the WNA with the optimal choices for parameter[1]. We can see that MLF_LT is more robust and offers a more accurate estimation.

[1]the best choice among all the candidate parameters we try, not the theoretical optimum

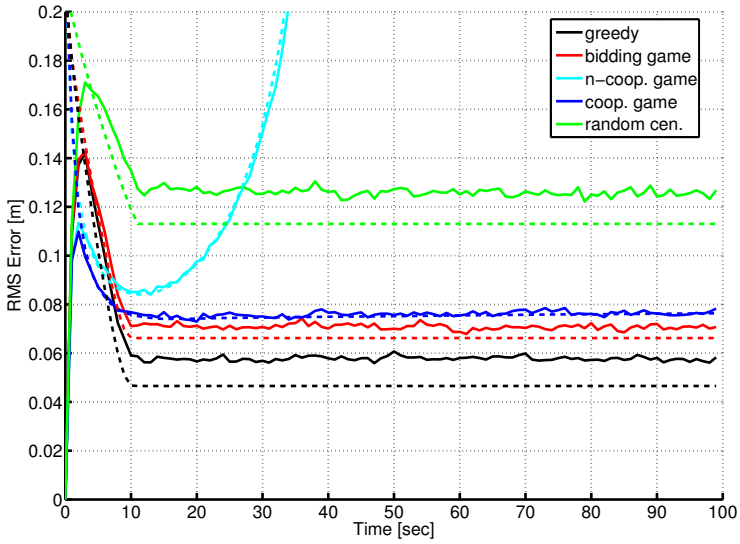

Figure 6.15: The comparison of different resource allocation schemes with stationary MTs in Scenario 3. The dashed lines show the corresponding CRLB

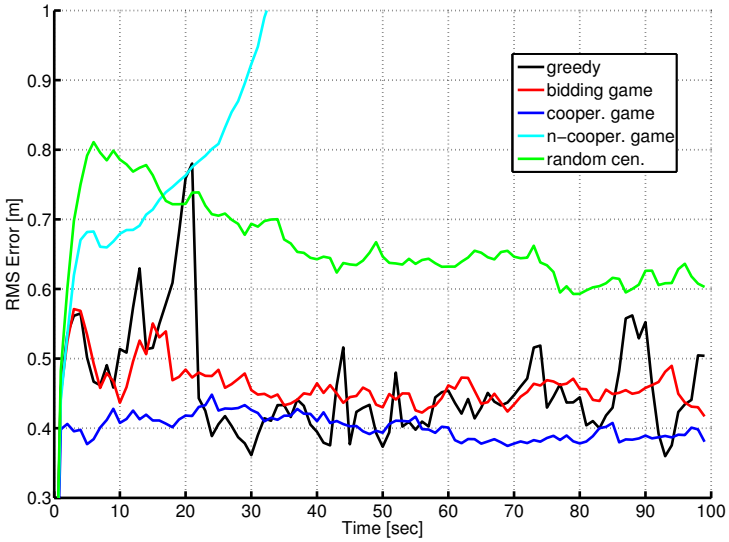

Figure 6.16: The RMS error comparison of different resource allocation schemes with moving MTs in Scenario 3, without link evaluation

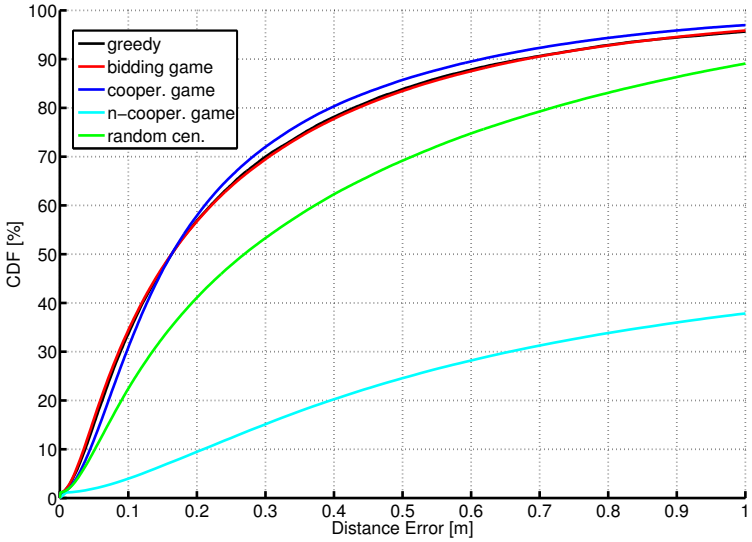

Figure 6.17: The CDF (cumulative distribution function) comparison of different resource allocation schemes with moving MTs in Scenario 3, without link evaluation

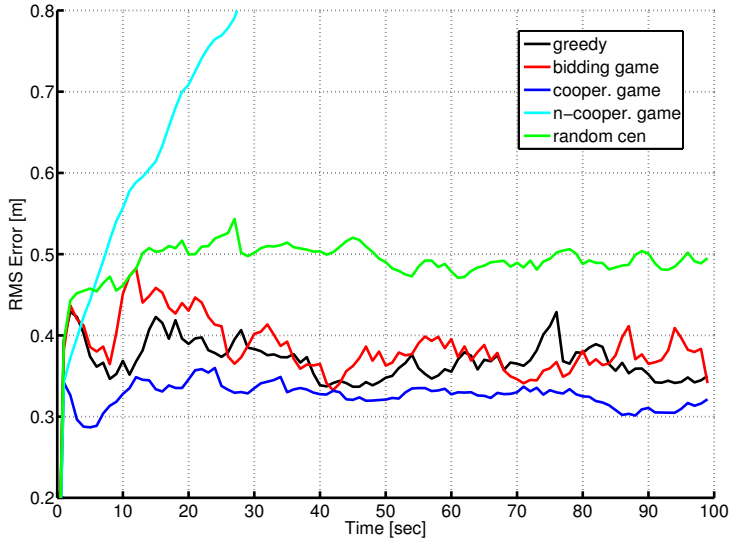

Figure 6.18: The RMS error comparison of different resource allocation schemes with moving MTs in Scenario 3, with link evaluation

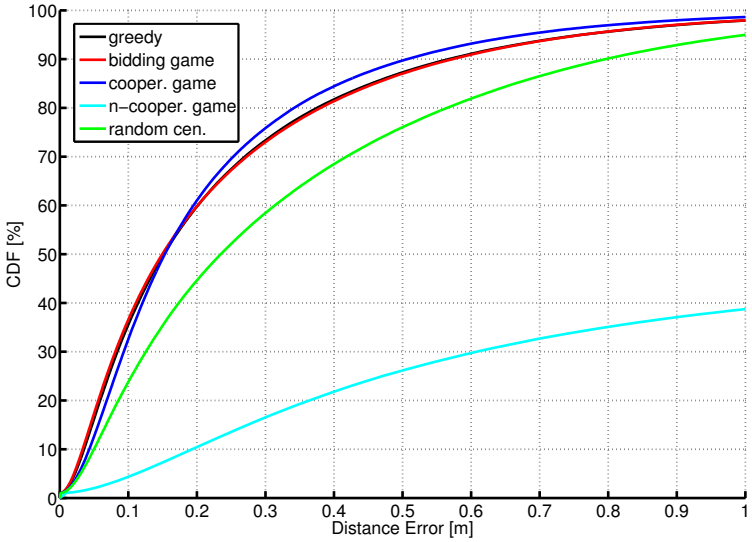

Figure 6.19: The CDF comparison of different resource allocation schemes with moving MTs in Scenario 3, with link evaluation

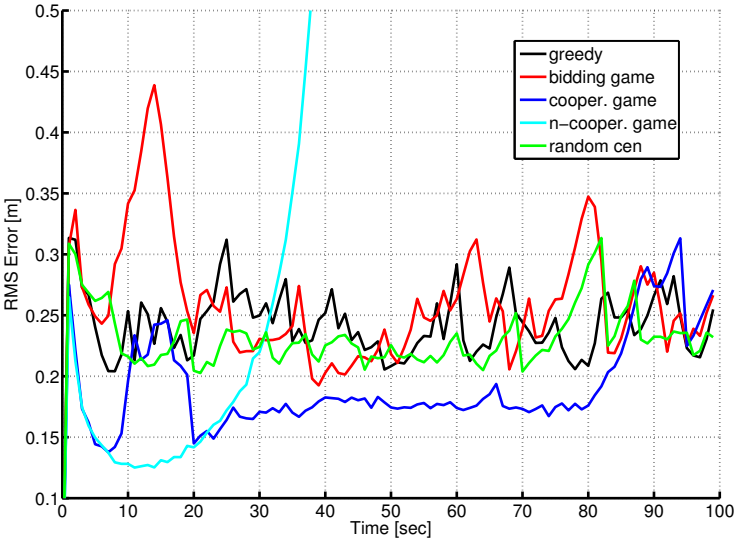

Figure 6.20: The RMS error comparison of different resource allocation schemes with moving MTs in Scenario 3, with link evaluation + speed estimation (adding v^2 as the additional variance caused by the movement)

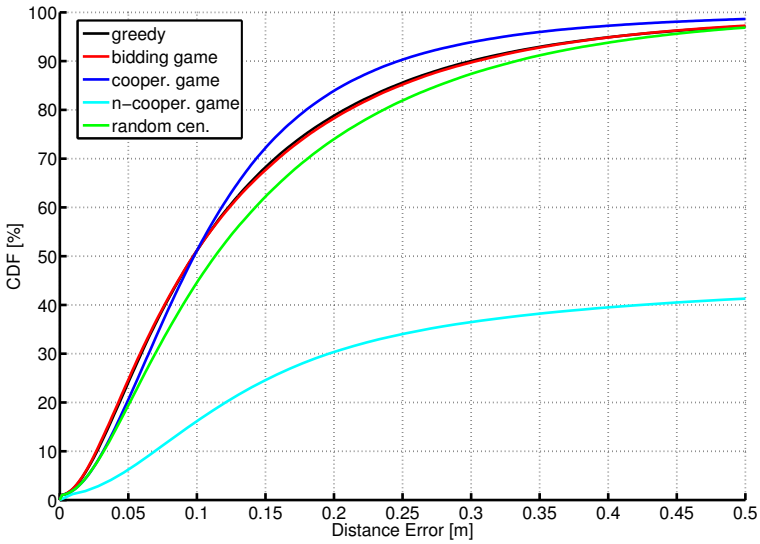

Figure 6.21: The CDF comparison of different resource allocation schemes with moving MTs in Scenario 3, with link evaluation + speed estimation (adding v^2 as the additional variance caused by the movement)

From Figure 6.15 we can see for the stationary scenario, the greedy algorithm is the best one. The bidding game and the cooperative game perform similarly. The random centralized is not as good as the former three. The non-cooperative game performs well at the beginning, and then loses the accuracy because the interference becomes severe. We can also see that for stationary case, the performance is close to the CRLB. From Figure 6.16 and 6.17 we can find the positioning accuracy decreases if the system is dynamic. However, a significant improvement can still be observed by applying the resource allocation schemes. If the link evaluation scheme is used (Figure 6.18 and 6.19), an improvement can be obtained. If we additionally consider the mobility uncertainty for the link evaluation scheme (Figure 6.20 and 6.21), a more accurate estimation is achievable. However, in this case, the resource allocation gain is less significant. The greedy scheme and the bidding game perform similarly as randomly allocating the resources. One reason could be that the movement variance information is not accurate enough. In this scenario, the cooperative game performs slightly better than the greedy algorithm and the bidding game. Even the non-cooperative game performances better than the greedy algorithm at the first twenty time steps. It may comes from the different scheme criteria or because the advantage of resource reusing is more significant than the interference effect.

Chapter 7

Conclusion and Future Work

7.1 Conclusion

In this thesis, we look into distributed cooperative positioning with the next generation mobile radio system. We introduce two distributed cooperative positioning algorithms: the distributed Gauss-Newton method (GN) and the particle filter (PF) and a nature-inspired mobility model: Lévy-Flight (LF). Several modified versions of the LF are proposed. We test the modified Lévy-Flight (MLF) and the modified Lévy-Flight and Lévy-Track (MLF_LT) and compare the performance with the conventional white noise acceleration (WNA). It is shown that the MLF_LT outperforms the WNA with different velocities (0.1 m/s, 1 m/s and 2 m/s).

We propose a link evaluation scheme to reduce the error propagation effect. The simulation results show that by this scheme, the performance can be improved. It can also be used to consider the dynamic uncertainty which offers a further improvement.

We explore the delay-pathloss dependency. With this dependency, the delay estimation can be corrected by the RSS. It is shown that for a short distance ranging, exploring this dependency can offer a significant gain. Whereas when the neighbor is far, the RSS is less reliable, and the accuracy of this TOA-RSS hybrid metric is almost the same as to use only the TOA. For cooperative positioning, because of the interaction, it is difficult to calculate the CRLB for a specific user. We combine the link evaluation scheme and the positioning CRLB and present a local approximation of the cooperative CRLB. The simulation results show that it will become stable slightly above the true cooperative CRLB within several iterations.

In Chapter 5 we consider the resources limitation of a real wireless system and proposed several resource allocation schemes. The derived CRLB acts as a crucial factor for allocating the resources. For a centralized system, a greedy algorithm is introduced which divides the problem into many sub-problems and tries to find the optimum for each sub-problem. The complexity of the greedy algorithm is high ($O(M^5 N_{\text{res}})$). To reduce the complexity, a partial decentralized allocation scheme - bidding game is presented. The local approximated CRLB instead of the global CRLB is used to calculate the potential improvement for an MT. The simulation

results show that the solution from bidding game is similar as the one from the greedy algorithm. The overall complexity is reduced to $O(M^2 N_{\text{res}})$. For a purely decentralized system, The resource allocation can be considered as a non-cooperative game. we evaluate the Nash equilibrium point where every MT behaves greedy and selfish. The interference becomes severe and jeopardizes the positioning estimation. To solve this problem, a cooperative game is presented. As a probabilistic approach, we design the utility function which fulfills the constraints. The simulation results show it works well in both stationary and dynamic cases.

Due to the interference avoidance, the centralized schemes should in general outperforms the decentralized ones. However, from the simulation results we find out that sometimes the cooperative game performs better than the centralized greedy scheme. One reason could be that the gain from subcarrier reuse is higher than the interference effect.

7.2 Future Work

For the future work, some of the remaining problems are interesting. The link evaluation is an essential scheme because other relevant schemes are based on it, e.g. local cooperative CRLB approximation, bidding game, cooperative game, etc. Therefore, it would be valuable to find a scheme better than the variance approximation. One idea could be for the PF, integrating the neighbors' positions into the local state space and directly draw particles to estimate the marginal posterior function jointly for both own position and neighbor's position. The computational redundancy reduction for this approach would be of interest. For the delay-pathloss dependency, we only derived a bound for it. How to fuse these two metrics will be an interesting topic in practice. Another interesting topic is for the centralized greedy scheme, the correlation of the sub-problems can be explored to reduce the complexity. The optimal subcarrier reuse rate is also worth to be investigated. At the end, using a real system to test the constraints and the performance in reality will also be an interesting step forward.

Bibliography

[1] I. F. Progri, "Wireless-enabled GPS Indoor Geolocation System," in *Position Location and Navigation Symposium (PLANS), 2010 IEEE/ION*, pp. 526 –538, may 2010.

[2] R. Ouyang, A.-S. Wong, and K. T. Woo, "GPS Localization Accuracy Improvement by Fusing Terrestrial TOA Measurements," in *Communications (ICC), 2010 IEEE International Conference on*, pp. 1 –5, may 2010.

[3] S. Gezici, Z. Tian, G. Giannakis, H. Kobayashi, A. Molisch, H. Poor, and Z. Sahinoglu, "Localization via Ultra-Wideband Radios: a Look at Positioning Aspects for Future Sensor Networks," *Signal Processing Magazine, IEEE*, vol. 22, pp. 70 – 84, july 2005.

[4] Y. Shen and M. Win, "Fundamental Limits of Wideband Localization - Part I: A General Framework," *Information Theory, IEEE Transactions on*, vol. 56, pp. 4956 –4980, oct. 2010.

[5] D. Porcino, "Location of Third Generation Mobile Devices: A Comparison between Terrestrial and Satellite Positioning Systems," in *Vehicular Technology Conference, 2001. VTC 2001 Spring. IEEE VTS 53rd*, vol. 4, pp. 2970 –2974 vol.4, 2001.

[6] Y. Jin, W.-S. Soh, and W.-C. Wong, "Indoor Localization with Channel Impulse Response based Fingerprint and Non-parametric Regression," *Wireless Communications, IEEE Transactions on*, vol. 9, pp. 1120 –1127, march 2010.

[7] Y. Qi and H. Kobayashi, "On Relation Among Time Delay and Signal Strength based Geolocation Methods," in *Global Telecommunications Conference, 2003. GLOBECOM '03. IEEE*, vol. 7, pp. 4079 – 4083 vol.7, dec. 2003.

[8] N. Patwari, J. Ash, S. Kyperountas, I. Hero, A.O., R. Moses, and N. Correal, "Locating the Nodes: Cooperative Localization in Wireless Sensor Networks," *Signal Processing Magazine, IEEE*, vol. 22, pp. 54 – 69, july 2005.

[9] Claus Pedersen, et al., "Hybrid Localization Techniques," *WHERE (FP6-ICT-217033), Deliverable D2.3 Version 1.0*, May 2010.

[10] J. Figueiras and S. Frattasi, *Mobile Positioning and Tracking: From Conventional to Cooperative Techniques*. John Wiley & Sons, 2010.

[11] B. Uguen, "Scenarios and Parameters," *WHERE2 (FP7-ICT-2009-4), Deliverable D1.1*, August 2011.

[12] K. Doppler, M. Rinne, C. Wijting, C. Ribeiro, and K. Hugl, "Device-to-Device Communication as an Underlay to LTE-Advanced Networks," *Communications Magazine, IEEE*, vol. 47, pp. 42 –49, dec. 2009.

[13] R. Raulefs, S. Zhang, C. Mensing, C. Ghali, and J. Hachem, "Dynamic Cooperative Positioning," *Wireless Conference 2011 - Sustainable Wireless Technologies (European Wireless), 11th European*, pp. 1 –5, april 2011.

[14] Y. Shen, H. Wymeersch, and M. Win, "Fundamental Limits of Wideband Localization - Part II: Cooperative Networks," *Information Theory, IEEE Transactions on*, vol. 56, pp. 4981 –5000, oct. 2010.

[15] F. Penna, M. Caceres, and H. Wymeersch, "Cramér-Rao Bound for Hybrid GNSS-Terrestrial Cooperative Positioning," *Communications Letters, IEEE*, vol. 14, pp. 1005 –1007, november 2010.

[16] C. Savarese, J. Rabaey, and K. Langendoen, "Robust Positioning Algorithms for Distributed Ad-Hoc Wireless Sensor Networks," *USENIX technical annual conference*, vol. 2, pp. 317–327, 2002.

[17] H. Wymeersch, J. Lien, and M. Win, "Cooperative Localization in Wireless Networks," *Proceedings of the IEEE*, vol. 97, pp. 427 –450, feb. 2009.

[18] M. Caceres, F. Penna, H. Wymeersch, and R. Garello, "Hybrid GNSS-Terrestrial Cooperative Positioning via Distributed Belief Propagation," in *GLOBECOM 2010, 2010 IEEE Global Telecommunications Conference*, pp. 1 –5, dec. 2010.

[19] K. Das and H. Wymeersch, "Censored Cooperative Positioning for Dense Wireless Networks," in *Personal, Indoor and Mobile Radio Communications Workshops (PIMRC Workshops), 2010 IEEE 21st International Symposium on*, pp. 262 –266, sept. 2010.

[20] X.-S. Yang and S. Deb, "Cuckoo Search via Lévy Flights," in *Nature Biologically Inspired Computing, 2009. NaBIC 2009. World Congress on*, pp. 210 –214, dec. 2009.

[21] C. Günther, *Lecture Notes: Satellite Navigation*. 2009.

[22] S. M. Kay, *Fundamentals of Statistical Signal Processing: Estimation Theory*. Upper Saddle River, NJ, USA: Prentice-Hall, Inc., 1993.

[23] F. Gustafsson and F. Gunnarsson, "Mobile Positioning Using Wireless Networks: Possibilities and Fundamental Limitations based on Available Wireless Network Measurements," *Signal Processing Magazine, IEEE*, vol. 22, pp. 41 – 53, july 2005.

[24] M. S. Arulampalam, S. Maskell, N. Gordon, and T. Clapp, "A Tutorial on Particle Filters for Online Nonlinear/Non-Gaussian Bayesian Tracking," *IEEE Transactions on Signal Processing*, vol. 50, pp. 174–188, February 2002.

[25] B. Ristic, S. Arulampalam, and N. Gordon, *Beyond the Kalman Filter - Particle Filters for Tracking Applications*. Artech House, 2004.

[26] Injong Rhee and Minsu Shin and Seongik Hong and Kyunghan Lee and Song Chong, "On the Levy-walk Nature of Human Mobility," *IEEE 27th Conference on Computer Communications (INFOCOM), Phoenix, USA* , vol. 27, April 2008.

[27] H. Cramér, *Mathematical Methods of Statistics*. Princeton University Press, 1946.

[28] C. R. Rao, "Information and the Accuracy Attainable in the Estimation of Statistical Parameters," *Bull. Calcutta Math. Soc.*, 1945.

[29] A. Dammann, *Lecture Notes: System Aspects in Signal Processing*. 2010.

[30] I. Viering, *Lecture Notes: System Aspects in Communications Engineering*. 2010.

[31] L. Dai, Z. Wang, J. Wang, and Z. Yang, "Positioning with OFDM Signals for the Next- Generation GNSS," *Consumer Electronics, IEEE Transactions on*, vol. 56, pp. 374 –379, may 2010.

[32] A. B. MacKenzie and L. A. DaSilva, *Game Theory for Wireless Engineers (Synthesis Lectures on Communications)*. Morgan & Claypool Publishers.

[33] D. Schmidt, C. Shi, R. Berry, M. Honig, and W. Utschick, "Distributed Resource Allocation Schemes," *Signal Processing Magazine, IEEE*, vol. 26, pp. 53 –63, september 2009.

[34] L. Law, J. Huang, M. Liu, and S.-y. Li, "Price of Anarchy for Cognitive MAC Games," in *Global Telecommunications Conference, 2009. GLOBECOM 2009. IEEE*, pp. 1 –6, 30 2009-dec. 4 2009.

[35] J. Nash, "Non-Cooperative Games," *The Annals of Mathematics*, vol. 54, pp. 286–295, Sept. 1951.

[36] M. J. Osborne and A. Rubinstein, *A Course in Game Theory*, vol. 1 of *MIT Press Books*. The MIT Press, 1994.